AD-A058 533 DAVID W TAYLOR NAVAL SHIP RESEARCH AND DEVELOPMENT CE--ETC F/G 13/10
LIFTING LINE CALCULATIONS FOR HYDROFOIL PERFORMANCE AT ARBITRAR--ETC(U)
JUN 78 M B WILSON
UNCLASSIFIED DTNSRDC/SPD-0839-01 NL

1 OF 2
ADA
058533

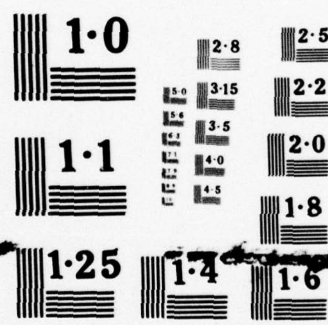
1·0
2·8
2·5
3·15
2·2
3·5
2·0
4·0
1·1
4·5
1·8
1·25
1·4
1·6

LIFTING LINE CALCULATIONS FOR HYDROFOIL PERFORMANCE AT ARBITRARY FROUDE NUMBER AND SUBMERGENCE - PART 1 - FIXED SHAPE ELLIPTICAL CIRCULATION DISTRIBUTION

DTNSRDC/SPD-0839-01

ADA058533

AD No.

DDC FILE COPY

DAVID W. TAYLOR NAVAL SHIP RESEARCH AND DEVELOPMENT CENTER

Bethesda, Md. 20084

LIFTING LINE CALCULATIONS FOR HYDROFOIL PERFORMANCE

AT ARBITRARY FROUDE NUMBER AND SUBMERGENCE

PART 1

FIXED SHAPE ELLIPTICAL CIRCULATION DISTRIBUTION

by

Michael B. Wilson

APPROVED FOR PUBLIC RELEASE: DISTRIBUTION UNLIMITED

SHIP PERFORMANCE DEPARTMENT

DEPARTMENTAL REPORT

78 14 08 031

June 1978 DTNSRDC/SPD-0839-01

MAJOR DTNSRDC ORGANIZATIONAL COMPONENTS

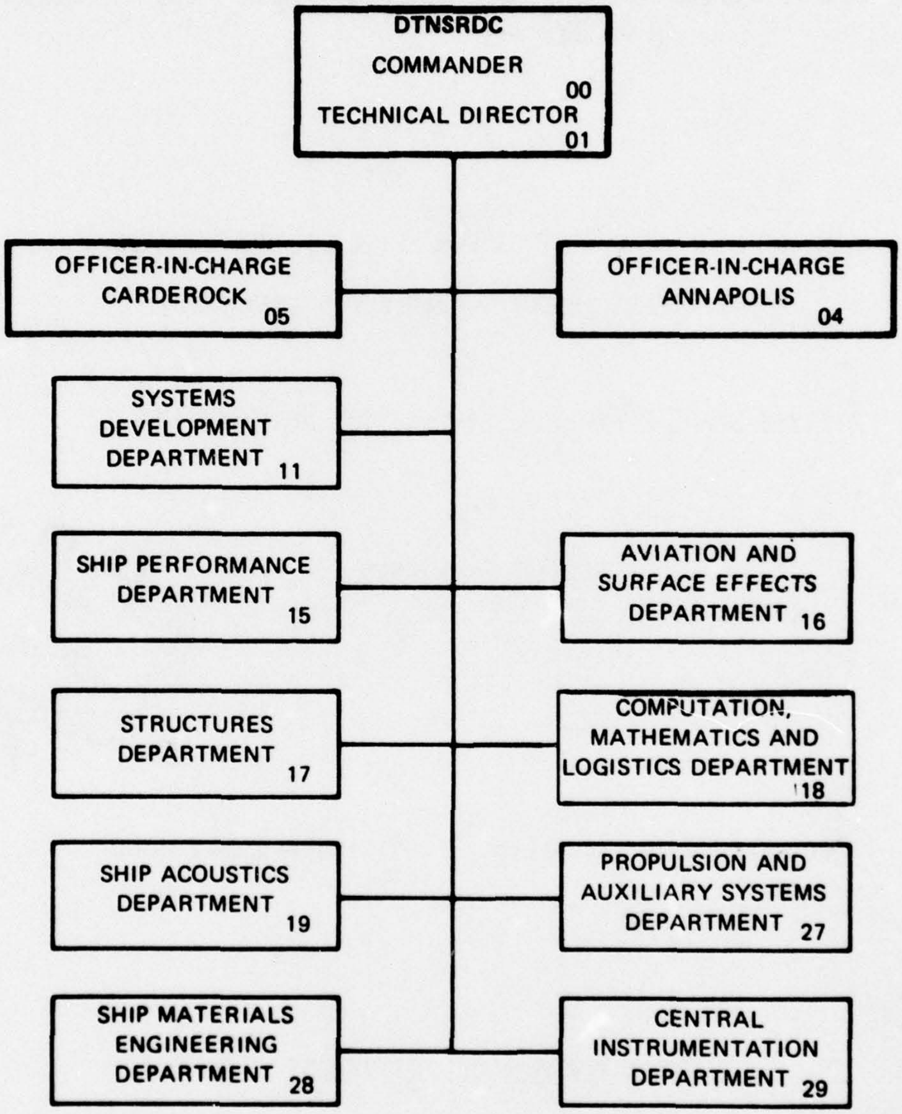

UNCLASSIFIED

SECURITY CLASSIFICATION OF THIS PAGE (When Data Entered)

REPORT DOCUMENTATION PAGE

READ INSTRUCTIONS BEFORE COMPLETING FORM

1. REPORT NUMBER: (14) DTNSRDC/SPD-0839-01
2. GOVT ACCESSION NO.
3. RECIPIENT'S CATALOG NUMBER

4. TITLE (and Subtitle): (6) LIFTING LINE CALCULATIONS FOR HYDROFOIL PERFORMANCE AT ARBITRARY FROUDE NUMBER AND SUBMERGENCE. PART 1. FIXED SHAPE ELLIPTICAL CIRCULATION DISTRIBUTION.
5. TYPE OF REPORT & PERIOD COVERED
6. PERFORMING ORG. REPORT NUMBER

7. AUTHOR(s): (10) Michael B. Wilson
8. CONTRACT OR GRANT NUMBER(s): (16) F43421

9. PERFORMING ORGANIZATION NAME AND ADDRESS: David W. Taylor Naval Ship R&D Center, Bethesda, MD 20084
10. PROGRAM ELEMENT, PROJECT, TASK AREA & WORK UNIT NUMBERS: (17) Task Area ZF43421001, Element 62543N, Work Unit 1-1500-100

11. CONTROLLING OFFICE NAME AND ADDRESS: Naval Material Command, Navy Department, Washington, D.C. 20360
12. REPORT DATE: (11) June 1978
13. NUMBER OF PAGES: 95

14. MONITORING AGENCY NAME & ADDRESS (if different from Controlling Office): (12) 97p.
15. SECURITY CLASS. (of this report): UNCLASSIFIED
15a. DECLASSIFICATION/DOWNGRADING SCHEDULE

16. DISTRIBUTION STATEMENT (of this Report)

APPROVED FOR PUBLIC RELEASE: DISTRIBUTION UNLIMITED

17. DISTRIBUTION STATEMENT (of the abstract entered in Block 20, if different from Report)

18. SUPPLEMENTARY NOTES

78 14 08 031

19. KEY WORDS (Continue on reverse side if necessary and identify by block number)

Hydrofoil, Wave Resistance, Froude Number, Finite Aspect Ratio, Lifting Line, Free Surface Effect, Lift Correction

20. ABSTRACT (Continue on reverse side if necessary and identify by block number)

Hydrofoil drag and lift prediction formulas derived by T.Y. Wu using the lifting line approximation are evaluated numerically using a computer program developed for the purpose. Some results for selected aspect ratios and foil submergences are displayed in several plots of general interest and usefulness, for the case of an elliptic planform hydrofoil supporting an elliptic circulation distribution of fixed shape, but variable strength.

DD FORM 1 JAN 73 1473 EDITION OF 1 NOV 65 IS OBSOLETE

S/N 0102-LF-014-6601

UNCLASSIFIED

SECURITY CLASSIFICATION OF THIS PAGE (When Data Entered)

LB

389 694

UNCLASSIFIED

SECURITY CLASSIFICATION OF THIS PAGE (When Data Entered)

Some preliminary comparisons between results obtained numerically and from Wu's asymptotic formulas are discussed. These show that for certain extreme cases, the wave drag and the Froude-independent part of the lift correction are well predicted by asymptotic relations. For intermediate values of both Froude number and submergence ratio, the asymptotic relations give poor results for wave drag. At most all submergences and Froude numbers the existing asymptotic expressions for the Froude-dependent part of lift correction give poor results.

UNCLASSIFIED

SECURITY CLASSIFICATION OF THIS PAGE (When Data Entered)

TABLE OF CONTENTS

LIST OF FIGURES

LIST OF TABLES

NOTATION

		Dimensions*
A	Planform aspect ratio = $(2b)^2/S$	L^2
b	Half-span of hydrofoil	L
c(y)	Chord length distribution	L
c_a	Average chord length	L
c_o	Midspan chord length	L
C_D	Total inviscid lift-dependent drag coefficient = $D/\frac{1}{2}\,\rho U^2 S$	-
$C_{D_{i\infty}}$	Unbounded flow induced drag coefficient; corresponds to $D_1/\frac{1}{2}\,\rho U^2 S$	-
$C_{D_{si}}$	Surface induced drag coefficient; corresponds to $(D_2+D_3)/\frac{1}{2}\,\rho U^2 S$	-
$C_{D_{sw}}$	Surface wave part of wave drag coefficient at large Froude number	-
C_L	Total lift coefficient = $L/\frac{1}{2}\,\rho U^2 S$	-
C_{L_o}	Reference lift coefficient = $2\Gamma_o/Uc_o$	-
C_W	Wave drag coefficient, corresponds to $D_4/\frac{1}{2}\,\rho U^2 S$	-
$C_{W(d)}$, $C_{W(t)}$	Diverging and transverse wave components of C_W $(C_W = C_{W(d)} + C_{W(t)})$	-
D	Total inviscid lift-dependent drag	ML/T^2
$D_1,(D_2+D_3),D_4$	Components of total lift-dependent drag (Wu's designations)	ML/T^2
F_b	Half span Froude number = $U/\sqrt{gb}$	-

* L = length, T = time, M = mass

		Dimensions
F_c	Average chord Froude number = $U/\sqrt{gc_a}$	-
F_h	Depth Froude number = $U/\sqrt{gh}$	-
F_L	Kernel function in integral of ΔC_{L_2}	-
$F_L(o)$	Value of $F_L(u)$ at $u = 0$, function of λ only	-
g	Acceleration of gravity	L/T^2
h	Depth of submergence	L
J_W	Wave drag integral	-
k_λ	Modulus appearing in complete elliptic integrals = $1/(1 + \lambda^2)^{\frac{1}{2}}$	-
L	Total lift force	ML/T^2
L_o	Reference lift force	ML/T^2
S	Planform area of hydrofoil	L^2
U	Free stream velocity	L/T
x, y, z	Coordinate variables (see Fig. 1)	L
β	Half-span Froude number squared = U^2/gb	-
γ_W	Wave drag function; related to $C_{D_{sw}}$ term	-
$\Gamma(y)$	Distribution of circulation strength across span	L^2/T
Γ_o	Value of $\Gamma(y)$ at midspan (y=0); 'strength' of circulation	L^2/T
Δ_{LC}	Lift correction coefficient ratio = $\Delta C_L/C_{L_o}^2$	-

		Dimensions
ΔC_L	Lift correction coefficient = $\Delta L/\frac{1}{2}\rho U^2 S$	-
ΔC_{L_1}, ΔC_{L_2}	Froude-independent and dependent terms, respectively, of lift correction coefficient	-
ΔL	Lift correction due to u-component induced velocity	ML/T^2
κ_o	Free surface wave number = g/U^2	L^{-1}
λ	Depth-to-half span ratio = h/b	-
σ_i	Biplane factor	-
ϕ	Perturbation velocity potential	L^2/T

ABSTRACT

Hydrofoil drag and lift prediction formulas derived by T.Y. Wu using the lifting line approximation are evaluated numerically using a computer program developed for the purpose. Some results for selected aspect ratios and foil submergences are displayed in several plots of general interest and usefulness, for the case of an elliptic planform hydrofoil supporting an elliptic circulation distribution of fixed shape, but variable strength.

Some preliminary comparisons between results obtained numerically and from Wu's asymptotic formulas are discussed. These show that for certain extreme cases, the wave drag and the Froude-independent part of the lift correction are well predicted by asymptotic relations. For intermediate values of both Froude number and submergence ratio, the asymptotic relations give poor results for wave drag. At most all submergences and Froude numbers the existing asymptotic expressions for the Froude-dependent part of lift correction give poor results.

ADMINISTRATIVE INFORMATION

This work was authorized by the Naval Material Command (08T), funded under the Ships, Subs and Boats Program, Task Area ZF43-421, and administered by the Ship Performance Department High Performance Vehicles Program (1507).

INTRODUCTION

Growing interest in very large hydrofoil support systems has focused attention on a low Froude number range of operation (at or near takeoff speeds) generally regarded previously as being below anything of practical utility. This has created a renewed interest in the analytical properties of a hydrofoil moving near the free surface. A recent experiment[1*] specifically intended to produce data for a hydrofoil operating at low Froude numbers has also pointed out a distinct need for

---

* A complete list of references is given on page 88

well-founded analytical predictions of foil-alone performance for use in direct comparisons with experimental results, for preliminary design studies, and possibly for refined data analysis of interference effects.

There are available several published lifting line theories for submerged hydrofoils, and though there may be differences as to the form of the final expressions or in the degree of completeness of the calculated results, these theories all share common fundamental assumptions and therefore must ultimately be versions of the same theory. A recent comprehensive summary of published work on the linearized theory of hydrofoils has been presented by T. Nishiyama,[2] whose own extensive work with the hydrofoil lifting line theory appears prominently in the discussion offered in Reference 2. Unfortunately there are only limited examples of hydrofoil aspect ratios and depths of submergence carried out in Nishiyama's papers, and his computer programs are not available. Therefore it was decided to start to build up a computational capability for predicting hydrofoil performance based on the lifting line theory by T.Y. Wu developed in 1953,[3a] and published in 1954.[3b] Hallmarks of this work are the careful formulation and solution of the problem within the framework of the linearized free surface potential theory, and the extensive asymptotic analyses that show the effects of Froude number and sumbergence depth on drag, lift, and induced velocities. As far as is known, there has never been a systematic attempt made to exploit numerically Wu's derived formulas for the purpose of presenting general information useful for preliminary design or comparison with experiments. It may be noted that in an independent effort, J. Breslin and his associates obtained formulas similar to those

of Wu. Also, Breslin[4] organized what look like part of Wu's asymptotic results for wave drag into an approximate scheme for estimating hydrofoil performance at large Froude number. This scheme has been unverified, however, both as to its accuracy and regions of its application.

The present work has been directed mainly toward the development of numerical procedures and a computer program for evaluating Wu's results for the prediction of hydrofoil total lift-dependent-drag and lift correction.

SUMMARY OF RESULTS FROM LIFTING LINE SOLUTION

The complete potential flow solution for a submerged flat hydrofoil of span 2b, submergence h, zero thickness, and arbitrary planform shape of aspect ratio $A = (2b)^2/S$ moving with steady velocity U beneath the free surface of an otherwise undisturbed fluid has been presented by Wu.[3] Formulas have been given for the solution of the perturbation velocity potential $\phi(x, y, z)$ which satisfies the Laplace equation throughout the fluid region and the linearized free surface boundary conditions on the plane $z = 0$. Details should be sought in the original reference. Figure 1 shows the geometry and coordinate system for the hydrofoil lifting line problem.

In accordance with the classical lifting line approach, the spanwise-varying bound vortex distribution $\Gamma(y)$ has a strength at each y-value that represents the chordwise-integrated effect of bound

vorticity concentrated at the quarter-chord line---a reasonable approximation for 'large' aspect ratios. In practice, this means for aspect ratios larger than about four.

If we suppose that the circulation distribution $\Gamma(y)$ is known, either by specification or as part of the solution, Wu's expressions are summarized here for the hydrofoil lift-dependent drag and total lift, given in terms of $\Gamma(y)$ and the induced velocity field at the location of the lifting line.

GENERAL

Drag Due-to-Lift

The total drag due-to-lift has been obtained from the expression

$$D = -\rho \int_{-\infty}^{\infty} \Gamma(y) \left(\frac{\partial \phi}{\partial z} \right)_{\substack{x=0 \\ z=-h}} dy \tag{1}$$

Of course the perturbation velocity potential ϕ is itself proportional to the circulation strength, and has been determined by Wu as the sum of four parts, with corresponding drag components. Thus

$$D = D_1 + D_2 + D_3 + D_4 \tag{2}$$

where

$$D_1 = \frac{\pi}{4}\rho\int_0^{\infty}\left[f^2(\mu) + g^2(\mu)\right]\mu d\mu \tag{3}$$

$$(D_2+D_3) = -\frac{\pi}{4}\rho\int_0^{\infty} e^{-2h\mu}\left[f^2(\mu) + g^2(\mu)\right]\mu d\mu \tag{4}$$

$$\begin{aligned} D_4 = \pi\,\rho\kappa_o{}^2\int_0^{\pi/2} e^{-2h\kappa_o\sec^2\theta}\Big[&f^2(\kappa_o\sec^2\theta\ \sin\theta) \\ &+ g^2(\kappa_o\sec^2\theta\ \sin\theta)\Big]\sec^5\theta\, d\theta \end{aligned} \tag{5}$$

with

$$f(\mu) = \frac{1}{\pi}\int_{-\infty}^{\infty}\Gamma(\eta)\cos\mu\eta\, d\eta$$

$$g(\mu) = \frac{1}{\pi}\int_{-\infty}^{\infty}\Gamma(\eta)\sin\mu\eta\, d\eta \tag{6}$$

$$\kappa_o = g/U^2$$

Viscous drag is not included in this potential flow result. The functions $f(\mu)$ and $g(\mu)$ are the Fourier coefficients of the circulation distribution.

Total Lift

For the hydrofoil, the x-component of total velocity is modified from the free stream U by the presence of the free surface, so that

total lift is given by

$$L = \rho \int_{-\infty}^{\infty} \Gamma(y) \left\{ U + \left[\frac{\partial\phi}{\partial x}\right]_{\substack{x=0 \\ z=-h}} \right\} dy \tag{7}$$

or

$$L = L_o + \Delta L \tag{8}$$

where

$$L_o = \rho U \int_{-\infty}^{\infty} \Gamma(y)\, dy \tag{9}$$

$$\Delta L = \rho \int_{-\infty}^{\infty} \Gamma(y) \left\{\frac{\partial}{\partial x} \phi(o,y,-h)\right\} dy$$

$$\Delta L = -\tfrac{1}{2} \rho \int_0^{\infty} e^{-2h\mu} \mu\, d\mu \int_0^{\pi/2} \left\{ f^2(\mu \sin\theta) + g^2(\mu \sin\theta) \right\} \times \left\{ \frac{\mu + \kappa_o \sec^2\theta}{\mu + \kappa_o \sec^2\theta} \right\} d\theta \tag{10}$$

with $f(\mu)$ and $g(\mu)$ given by Equations (6). It may be noted at this stage that in all of Nishiyama's work with the hydrofoil lifting line approach, the lift correction term ΔL has been neglected as being of a higher order and therefore not properly included in the results of a linearized theory (see, for example, Reference 2, Equation (195)). There is certainly no question that the numerical computation of ΔL is tedious and time consuming. However, it is not at all obvious that ΔL is of negligible size from the integral results in their primitive state. Rather, it is fair to state that ΔL is of the same order of magnitude as the lift-dependent drag, and that it is one order smaller in magnitude than L_o.

ELLIPTICAL CIRCULATION

Because of the inherent simplifications, it is interesting to consider in detail the case of specified elliptical circulation distribution

$$\Gamma(y) = \begin{cases} \Gamma_o \sqrt{1-y^2/b^2}, & |y| \leq b \\ 0 \quad , & |y| > b \end{cases} \tag{11}$$

This is clearly a meaningful choice because the elliptic distribution is the correct linearized solution for an elliptic planform wing in an unbounded stream (no free surface present).

EXAMPLE PLANFORM GEOMETRY

The planform geometry chosen here is an ellipse, simply to remain consistent with the choice of the elliptical circulation distribution. As indicated in Figure 2, the elliptic planform, with chord distribution

$$c(y) = c_o \sqrt{1-y^2/b^2} \tag{12}$$

may be characterized by:

averaged chord $\qquad c_a = \frac{\pi}{4} c_o \qquad$ (13)

planform area $\qquad S = \frac{\pi}{2} c_o b = 2bc_a \qquad$ (14)

aspect ratio $$A = \frac{(2b)^2}{S} = \frac{8b}{\pi c_o} = \frac{2b}{c_a} \qquad (15)$$

The depth-to-chord ratio and depth-to-half span ratio are, respectively,

$$\frac{h}{c_a} = \frac{4}{\pi}\left(\frac{h}{c_o}\right) \qquad (16)$$

$$\lambda = \frac{h}{b} = \frac{8h}{\pi c_o A} = \left(\frac{2}{A}\right)\frac{h}{c_a} \qquad (17)$$

Then drag and lift coefficient are formed in the usual way, based on planform area

$$C_D = \frac{D}{\frac{1}{2}\rho U^2 S} \quad \text{and} \quad C_L = \frac{L}{\frac{1}{2}\rho U^2 S} \qquad (18)$$

Physically, the results of the present calculations pertain to a special situation where both the form and strength of the circulation distribution are maintained somehow on the specified planform shape; without regard to the angle of attack and changes in the effective angle due to vertical induced velocity. It should be emphasized that for a near-surface hydrofoil of any prescribed geometry, the actual circulation distribution $\Gamma(y)$ will be fixed in neither shape nor in strength, and in general must be determined as a function of Froude number and depth of submergence. Numerical calculations of the complete free surface hydrofoil problem are deferred to a later reporting of results.

The present calculations are very useful in showing the detailed Froude-dependent behavior and exact relative magnitudes of the various components of both $C_D/C_{L_o}^2$ and $\Delta C_L/C_{L_o}^2$ for the simplified version of the problem.

FROUDE NUMBERS

It is convenient to have several Froude numbers available when discussing hydrofoil performance. The reference length can be either a hydrofoil size parameter or the submergence depth.

$$
\begin{aligned}
&\text{chord Froude number} && F_c = U/\sqrt{gc_a} \\
&\text{depth Froude number} && F_h = U/\sqrt{gh} = \sqrt{c_a/h}\, F_c \\
&\text{half-span Froude number} && F_b = U/\sqrt{gb} = \sqrt{2/A}\, F_c \\
& && \beta = U^2/gb = F_b^2
\end{aligned}
\tag{19}
$$

Any one Froude number alone will not suffice to characterize the free surface flow geometry of a hydrofoil. There must be a nondimensional speed parameter (Froude number) accompanied by a relative depth of submergence parameter.

FORMULA SUMMARY

Drag Due-to-Lift

The total inviscid drag due-to-lift, in coefficient form, is hereafter written in components that can be identified in terms of C_{D_1},

C_{D_2}, C_{D_3}, and C_{D_4} (obtained from Wu's D_1, D_2, etc.), but with a notation more suggestive of their physical significance

$$C_D = C_{D_{i\infty}} + C_{D_{si}} + C_W \tag{20}$$

$$= C_{D_1} + (C_{D_2} + C_{D_3}) + C_{D_4} \qquad \text{(Wu's notation)}$$

where for the elliptic circulation distribution

$$C_{D_{i\infty}} = \frac{C_{L_o}^{\ 2}}{\pi A} \tag{21}$$

$$C_{D_{si}} = -\frac{\sigma_i}{\pi A} C_{L_o}^{\ 2} \tag{22}$$

$$C_W = \frac{8C_{L_o}^{\ 2}}{\pi A} \int_0^{\pi/2} e^{-2F_h^{-2}\sec^2\theta} J_1^{\ 2}\left(\frac{1}{\beta}\sec^2\theta \sin\theta\right) \times \frac{\sec\theta}{\sin^2\theta}\, d\theta \tag{23}$$

where J_1 is the Bessel function of the first kind, of order one. The reference lift coefficient C_{L_o} is proportional to the circulation strength Γ_o,

$$C_{L_o} = \frac{2\,\Gamma_o}{Uc_o} \tag{24}$$

The image induced drag factor σ_i can be identified as the Prandtl 'biplane factor' discussed, for example, by von Kármán and Burgers,[5] pp. 217-219, in connection with the combined drag of biplane arrangements. Wu[3] has obtained a compact formula for the biplane factor, expressed purely as a function of λ

$$\sigma_i(\lambda) = 1 - \frac{4}{\pi} \lambda \sqrt{1+\lambda^2} \left[K(k_\lambda) - E(k_\lambda)\right] \qquad (25)$$

where λ = depth-to-half span ratio = h/b

$$k_\lambda = 1/(1 + \lambda^2)^{\frac{1}{2}}$$

and $K(k)$ and $E(k)$ are, respectively, the complete elliptic integrals of the first and second kind.

The term $C_{D_{i\infty}}$ is the familiar unbounded flow induced drag coefficient for an elliptic planform wing with total lift coefficient C_{L_o}. The negative quantity $C_{D_{si}}$ represents part of the surface induced drag, independent of Froude number. We note that $C_{D_{si}}$ depends only on the depth-to-half span ratio λ, as contained in the biplane factor $\sigma_i(\lambda)$ described above. The 'wave drag' coefficient, C_W, is the Froude-dependent drag contribution, denoted as such to conform with past notations (e.g. Breslin[4]). However, C_W embodies more than the usual wavemaking drag coefficient that one would obtain, say, for a submerged <u>non-lifting</u> body. While C_W has the expected zero-value lower limit (Froude number $\rightarrow 0$), it approaches a non-zero upper limit (as Froude number $\rightarrow \infty$). This upper limit value combines directly with the $C_{D_{si}}$ term; and in the infinite Froude number limit, changes the sign of the

resulting surface induced drag contribution. Specifically, the wave drag coefficient can be written for the large Froude number regime as

$$C_W = \frac{2\sigma_i}{\pi A} C_{L_o}^{\,2} + C_{D_{sw}} \tag{26}$$

where the new term, $C_{D_{sw}}$, is the 'surface wave' part of C_W that has a <u>zero</u> limit as Froude number grows infinitely large. This form is inappropriate for use at small Froude numbers.

The two limiting values with respect to Froude number of the total drag coefficient due-to-lift are simple modifications to the induced drag, and involve only the biplane factor

$$\lim_{F_c \to 0} C_D = \frac{C_{L_o}^{\,2}}{\pi A}\left[1 - \sigma_i(\lambda)\right] \quad \text{(lower limit)} \tag{27}$$

$$\lim_{F_c \to \infty} C_D = \frac{C_{L_o}^{\,2}}{\pi A}\left[1 + \sigma_i(\lambda)\right] \quad \text{(upper limit)} \tag{28}$$

Total Lift

The total lift coefficient for a hydrofoil having an elliptic circulation distribution of strength Γ_o is given by

$$C_L = C_{L_o} + \Delta C_L \tag{29}$$

where

$$C_{L_o} = \frac{\Gamma_o}{bc_a U} \int_{-b}^{b} \sqrt{1-y^2/b^2}\; dy = \frac{\pi\Gamma_o}{2Uc_a} = \frac{2\Gamma_o}{Uc_o} \tag{30}$$

$$\Delta C_L = \Delta C_{L_1} + \Delta C_{L_2} \tag{31}$$

The two parts of the lift correction coefficient, ΔC_L, can be written directly from Wu's[3] results as

$$\Delta C_{L_1} = -\frac{8C_{L_o}^2}{\pi^3 \lambda A} \int_0^{k_\lambda} \left[\frac{1-(k_1/k_\lambda)^2}{1-k_1^2}\right]^{\frac{1}{2}} \mathbf{C}(k_1)dk_1 \tag{32}$$

$$\begin{aligned}\Delta C_{L_2} = -\frac{8C_{L_o}^2}{\pi^2 A} \int_0^{\infty} \frac{du}{u(u-1)} \int_0^{\pi/2} e^{-2uF_h^{-2}\sec^2\theta} \\ \times J_1^2\left(\frac{u}{\beta}\sec^2\theta \sin\theta\right) \frac{d\theta}{\sin^2\theta}\end{aligned} \tag{33}$$

where $\mathbf{C}(k_1)$ is a derived complete elliptic integral that can be written (see Reference 6, p. 321) in terms of the complete elliptic integrals $K(k_1)$ and $E(k_1)$ as follows

$$\mathbf{C}(k_1) = \frac{1}{k_1^4}\left[(2-k_1^2)\,K(k_1) - 2E(k_1)\right] \tag{34}$$

with

$$k_\lambda = 1/(1+\lambda^2)^{\frac{1}{2}}$$

It is clear that the reference lift coefficient C_{L_o} is the first order lift quantity, and that ΔC_L is a second order quantity proportional to $C_{L_o}^{\,2}$ and therefore roughly of the same magnitude as C_D.

EXAMPLE NUMERICAL RESULTS

In this section the results of some numerical calculations for hydrofoil drag and lift correction are presented for representative values of planform aspect ratio, depth of submergence, and a range of Froude numbers. Table 1 indicates the matrix of cases considered. To produce these results, numerical evaluations of the integrals appearing in the wave drag coefficient and lift correction coefficient expressions have been carried out with a digital computer program consisting of several subroutines guided by a main program entitled SUBMFL. A complete listing of this computer program is given in Appendix A. No approximate or asymptotic formulas or series solutions are used; only numerical quadrature has been employed. However, rather extensive intermediate and check-out tests of most of Wu's asymptotic results have been performed in the course of debugging the individual subroutines.

Certain details of the manipulations of integration variables and general outlines of the numerical integration procedures are covered in the appendices.

TABLE 1

MATRIX OF CALCULATED CASES

DEPTH-TO-CHORD RATIO, h/c_a	ASPECT RATIO, A: 4	6	10
0.25	x	x	
0.35	x		
0.5	x	x	
0.75	x		
1.0	x	x	x
1.5	x		
2.0	x	x	
3.5	x		

DRAG DUE-TO-LIFT

Biplane Factor

The magnitude of image induced drag effect (see Equations (27) and (28)) is contained in the biplane factor $\sigma_i(\lambda)$, given by Equation (25). Owing to the ease of computation of K(k) and E(k), an approximate formula for σ_i is not needed. Appendix B presents brief remarks on the calculation of σ_i and a table of its values. Figure 3 is a plot of $\sigma_i(\lambda)$ covering a practical range of λ-values.

Wave Drag

A convenient form for the expression for wave drag coefficient ratio, starting with Equation (23) is shown in Appendix C to be

$$\frac{C_W}{C_{L_o}^{\,2}} = \frac{e^{-F_h^{-2}}}{\pi F_c^{\,2}} J_W \tag{35}$$

where the wave drag integral is

$$J_W = \int_0^\infty \frac{\exp(-F_h^{-2}\sqrt{1+4\beta^2t^2})\left[1+\sqrt{1+4\beta^2t^2}\right]^2}{t^2\sqrt{1+4\beta^2t^2}} J_1^{\,2}(t)dt \tag{36}$$

Numerical results for the wave drag coefficient ratio versus the chord Froude number F_c are plotted in Figure 4 for an aspect ratio A = 4 hydrofoil, with contours of eight depth-to-chord ratios. Some of the same results are replotted versus depth Froude number F_h in Figure 5 to show that the peaks in the wave drag ratio $C_W/C_{L_o}^{\,2}$ apparently line up at

a Froude number of $F_h \approx 1.4$, regardless of the depth of submergence. From Figure 4, it is seen that in the chord Froude number plot, the peaks shift to higher F_c-values as the submergence depth increases. Figure 6 displays wave drag results for aspect ratio A = 6 at four depth-to-chord ratios.

In all three Figures 4, 5, and 6, the upper limit values of wave drag ratio (see Equation (26))

$$\lim_{F_c \to \infty} \frac{C_W}{C_{L_o}^2} = \frac{2\sigma_i}{\pi A} \tag{37}$$

are indicated by horizontal lines along the right hand borders of the graphs. Evidently the $C_W/C_{L_o}^2$ curves approach the limiting values more quickly for the deep submergence cases than for the shallow submergence cases.

For a constant depth-to-chord ratio $h/c_a = 1.0$, Figure 7 is a graph of $C_W/C_{L_o}^2$ versus F_c for three different aspect ratios A = 4, 6, and 10. This shows that the wave drag peaks become relatively higher for hydrofoils with larger aspect ratios. Although at first glance this may seem contrary to one's intuition, the result is true only for the wavemaking part of the drag due-to-lift at a low Froude number, and can be understood by a separate study of the relative magnitudes of the drag components associated with the transverse and diverging wave systems.

Transverse and Diverging Wave Contributions

The free surface wave pattern produced by a submerged disturbance is the superposition of two families of waves, the transverse and diverging systems. It is interesting to decompose the total wave drag into corresponding wave system components as was accomplished by Wigley (see Lunde[7]) using the thin ship theory for wave resistance for surface ships, and by Breslin[4] for hydrofoil wave drag. In the θ-integral representation of wave drag in Equation (23), the transverse wave system is the integrated effect of the wave-direction-interval $0 \leq \theta \leq \theta_c$, and the diverging wave system comes from $\theta_c \leq \theta \leq \pi/2$. The critical angle dividing the two intervals is

$$\theta_c = \sin^{-1}\left(\sqrt{1/3}\right)$$

In the t-integral representation of wave drag, given in Equation (36), the critical t-value corresponding to θ_c is Froude dependent

$$t_c = \frac{1}{\beta} \sec^2\theta_c \sin\theta_c$$

Computations of the transverse wave drag contribution $C_{W(t)}$ and diverging wave part $C_{W(d)}$ correspond, then, to the intervals $0 \leq t \leq t_c$ and $t_c \leq t \leq \infty$, respectively.

Some example results for the wave drag decomposition are shown in Figures 8 and 9 for an aspect ratio 4 hydrofoil at submergence $h/c_a = 0.25$ and 1.0, respectively. For comparison, values of the wave drag coefficient ratio of a two-dimensional submerged hydrofoil[8]

$$\frac{C_W}{C_\ell^{\,2}} = \frac{e^{-2F_h^{-2}}}{2F_c^{\,2}} \tag{38}$$

are also plotted versus the chord Froude number in Figures 8 and 9. The C_W and C_ℓ denote the wave drag and lift coefficients per unit span, respectively. At low Froude numbers, the transverse wave component $C_{W(t)}$ dominates the total wave drag, reaches a peak value, then drops off rapidly as the diverging wave component slowly builds up. In Figure 8, there is a striking correspondence between the two-dimensional wave drag ratio and the total finite span wave drag ratio, $C_W/C_{L_o}^{\,2}$, at the chord Froude numbers below $F_c \approx 1.2$. There is a great temptation to suppose that this good correspondence could be used to generate an approximate prediction method for total hydrofoil lift-dependent drag based on the sum of the two-dimensional hydrofoil wave drag expression plus terms accounting for induced and biplane induced drag. In fact, this appears to be just what has been suggested in the well known drag estimation procedure introduced by Wadlin, Shuford, and McGehee.[9] However, the comparison in Figure 9, also for A = 4, but with $h/c_a = 1.0$, shows that any good correspondence observed earlier is fortuitous. Significant differences exist, particularly near the peak of wave drag, or in other words in the low Froude number regime. The wave drag decomposition curves in Figures 10 and 11, for $h/c_a = 0.75$ and 1.0 respectively, show similar trends in the comparison between the two-dimensional wave drag ratio and the finite span values of $C_W/C_{L_o}^{\,2}$, but for aspect ratio A = 6. Apparently the good correspondence noted in

Figure 8 improves with decreasing λ-values. Figure 12 is the wave drag decomposition for a aspect ratio 10 hydrofoil at submergence $h/c_a = 1.0$.

Total Drag Due-to- Lift

Summary curves of total inviscid drag ratio due-to-lift (from Equation (20)) plotted versus chord Froude number are given in Figure 13 for aspect ratio A = 4, and in Figure 14 for aspect ratio A = 6. The low and high Froude number limits given by Equations (27) and (28) are indicated by horizontal lines at the left and right borders of the graphs, respectively.

Figure 15 is a plot of $C_D/C_{L_o}^2$ versus F_c, comparing curves for aspect ratio 4, 6, and 10 hydrofoils at the same submergence $h/c_a = 1.0$. The horizontal broken lines indicate the magnitudes of the unbounded flow induced drag ratio $C_{D_{i\infty}}/C_{L_o}^2 = 1/\pi A$. This figure is also a representation of the relative magnitudes of the inviscid drag components, for this typical value of hydrofoil submergence. Now it is seen that the total drag due-to-lift increases for decreasing aspect ratio hydrofoils, but that the relative contribution of wavemaking drag increases with increasing ratio cases at low Froude numbers. As we have seen previously, this is caused by the large transverse wavemaking contribution that approaches the two-dimensional limit as the aspect ratio increases, but the effect is localized with respect to Froude number in the speed range $F_h \leq 1.4$.

TOTAL LIFT

As indicated in Equations (31)-(33), there are two parts to the lift correction ratio $\Delta C_L/C_{L_o}^2$. The form for the $\Delta C_{L_1}/C_{L_o}^2$ term, given in Equation (32), is directly suitable for numerical evaluation by Simpson's Rule.

A convenient form for the second term, $\Delta C_{L_2}/C_{L_o}^2$, starting with Equation (33) is shown in Appendix D to be

$$\frac{\Delta C_{L_2}}{C_{L_o}^2} = -\frac{4}{\pi^2 A F_h} \int_0^\infty \frac{e^{-u/F_h^2}}{\sqrt{u}\,(u-1)} F_L(u)\, du \qquad (39)$$

where

$$F_L(u) = \int_0^\infty \frac{\exp\left(-2\sqrt{t_1^2+u^2/4F_h^4}\right)\left[u/2F_h^2+\sqrt{t_1^2+u^2/4F_h^4}\right]^{3/2}}{t_1^2\sqrt{t_1^2+u^2/4F_h^4}} \times J_1^2\left(\frac{t_1}{\lambda}\right) dt_1 \qquad (40)$$

The kernel function $F_L(u)$ resembles the wave resistance integral J_W, and has been computed numerically in the same manner. The u-integral in Equation (39) must be evaluated in terms of its principal value, and some details of its numerical treatment are outlined in Appendix D. Completely numerical evaluation of the double integral for $\Delta C_{L_2}/C_{L_o}^2$ is very time consuming, much more so than the numerical computation of either the $C_W/C_{L_o}^2$ or $\Delta C_{L_1}/C_{L_o}^2$ terms.

Sample numerical results for the total lift correction ratio $\Delta C_L/C_{L_o}^2$ versus depth Froude number F_h are plotted in Figure 16 for an aspect ratio 4 hydrofoil, with contours of depth-to-chord ratio. Similar

results for aspect ratio 6 are plotted in Figure 17 versus chord Froude number F_c. At a constant depth-to-chord ratio $h/c_a = 1.0$, Figure 18 shows the variation of $\Delta C_L/C_{L_o}^2$ versus F_c for aspect ratios A = 4, 6, and 10. There is a distinctive effect of the free surface that causes a sharply peaked, positive lift correction at depth Froude numbers smaller than $F_h = 1.5$ and a broad, persistent, negative lift correction at Froude numbers larger than 1.5. The cross-over point appears to occur at $F_h \approx 1.5$ regardless of depth of submergence or aspect ratio. Apparently the influence of aspect ratio on the magnitude of $\Delta C_L/C_{L_o}^2$ is relatively slight, but Figure 18 shows that the peak values of lift correction (both positive and negative) increase somewhat with aspect ratio. It should be reiterated that this Froude-dependent behavior of $\Delta C_L/C_{L_o}^2$ has been computed with the assumption of fixed circulation distribution shape, and that the full Froude-dependent effects on both the strength and distribution of $\Gamma(y)$ have not been taken into account in these preliminary calculations.

TOTAL LIFT AND DRAG RATIOS

It is interesting to consider the ratio of total lift C_L to the reference lift coefficient C_{L_o} and how this affects the expected ratio of total lift-dependent drag to total lift squared. If the lift correction ratio is denoted as

$$\Delta_{LC} = \frac{\Delta C_{L_1} + \Delta C_{L_2}}{C_{L_o}^2} \tag{41}$$

then

$$\frac{C_L}{C_{L_o}} = 1 + \Delta_{LC}\, C_{L_o} \tag{42}$$

and so

$$\frac{C_D}{C_L{}^2} = \left(\frac{C_D}{C_{L_o}{}^2}\right) \frac{1}{(1 + \Delta_{LC}\, C_{L_o})^2} \tag{43}$$

This shows that the absolute magnitude of the reference lift coefficient C_{L_o} is important in determining to what extent the free surface effect will alter both C_L/C_{L_o} and $C_D/C_L{}^2$.

If the reference lift coefficient is held fixed at $C_{L_o} = 1.0$ throughout the speed range, then curves of the variation of C_L/C_{L_o} versus depth Froude *number* F_h are shown in Figures 19 and 20, for aspect ratio A = 4 and 6 respectively, with contours of two different submergence ratios $h/c_a = 0.25$ and 1.0. Some care must be exercised in interpreting these C_L/C_{L_o} curves with respect to determining the influence of the free surface on the lift produced by a submerged hydrofoil. Because the circulation distribution shape has been assumed to remain elliptical, the only adjustment accommodated by the present computations is the circulation strength Γ_o, or equivalently, the reference coefficient C_{L_o}. It should be noted that C_{L_o} is not the same as the unbounded flow lift coefficient denoted as C_{L_∞} by Nishiyama.[2]

Effectively, the only free surface influence accounted for here in the calculation of the lift correction, ΔC_L, enters through the induced changes in the x-component of the perturbation velocity multiplied by

the circulation distribution and integrated over the span. See Equation 10. This results in the rather modest variations in the ratio C_L/C_{L_o} versus Froude number shown in Figures 19 and 20. It is reasonable to predict that when a full accounting is made for adjustments of both the strength and shape of the circulation distribution, the variations will be different and possibly more extreme. An important improvement anticipated with complete solution is a detailed description of the induced changes due to both the horizontal and vertical perturbation velocities.

Curves of $C_D/C_{L_o}^2$ versus chord Froude number for an aspect ratio 6 hydrofoil at submergence $h/c_a = 0.25$ are plotted in Figure 21 for several different constant values of $C_{L_o} = 0.25$, 0.5, and 1.0. For comparison, the reference total drag ratio, $C_D/C_{L_o}^2$, is included. The effect of varying the magnitude of C_{L_o} is to separate the several contours of $C_D/C_{L_o}^2$, and to shift the peaks of the curves to somewhat higher Froude numbers.

A more realistic display of these results is shown in Figure 22, where a curve of C_D/C_L^2 versus F_c is plotted for a reference lift coefficient C_{L_o} that is based on a constant reference foil loading equal to $(L/S)_o = \frac{1}{2}\rho U^2 C_{L_o} = 1200$ pounds/foot^2 (57,456 N/m^2) on an aspect ratio 4 hydrofoil having an average chord length of $c_a = 20$ feet (6.1 m), operating at submergence $h/c_a = 1.0$. In this case the reference C_{L_o} is speed-dependent

$$C_{L_o} = \frac{1237}{U^2} \tag{44}$$

The curve is terminated for this example at a speed corresponding to $C_{L_o} = 2.0$. In the comparison with the $C_D/C_{L_o}^2$ curve in Figure 22, the main effect is to shift the peak of C_D/C_L^2 with respect to Froude number. The changes in magnitude between C_D/C_L^2 and $C_D/C_{L_o}^2$ become rather small for the higher Froude numbers because C_{L_o} becomes progressively smaller with speed increasing.

COMPUTATION TIME

The execution time for computation of a single case (given aspect ratio, submergence, and Froude number) varies widely as a function of both submergence ratio λ and Froude number, with the longest times being required for shallow submergence and small Froude numbers. Also, the execution time is dominated by the calculation of the ΔC_{L_2} term. Consider a representative case. With λ around 0.4 ($h/c_a \sim 1.0$), chord Froude number about 0.5, using 100 spaces per loop for the calculation of J_W and for ΔC_{L_1}, using 60 spaces per loop for F_L and for the non-singular integrals of ΔC_{L_2}, and with 61 spaces per half interval for the singular part of ΔC_{L_2} the total Central Processor (CP) execution time is around 55 seconds per case on the DTNSRDC CDC 6400 computer. Of this, approximately 0.5 to 0.75 seconds of CP time is devoted to each of the calculations of the wave drag C_W and lift correction term ΔC_{L_1}. The remainder, some 52 seconds, must be spent on the lift correction term ΔC_{L_2}.

COMPARISONS OF ASYMPTOTIC RESULTS

In consideration of how useful asymptotic results can be if they are accurate enough, some preliminary comparisons are included here between asymptotic estimates obtained in Reference 3 and the numerically determined values. This section is not intended as an exhaustive comparative study, but it does illustrate one important application of the present results.

It is crucial to consider asymptotic results only in the variable regimes where they are valid. In the case of the near surface hydrofoil, estimates produced by Wu[3] for large Froude number ($F_h^2 >> 1$) require simultaneously small submergence ($\lambda \rightarrow 0$). Similarly, formulas for small Froude number ($F_h^2 >> 1$) must be accompanied by large submergence ($\lambda \rightarrow \infty$). The present numerical tests of Wu's results were made on the following basis

$$\text{Large } F_h, \text{ small } \lambda: \qquad F_h^2 \geq 1.5, \quad \lambda < 1 \tag{45}$$

$$\text{Small } F_h, \text{ large } \lambda: \qquad F_h^2 \leq 1.5, \quad \lambda > 1 \tag{46}$$

DRAG DUE-TO-LIFT

Large Froude Number, Small Submergence

The asymptotic relation for wave drag at large Froude number obtained by Wu in Reference 3 (Equation (68)) can be written in coefficient form as

$$\frac{C_W}{C_{L_o}^2} \sim \frac{2\sigma_i}{\pi A} + \frac{1}{\pi F_c^2}\Bigg[\frac{4}{3}\Big\{\frac{2}{\pi}(1+\lambda^2)^{3/2}\;E(k_\lambda) - \frac{3}{2}\lambda \tag{47}$$

$$- \lambda^2\sqrt{1+\lambda^2}\;F(-\tfrac{1}{2}, \tfrac{3}{2}; 1; k_\lambda^2)\Big\} + O\Big(\frac{1}{\beta}\ln\beta, \frac{1}{\beta^2}, \frac{1}{F_h^2}\Big)\Bigg]$$

where F is the hypergeometric function, whose expansion for small λ was *determined in Reference 3a, Appendix E, p. 70 to be*

$$F(-\tfrac{1}{2}, \tfrac{3}{2}; 1; k_\lambda) \sim \frac{2}{\pi}\Big(2 - \ln\frac{4\sqrt{1+\lambda^2}}{\lambda}\Big) - \frac{3}{2\pi^2}\Big(\frac{1}{3} - \ln\frac{4\sqrt{1+\lambda^2}}{\lambda}\Big)$$

$$\times\Big(\frac{\lambda^2}{1+\lambda^2}\Big) + O(\lambda^2\ln\lambda) \tag{48}$$

with $k_\lambda = 1/(1+\lambda^2)^{1/2}$.

Now, this result can be used to write an asymptotic formula for the 'surface wave' drag term, $C_{D_{SW}}$, introduced in Equation (26). Following a suggestion and notation similar to that of Breslin,[4] the large Froude number, small submergence approximation for the surface wave drag is

$$\frac{C_{D_{sw}}}{C_{L_o}^2} \sim \frac{\gamma_W(\lambda)}{F_c^2} \tag{49}$$

where the wave drag function γ_W is purely a function of the depth-to-half span ratio, and from (47) and (48), is given in its complete asymptotic form by

$$\gamma_W(\lambda) \sim \frac{4}{3\pi}\left[\frac{2}{\pi}(1+\lambda^2)^{3/2} E(k_\lambda) - \frac{3}{2}\lambda - \lambda^2\sqrt{1+\lambda^2}\left\{\frac{2}{\pi}\right.\right.$$

$$\left.\left.\times\left(2 - \ln\frac{4\sqrt{1+\lambda^2}}{\lambda}\right) - \frac{3}{2\pi^2}\left(\frac{1}{3} - \ln\frac{4\sqrt{1+\lambda^2}}{\lambda}\right)\left(\frac{\lambda^2}{1+\lambda^2}\right)\right\}\right] \tag{50}$$

provided $\lambda \to 0$.

Breslin[4] proposed an abbreviated form of this function

$$\gamma_{W,Bres} \sim \frac{4}{3\pi}\left[\frac{2}{\pi}(1+\lambda^2)^{3/2} E(k_\lambda) - \frac{3}{2}\lambda\right] \tag{51}$$

Example comparisons between the asymptotic results for γ_W and numerical values are shown in Figures 23 through 26, for an aspect ratio 6 hydrofoil at depth-to-chord ratios h/c_a = 0.25, 0.5, 1.0, and 2.0 with corresponding depth-to-half span ratios of λ = 0.0833, 0.1667, 0.3333, and 0.6667 respectively. For the smallest submergence of λ = 0.08333, in Figure 23, good correspondence between the asymptotic and numerical results for γ_W is observed, but not until the Froude number exceeds $F_h \sim 9$ or 10. The difference between the two expressions for γ_W in this case is negligible.

For larger and larger values of λ, the agreement between asymptotic and numerical values for the wave drag function γ_W becomes poorer. Also the disparity between the values of γ_W calculated using the complete asymptotic expression in Equation (50) and Breslin's version in Equation (51) becomes greater as λ increases, although significant differences occur only for λ-values where the asymptotic formula no longer appears to be valid anyway.

Small Froude Number, Large Submergence

For very small values of depth Froude number, and large submergence ratio λ, the asymptotic relation for wave drag from Reference 3, (Equation (66)) can be expressed as

$$\frac{C_W}{C_{L_o}^2} \sim \frac{e^{-2/F_h^2}}{\sqrt{2\pi}\ \lambda^2 A F_h^3} \left[1 + \frac{3}{8}\left(1 - \frac{1}{6\lambda^2 F_h^4}\right) F_h^4 + O(F_h^4)\right] \tag{52}$$

for $F_h^2 \to 0$, $\lambda \to \infty$.

Figure 27 is an example comparison between results from the asymptotic estimate and numerical calculations, for an aspect ratio 4 hydrofoil at submergence $h/c_a = 3.5$, $\lambda = 1.75$. The curve for the asymptotic result is plotted out to $F_h^2 = 1.5$, and the agreement shown is excellent.

LIFT

The two parts of the lift correction ratio have somewhat different asymptotic behavior. The term $\Delta C_{L_1}/C_{L_o}^2$ is independent of Froude number,

and has approximating formulas that depend only on the relative size of the depth-to-half span ratio λ. The term $\Delta C_{L_2}/C_{L_o}^2$ requires careful attention to both Froude number and submergence ratio simultaneously, as prescribed earlier for wave drag in Equations (45) and (46).

Large Froude Number, Small Submergence

The asymptotic relation for the $\Delta C_{L_1}/C_{L_o}^2$ term, given in Equation (78a) of Reference 3, requires small values of submergence ratio, and can be written

$$\frac{\Delta C_{L_1}}{C_{L_o}^2} \sim -\frac{8}{3\pi^3 \lambda A}\left\{1 - 3\lambda^2\left(\ln 2 - \frac{3}{4} + \frac{5}{8}\ln\frac{\sqrt{1+\lambda^2}}{\lambda}\right)\right\} + O(\lambda^4 \ln\lambda) \tag{53}$$

provided $\lambda \to 0$.

For the $\Delta C_{L_2}/C_{L_o}^2$ term, the asymptotic expression from Equation (80) of Wu[3] can be written as

$$\frac{\Delta C_{L_2}}{C_{L_o}^2} \sim \frac{\sqrt{2}}{\pi^2 A}\Gamma(1/4)\left[1 - \frac{\Gamma(3/4)}{\sqrt{\pi}\,\Gamma(1/4)}\;\frac{\lambda}{\sqrt{1+\lambda^2}}\right] \times \left[1 + \sqrt{\frac{2}{\pi}}\frac{1}{F_h}\left(\gamma + \ln\frac{2}{F_h^2}\right)\right] \tag{54}$$

for $F_h^2 \to \infty$ and $\lambda \to 0$,

where Γ = the gamma function (c.f. Reference 10, p. 255)

γ = Euler's constant = 0.5772156649.

Example direct comparison of values for both $\Delta C_{L_1}/C_{L_o}^2$ and $\Delta C_{L_2}/C_{L_o}^2$, obtained both numerically and from the asymptotic expressions are plotted in Figures 28, 29 and 30 for the cases of an aspect ratio 6

hydrofoil at submergences $h/c_a = 0.25, 1.0,$ and 2.0, having corresponding values of $\lambda = 0.08333, 0.333, 0.667$ respectively. The agreement between the two curves for the $\Delta C_{L_1}/C_{L_o}^2$ part is excellent, even at the larger values of λ. However, the discrepencies between the asymptotic estimates and the numerical values for $\Delta C_{L_2}/C_{L_o}^2$ are substantial, even at the largest Froude numbers and smallest submergence ratio. Some preliminary checks on the series solution of the inner integral outlined by Wu[3a] in his Appendix IV(H) have shown some inconsistencies which may explain the differences.

The present calculations are undoubtedly more accurate, but at the expense of time-consuming computations, particularly for the $\Delta C_{L_2}/C_{L_o}^2$ term.

Small Froude Number, Large Submergence

For large submergence ratio λ, the approximate expression for the $\Delta C_{L_1}/C_{L_o}^2$ term, given by Wu[3] in his Equation (76), can be expressed as

$$\frac{\Delta C_{L_1}}{C_{L_o}^2} \sim \frac{-1}{8\pi\lambda\sqrt{1+\lambda^2}\,A}\left\{1 + \frac{0.3125}{(1+\lambda^2)} + \frac{0.70703}{(1+\lambda^2)^2} + \frac{0.0920105}{(1+\lambda^2)^3} + O\left(\frac{1}{(1+\lambda^2)^4}\right)\right\} \tag{55}$$

provided $\lambda \to \infty$.

For the $\Delta C_{L_2}/C_{L_o}^2$ term, the asymptotic relation from Equation (81) of Wu[3] can be written

$$\frac{\Delta C_{L_2}}{C_{L_o}^2} \sim \frac{1}{(2\pi)^{3/2}\lambda^2 A F_h} \left[1 + \frac{1}{2} F_h^{\,2} + O(F_h^{\,4})\right] \tag{56}$$

for $F_h^{\,2} << 1$, $\lambda \to \infty$.

Figure 31 is a comparison plot for both $\Delta C_{L_1}/C_{L_o}^2$ and $\Delta C_{L_2}/C_{L_o}^2$ versus Froude number for an aspect ratio 4 hydrofoil at submergence ratio $\lambda = 1.75$. Here again, the approximate formula for $\Delta C_{L_1}/C_{L_o}^2$ appears to be remarkably accurate. The same cannot be said for the $\Delta C_{L_2}/C_{L_o}^2$ term, where the asymptotic result shows a distinct divergence from the numerically obtained curve. There is good reason to suspect the validity of the asymptotic formula, which is the result of nested asymptotic evaluations of the double integral expression for ΔC_{L_2}. Although the example data are not provided here, a substantial number of numerical checks have been carried out on the inner integral, or the $F_L(u)$ function defined in Equation (40). These showed that the intermediate asymptotic formula obtained by Wu[3a*] gives inaccurate results, except for a limited range of large values for both $u/F_h^{\,2}$ and λ.

EXAMPLE DRAG FORCE ESTIMATES

In order to illustrate the relative importance of the major components of total drag experienced by large submerged hydrofoils moving at speeds between takeoff and subcavitating maximum, results of some simple estimates can be made using the computed predictions

---

* Asymptotic result for Wu's integral $I_2(u)$; his Equation (IV.34) in his Appendix IV

generated in this work. Two groups of comparison examples are included: (a) constant chord length (same chord Froude number range) and (b) constant total foil lift; both with the same foil loading

$$L/S = 1200 \text{ pounds/foot}^2 = 57{,}456 \text{ N/m}^2$$

and at submergence $h/c_a = 1.0$.

Consider first a family of three, uncambered, 10 percent thick, elliptic planform hydrofoils all having the same chord length

$$c_a = 20 \text{ feet } (6.1 \text{ m})$$

with aspect ratios A = 4, 6, and 10. The total foil-alone drag can be estimated from

$$\begin{aligned} D_T &= D_{visc} + D \\ &= \tfrac{1}{2}\,\rho\, U^2 S(C_{D_{visc}} + C_D) \end{aligned} \tag{57}$$

where $$C_{D_{visc}} \simeq 2(1 + f)\, C_f + K_{sep} C_L^{\,2}$$

$$C_D = C_{D_{i\infty}} + C_{D_{si}} + C_W \tag{58}$$

Here the total viscous drag contribution is estimated using

C_f = flat plate friction, 1957 ITTC correlation line, based on wetted surface

f = viscous pressure drag factor from Hoerner;[10] f = 0.206 for 10 percent thick foils

K_{sep} = incremental profile drag factor recommended in Reference 11, Appendix 8-B; assumed constant here as $K_{sep} = 0.005$, approximately true for $R_c \approx 10^8$.

The term C_D is the total drag coefficient due-to-lift, given by Equations (20)-(23).

The lift coefficient in sea water is speed dependent

$$C_L = \frac{1206}{U^2}$$

using U in feet/second. With the calculated, Froude-dependent values of Δ_{LC} defined by Equation (41), or

$$\Delta_{LC} = \frac{C_L - C_{L_o}}{C_{L_o}^{\,2}}$$

the reference lift coefficient C_{L_o} can be determined from

$$C_{L_o} = \frac{1}{2\Delta_{LC}} \left(\sqrt{1 + 4C_L\Delta_{LC}} - 1\right) \tag{59}$$

The Froude-dependent C_{L_o}-values together with the drag coefficient ratios, $C_D/C_{L_o}^{\,2}$, of Figures 13, 14, and 15 permit the final estimates of drag due-to-lift, C_D. Again it should be recalled that these lifting line predictions apply to the drag induced by an elliptical circulation distribution of fixed shape, but variable strength.

Figures 32, 33, and 34 are plots of drag force versus velocity for the speed range 20 to 50 knots, corresponding to aspect ratios A = 4, 6, and 10 respectively. The total foil lift is different for each case,

having corresponding values of L = 1,920,000 pounds (8.54×10^6 N), 2,880,000 pounds (12.81×10^6 N), and 4,800,000 pounds (21.35×10^6 N). Physically, it would be necessary to increase the foil angle of attack with decreasing speed in order to achieve the contours shown in Figures 32-34 and 35; but for the purposes of this comparison, the determination of the angle of attack schedule is superfluous. In each of these plots, the lower curve is the viscous drag D_{visc} and the upper curve is the total drag D_T. The dashed curve represents values of

$$(1 + \sigma_i)\, D'_{i\infty} \tag{60}$$

where $D'_{i\infty}$ is the unbounded flow induced drag determined from the coefficient

$$C'_{D_{i\infty}} = \frac{C_L^2}{\pi A} \tag{61}$$

The biplane factors corresponding to these cases are $\sigma_i = 0.2322$, 0.3409, and 0.4842 respectively. The difference between the D_T and $(1 + \sigma_i)\, D'_{i\infty}$ curves is the surface wave drag contribution, whose value goes to zero at infinite Froude number. It is clear from these graphs that for increasingly larger aspect ratios and physically larger hydrofoils, the surface wave drag becomes a relatively much more important factor in the speed range shown.

A second comparison is made on the basis of the same total foil lift. Figure 35 shows the drag variation with speed for an aspect ratio 10 hydrofoil having the same planform area, S = 1600 foot^2 (148.6 m^2),

and the same lift as the aspect ratio 4 hydrofoil example shown in Figure 32. Even with the smaller chord and therefore shifted Froude number range, the relatively greater importance of the surface wave drag contribution to the total drag is evident from looking at both Figures 32 and 35. It may also be noted that despite the increased surface wave drag, the total drag of the aspect ratio 10 hydrofoil is lower in this comparison at $h/c_a = 1$.

CONCLUSIONS AND RECOMMENDATIONS

1. A successful computer program has been developed for the numerical calculation of the integrals appearing in the prediction formulas for hydrofoil drag due-to-lift and total lift, for the special case of foil loading due to an elliptic circulation distribution of fixed shape on an elliptical planform.
2. Some results are displayed in a variety of useful graphs for aspect ratios 4, 6, and 10 at several depths of submergence, and for a range of Froude numbers $0.2 \leq F_c \leq 6.0$ and $F_h \leq 12.0$.
3. Although it was not the direct purpose of this work, some preliminary comparisons between numerical results and results from Wu's asymptotic relations have been made. These show mixed results. Excellent predictions are provided by asymptotic formulas for: (a) wave drag, $C_W/C_{L_o}^2$, at small Froude number and deep submergence, and (b) lift correction term, $\Delta C_{L_1}/C_{L_o}^2$, for both shallow and deep submergence.

A narrow range of good predictions are provided by the asymptotic relations for wave drag at large Froude number and shallow submergence.

Rather poor predictions are available from the asymptotic formulas for the lift correction term $\Delta C_{L_2}/C_{L_o}^2$ in both the large and small Froude number regimes.

4. More efficient means should be explored for the evaluation of the ΔC_{L_2} term to avoid performing both integrals by numerical quadrature. With faster computation of this term, it is recommended to include the ΔC_L correction to the drag and lift results of the linearized theoretical prediction of hydrofoil performance.

5. The lifting line results of Wu should be further implemented in a computer program capable of analyzing arbitrary planform shapes (those within the known limitations of the lifting line theory) and should be made available for evaluation for general hydrofoil support systems.

6. Example calculations of hydrofoil drag force illustrate the need to have accurate predictions of the surface wave drag contributions present at the low chord Froude numbers characteristic of very large hydrofoil planforms.

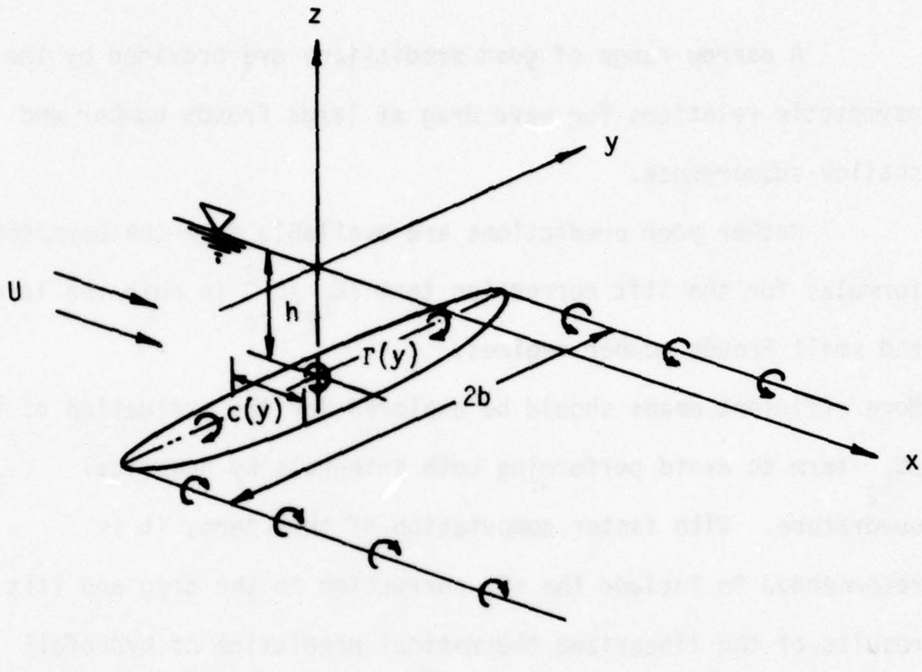

Figure 1 - Geometry and Coordinate System of Submerged Hydrofoil

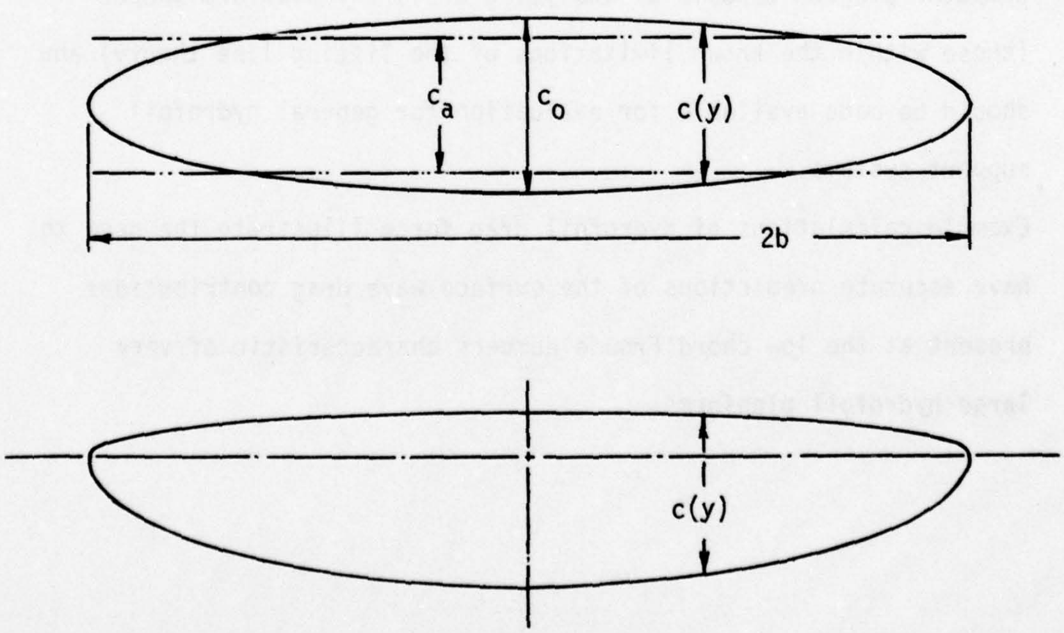

Figure 2 - Elliptic Planform Shape

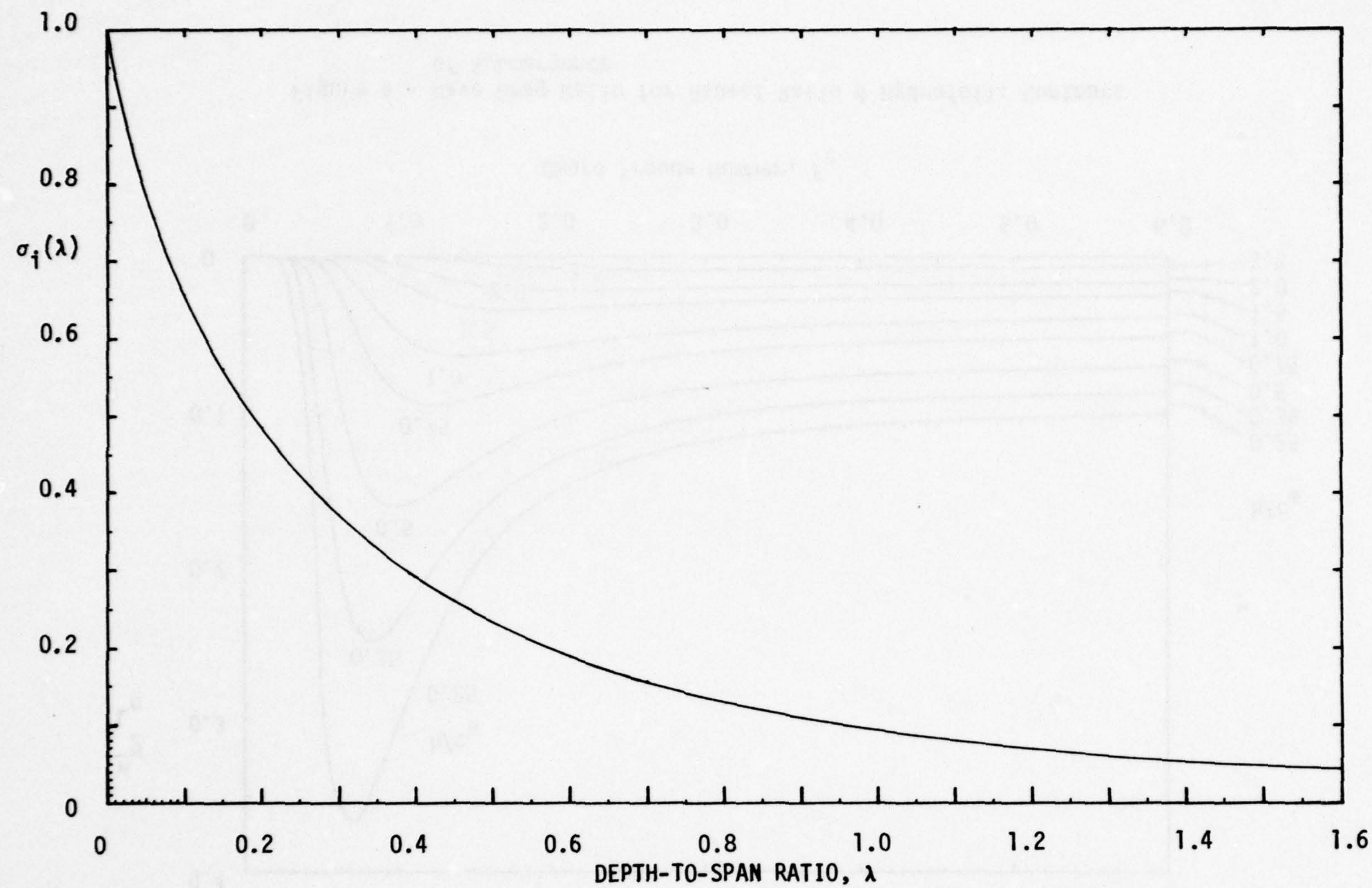

Figure 3 - The Biplane Factor $\sigma_i(\lambda)$

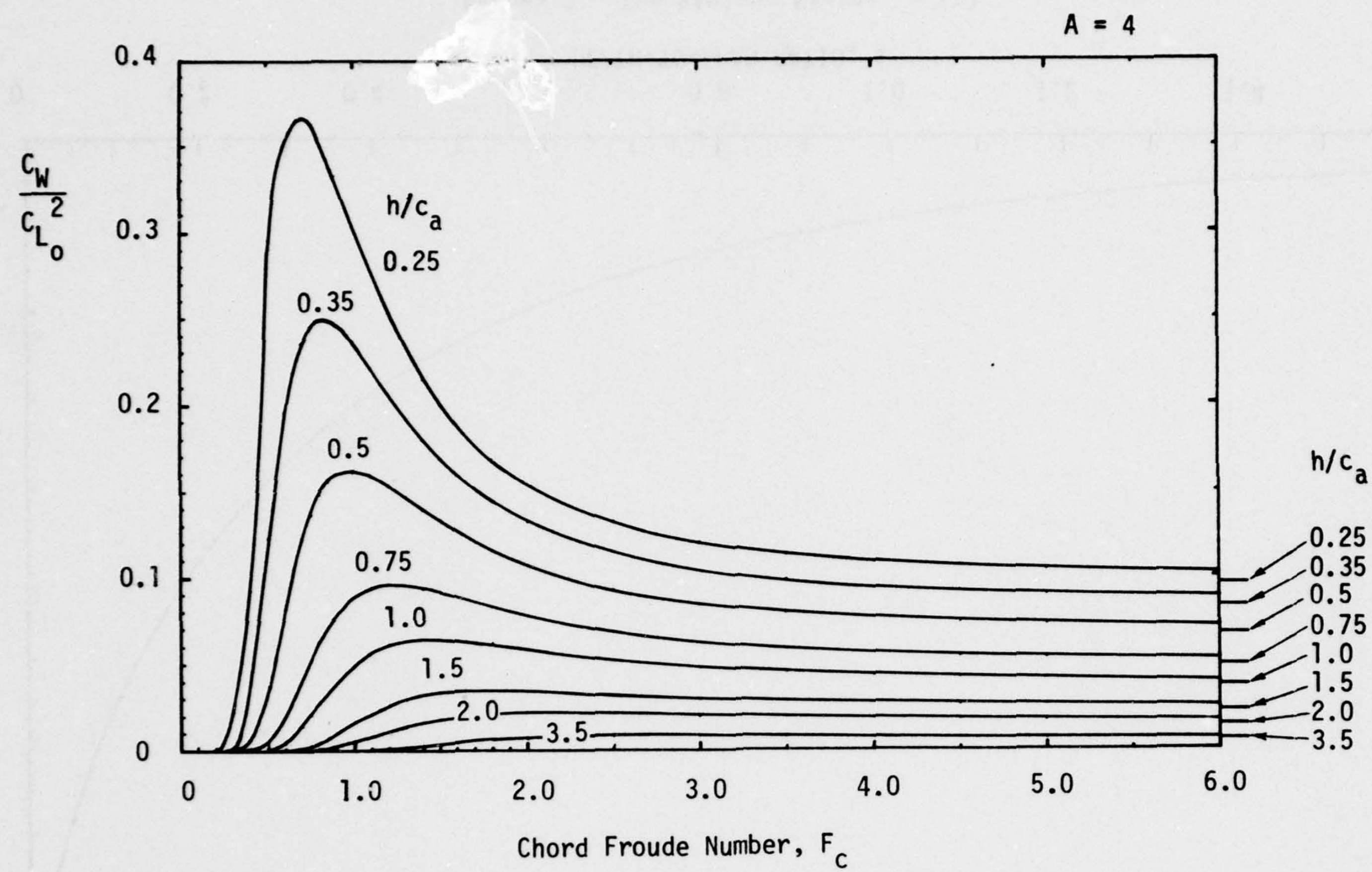

Figure 4 - Wave Drag Ratio for Aspect Ratio 4 Hydrofoil; Contours of Submergence

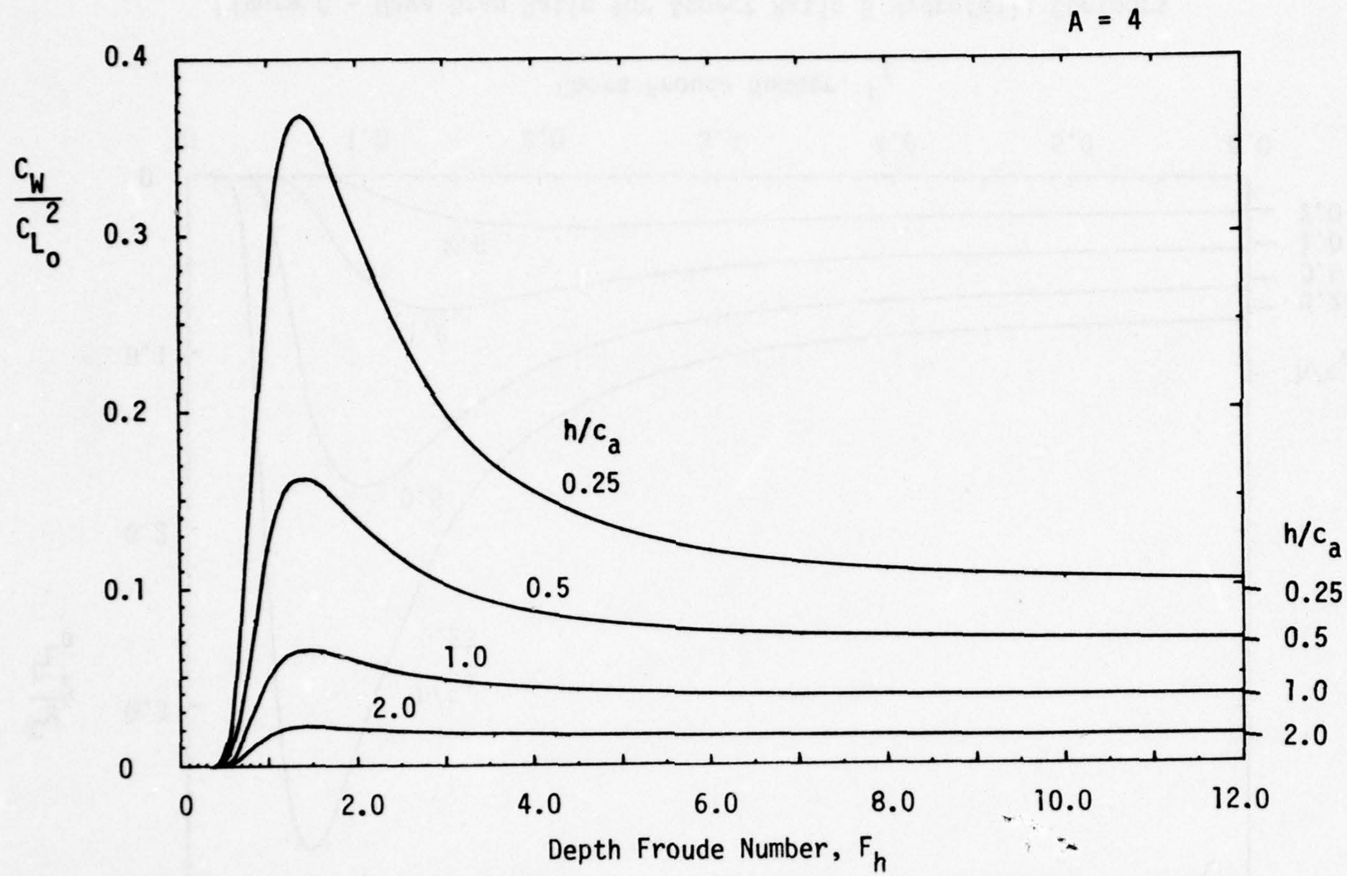

Figure 5 - Wave Drag Ratio Versus Depth Froude Number for Aspect Ratio 4 Hydrofoil

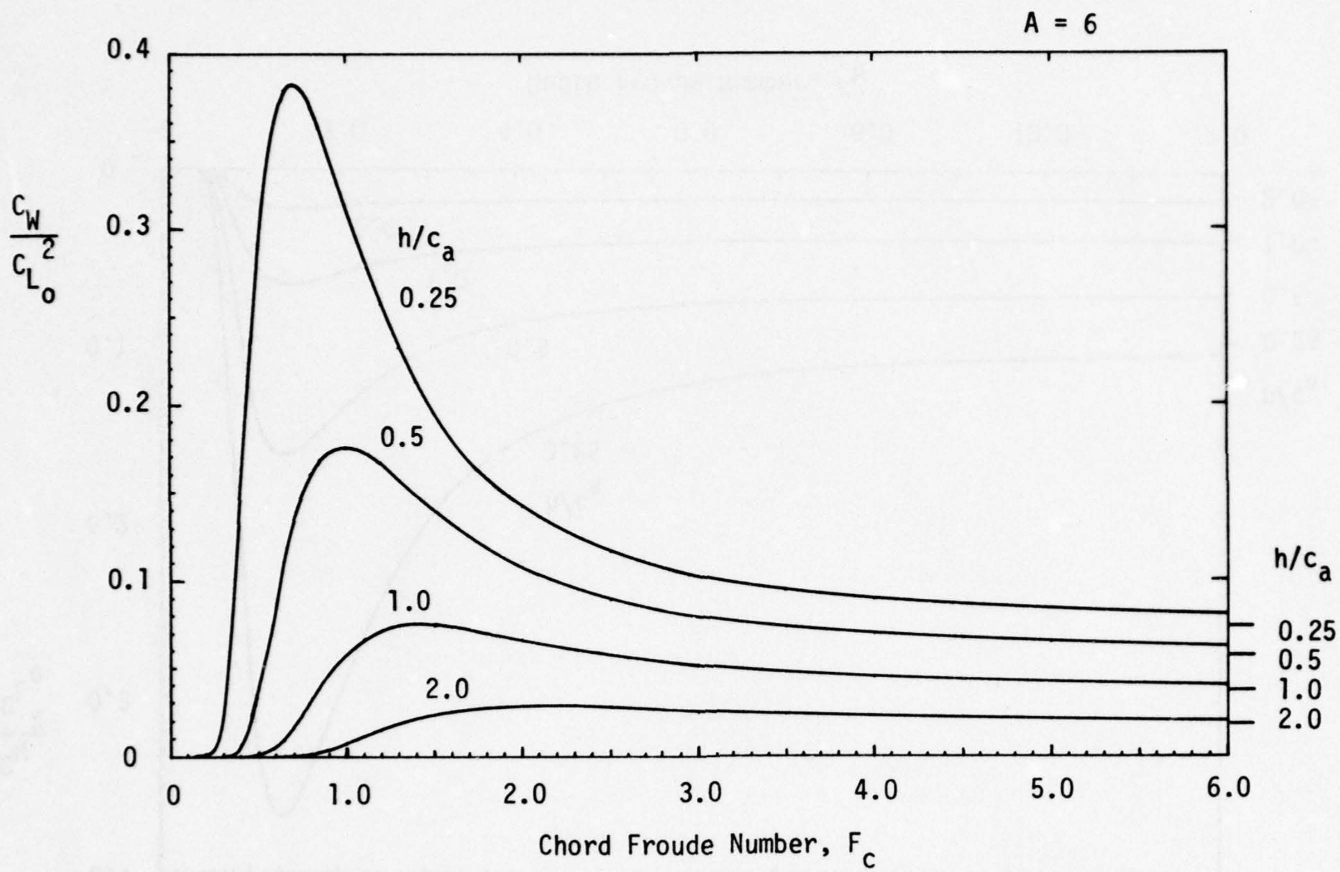

Figure 6 - Wave Drag Ratio for Aspect Ratio 6 Hydrofoil; Contours of Submergence

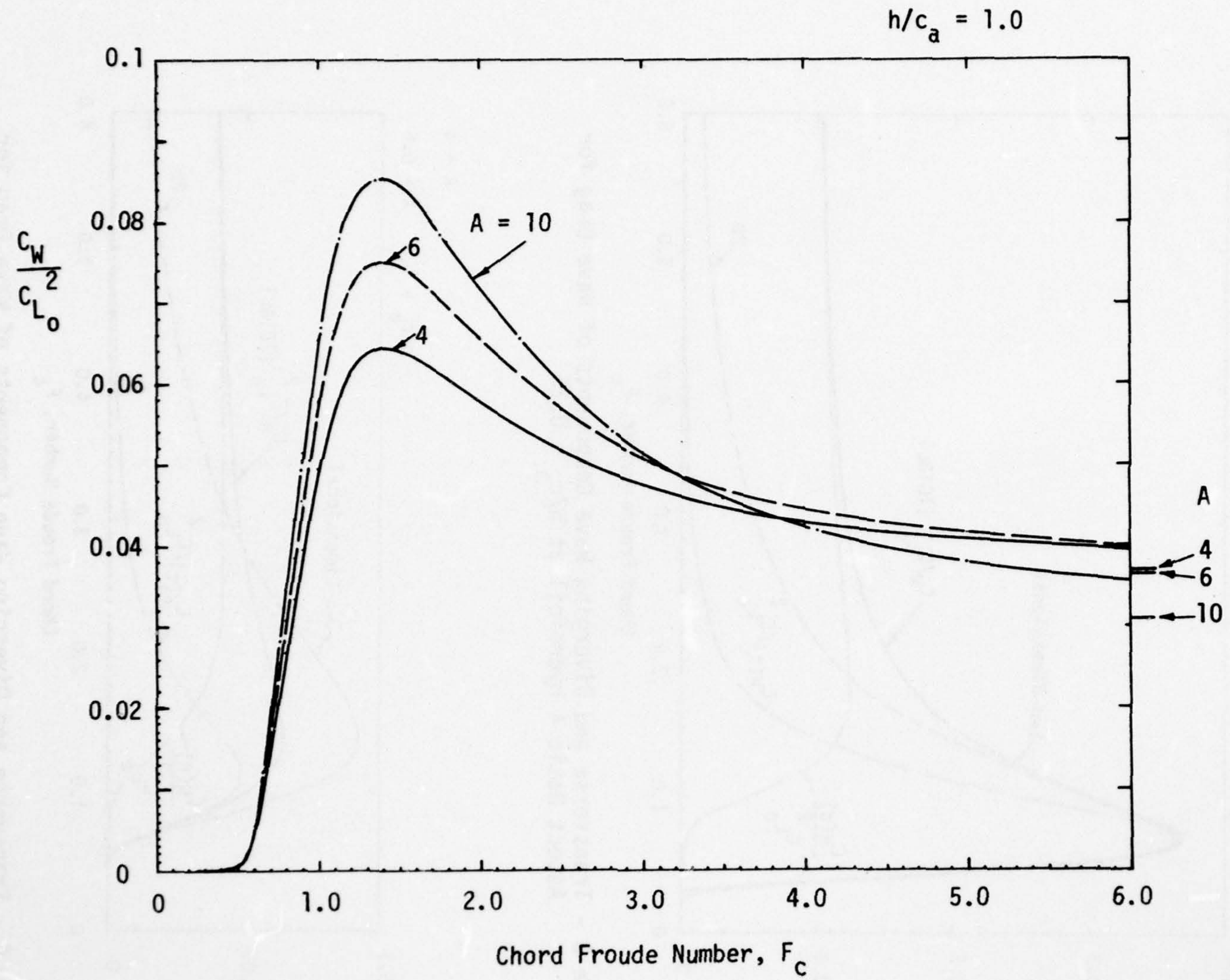

Figure 7 - Wave Drag Ratio for Aspect Ratios 4, 6, and 10 at Submergence $h/c_a = 1.0$

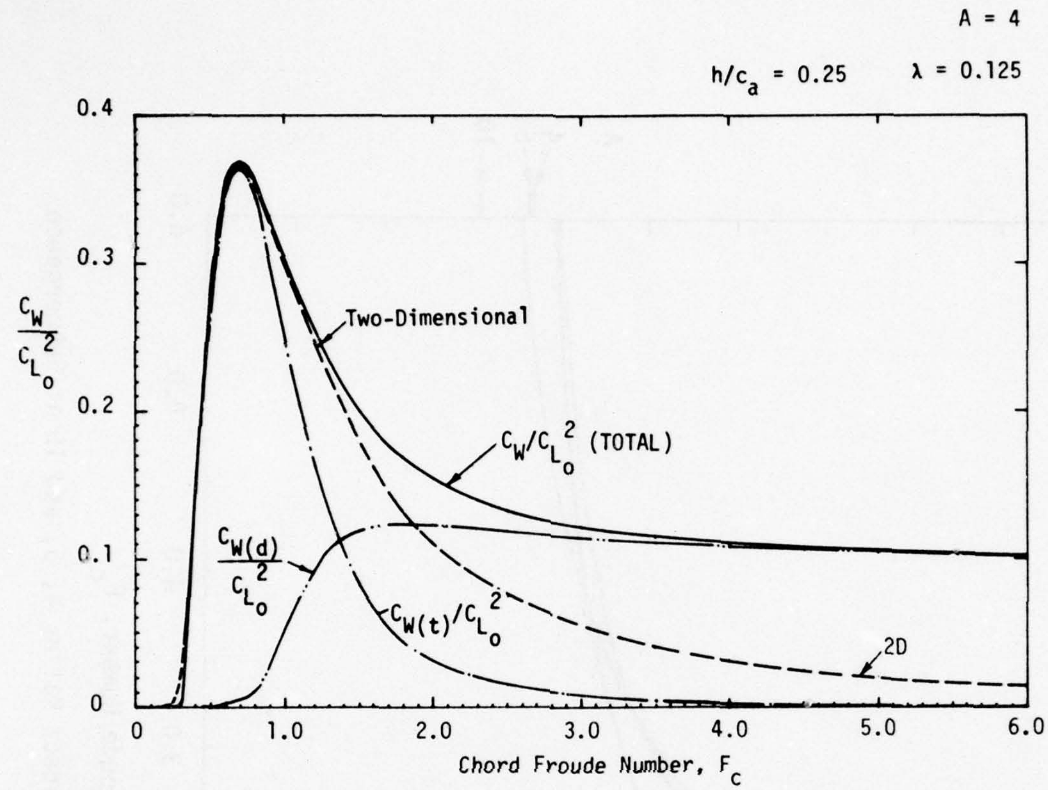

Figure 8 - Transverse and Diverging Wave Components of Wave Drag for Aspect Ratio 4 Hydrofoil at $h/c_a = 0.25$

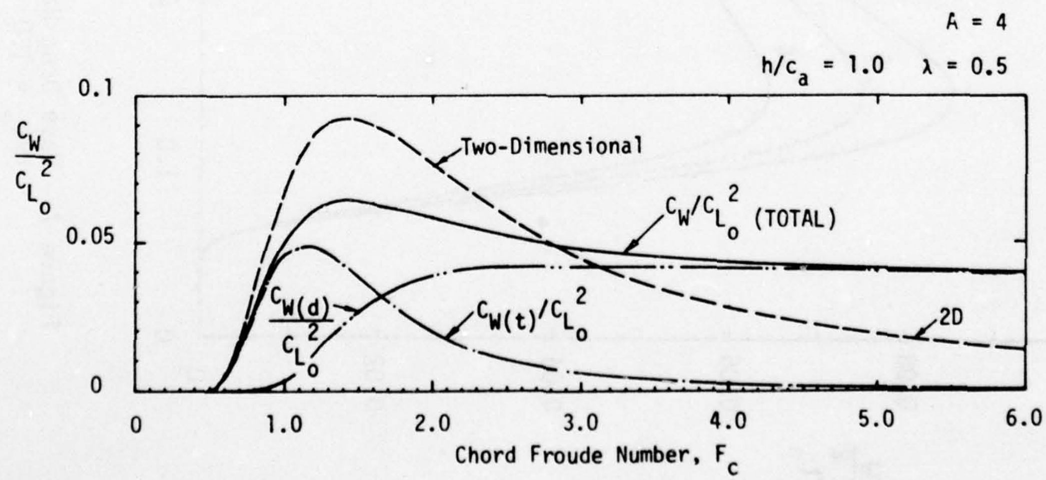

Figure 9 - Transverse and Diverging Wave Components of Wave Drag for Aspect Ratio 4 Hydrofoil at $h/c_a = 1.0$

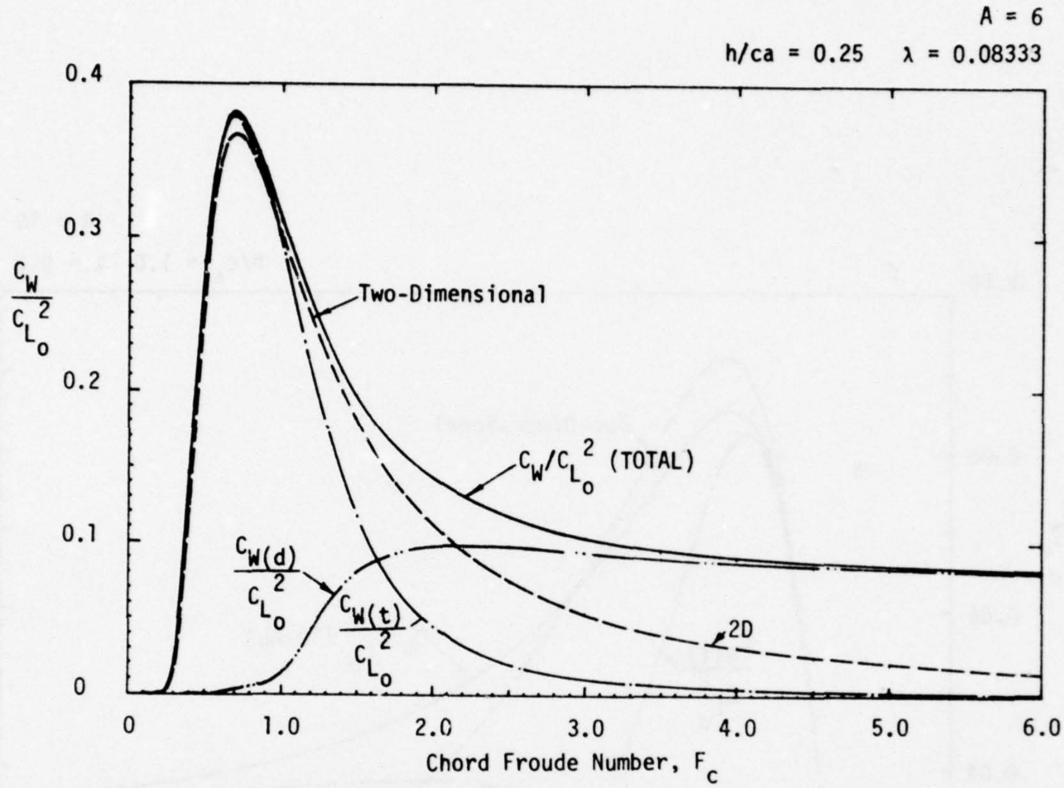

Figure 10 - Transverse and Diverging Wave Components of Wave Drag for Aspect Ratio 6 Hydrofoil at h/c_a = 0.25

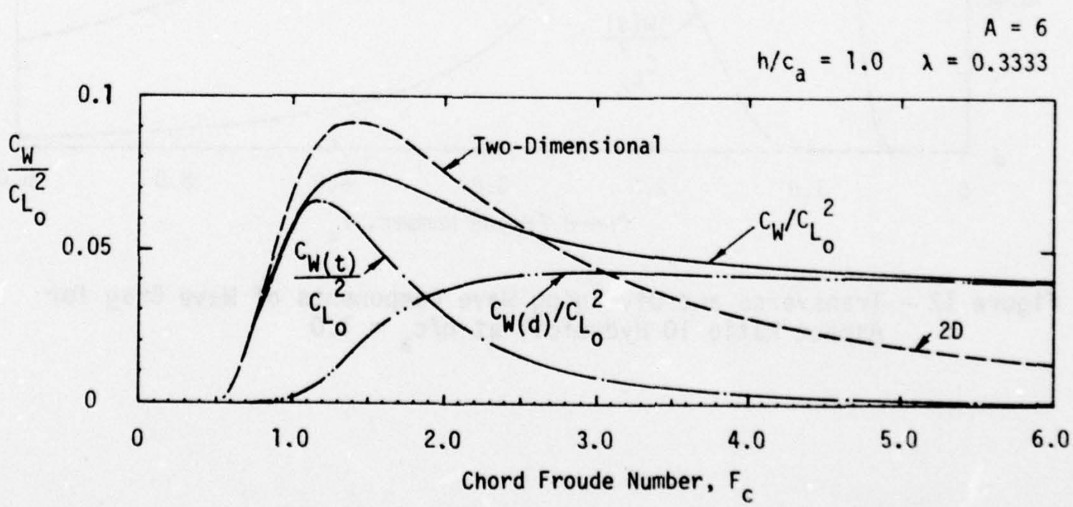

Figure 11 - Transverse and Diverging Wave Components of Wave Drag for Aspect Ratio 6 Hydrofoil at h/c_a = 1.0

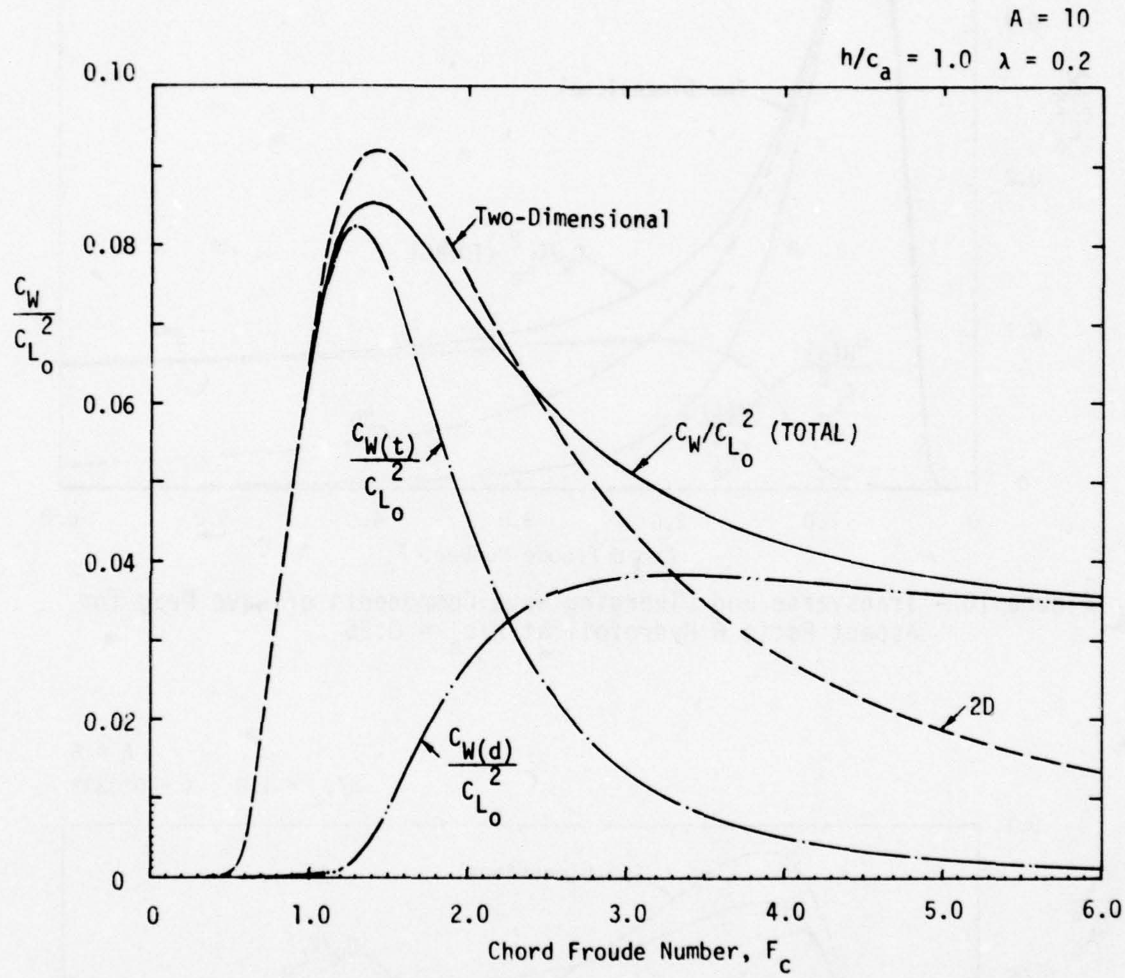

Figure 12 - Transverse and Diverging Wave Components of Wave Drag for Aspect Ratio 10 Hydrofoil at $h/c_a = 1.0$

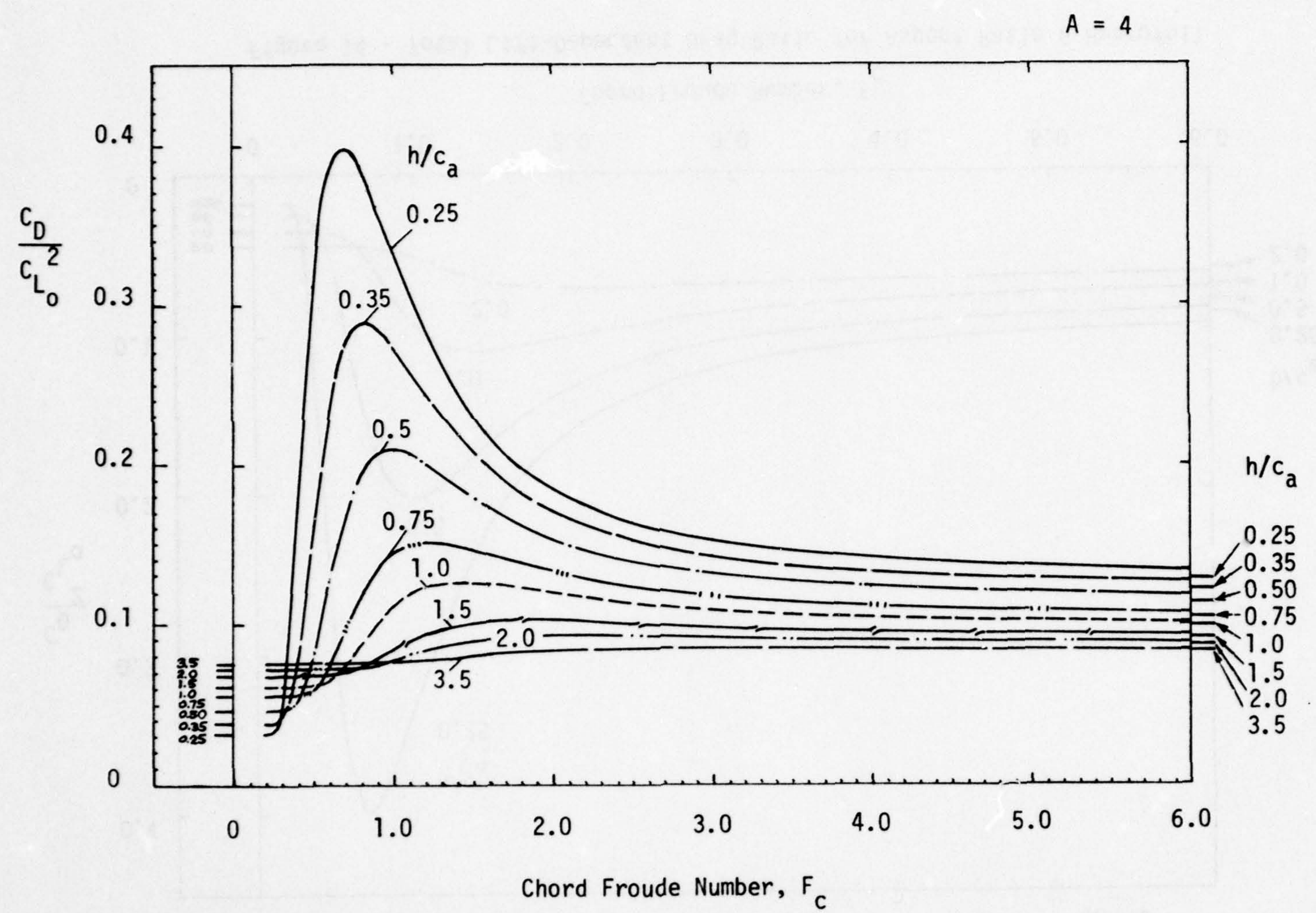

Figure 13 - Total Lift-Dependent Drag Ratio for Aspect Ratio 4 Hydrofoil

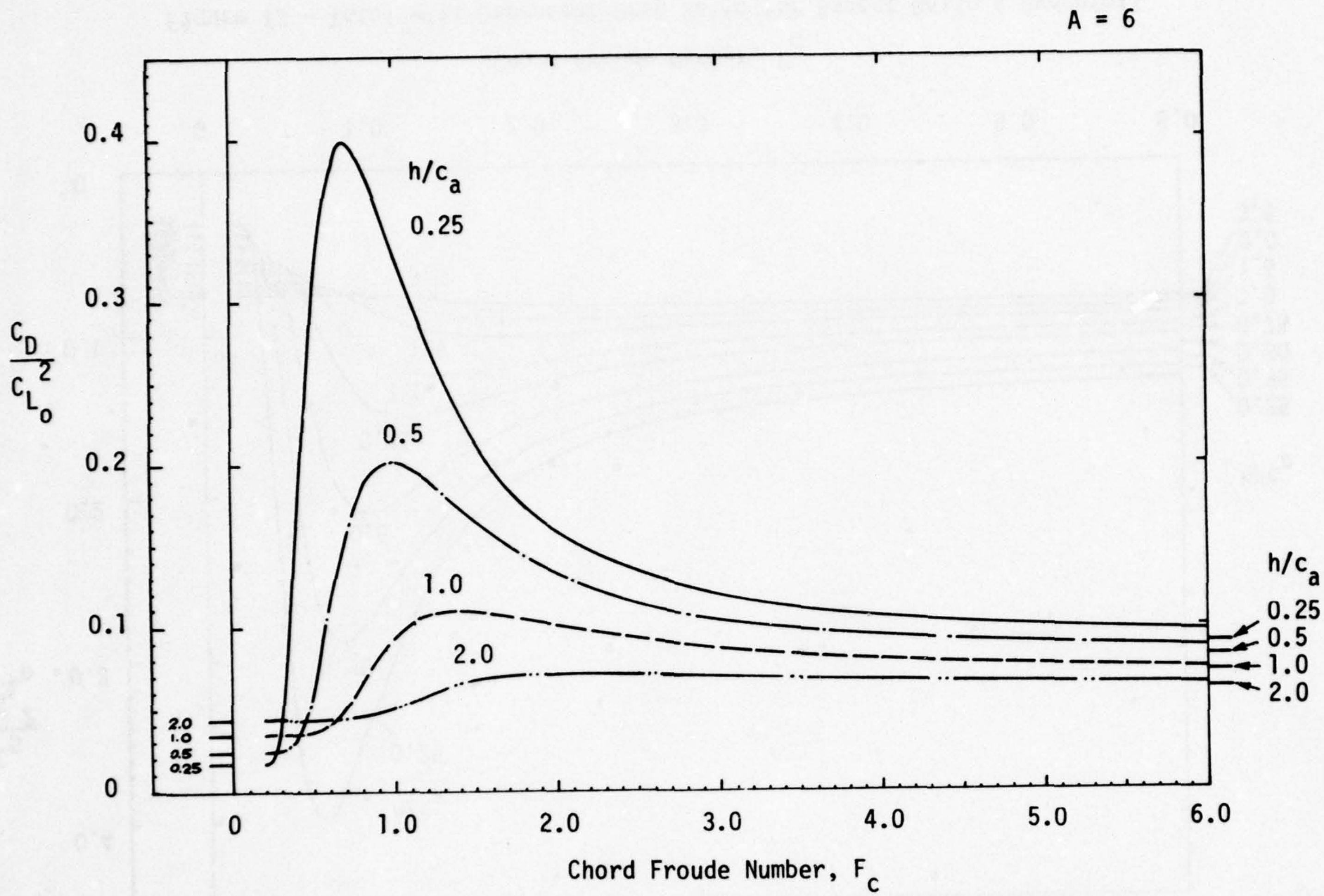

Figure 14 - Total Lift-Dependent Drag Ratio for Aspect Ratio 6 Hydrofoil

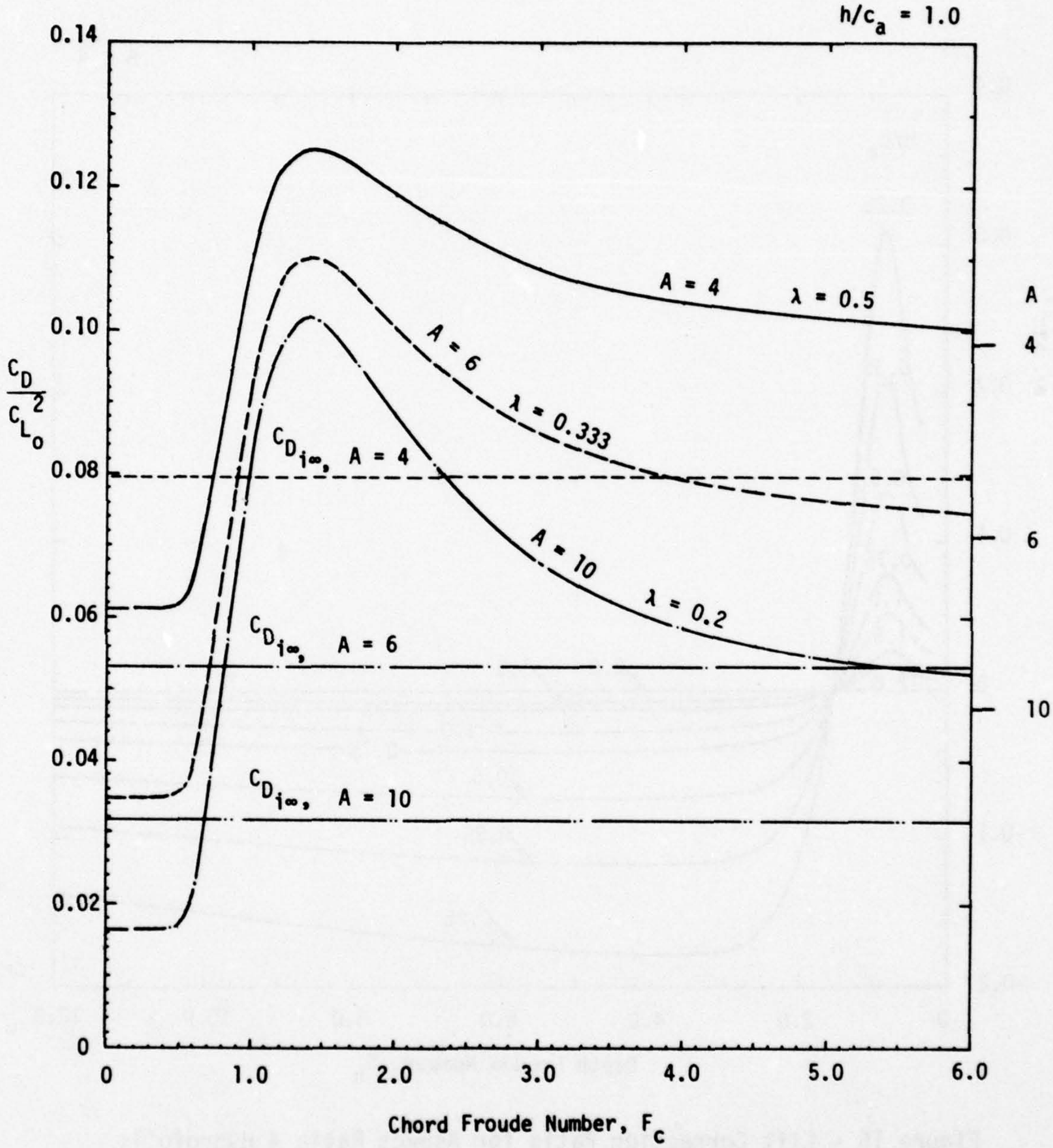

Figure 15 - Total Lift-Dependent Drag Ratio for Aspect Ratios 4, 6, and 10 at Submergence $h/c_a = 1.0$

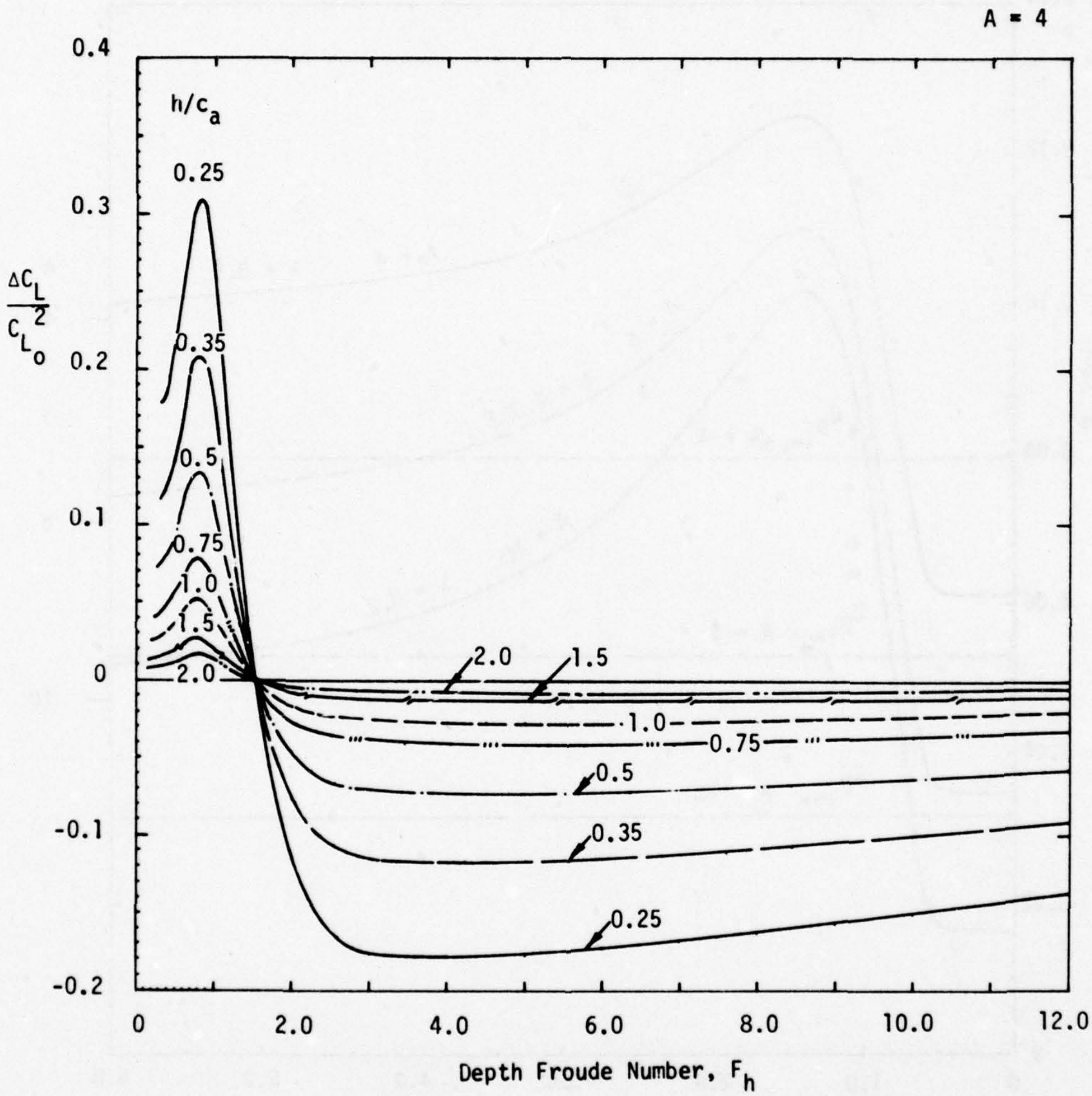

Figure 16 - Lift Correction Ratio for Aspect Ratio 4 Hydrofoil; Contours of Submergence

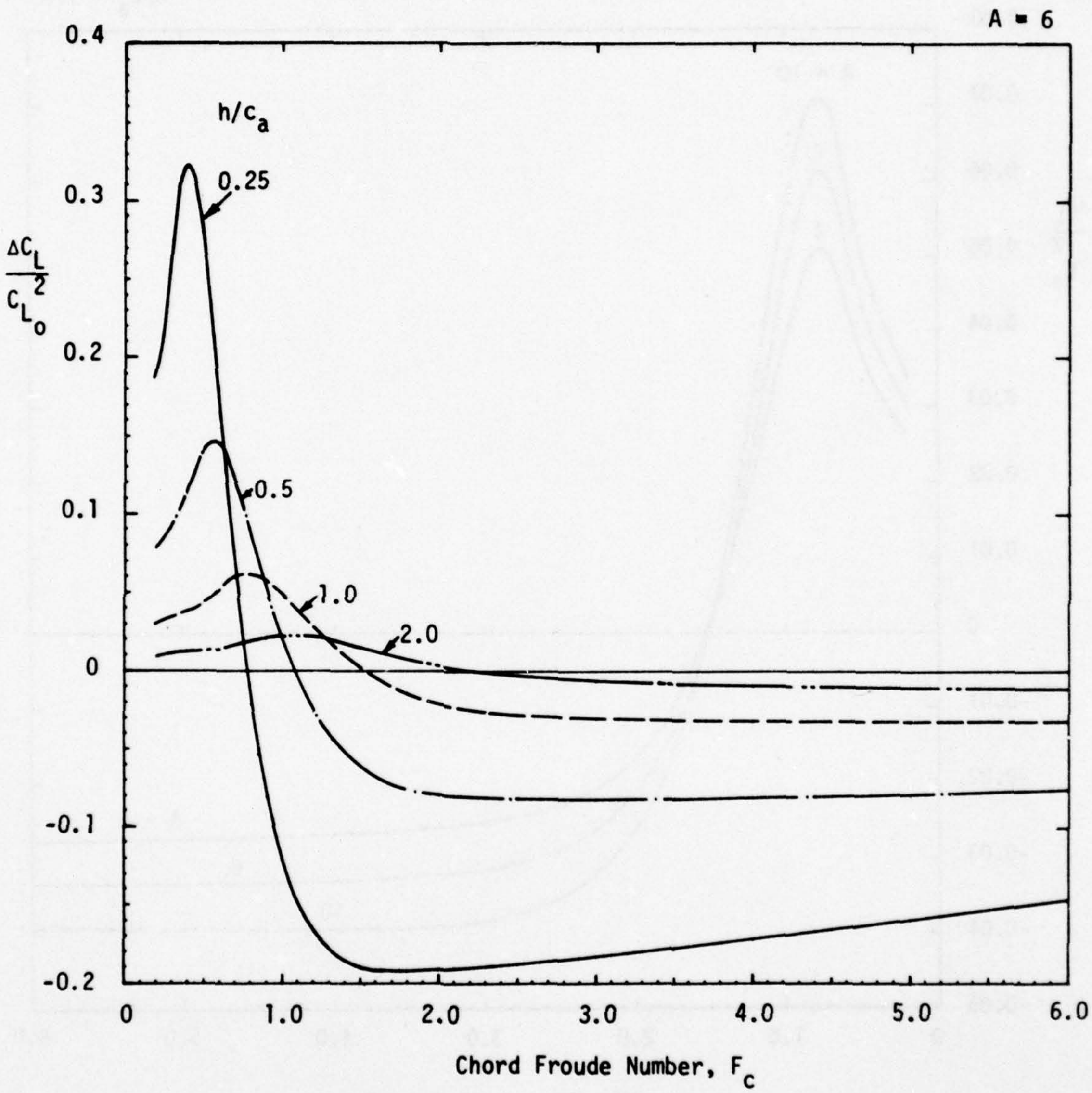

Figure 17 - Lift Correction Ratio for Aspect Ratio 6 Hydrofoil; Contours of Submergence

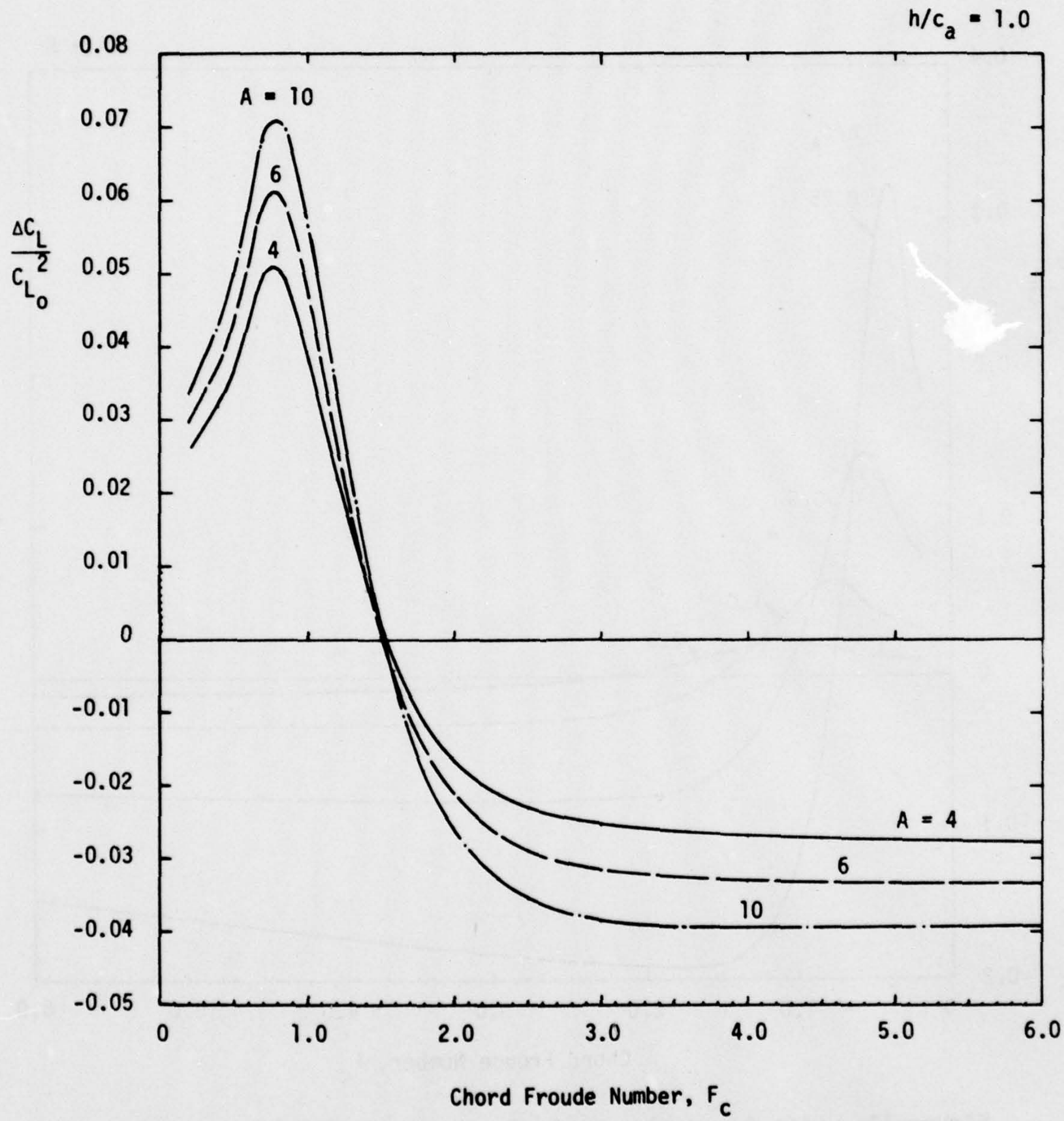

Figure 18 - Lift Correction Ratio for Aspect Ratios 4, 6, and 10 at Submergence $h/c_a = 1.0$

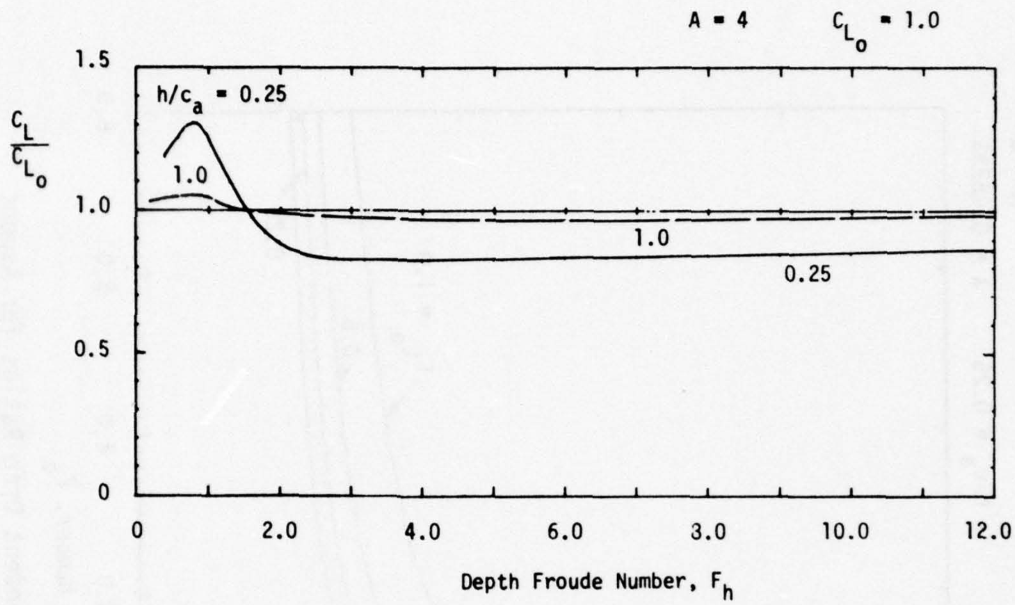

Figure 19 - Total Lift Ratio for Aspect Ratio 4 at C_{L_o} = 1.0

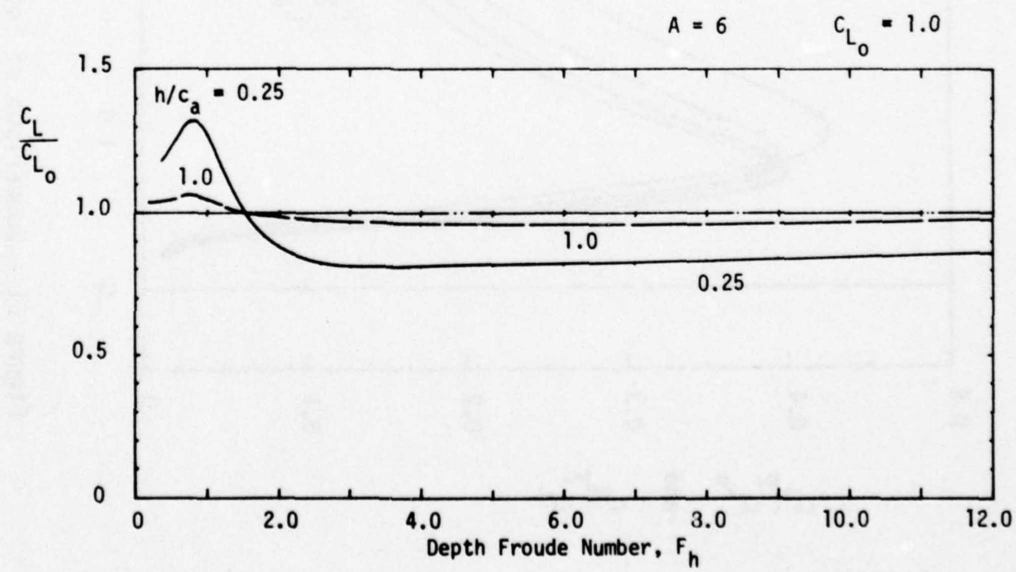

Figure 20 - Total Lift Ratio for Aspect Ratio 6 at C_{L_o} = 1.0

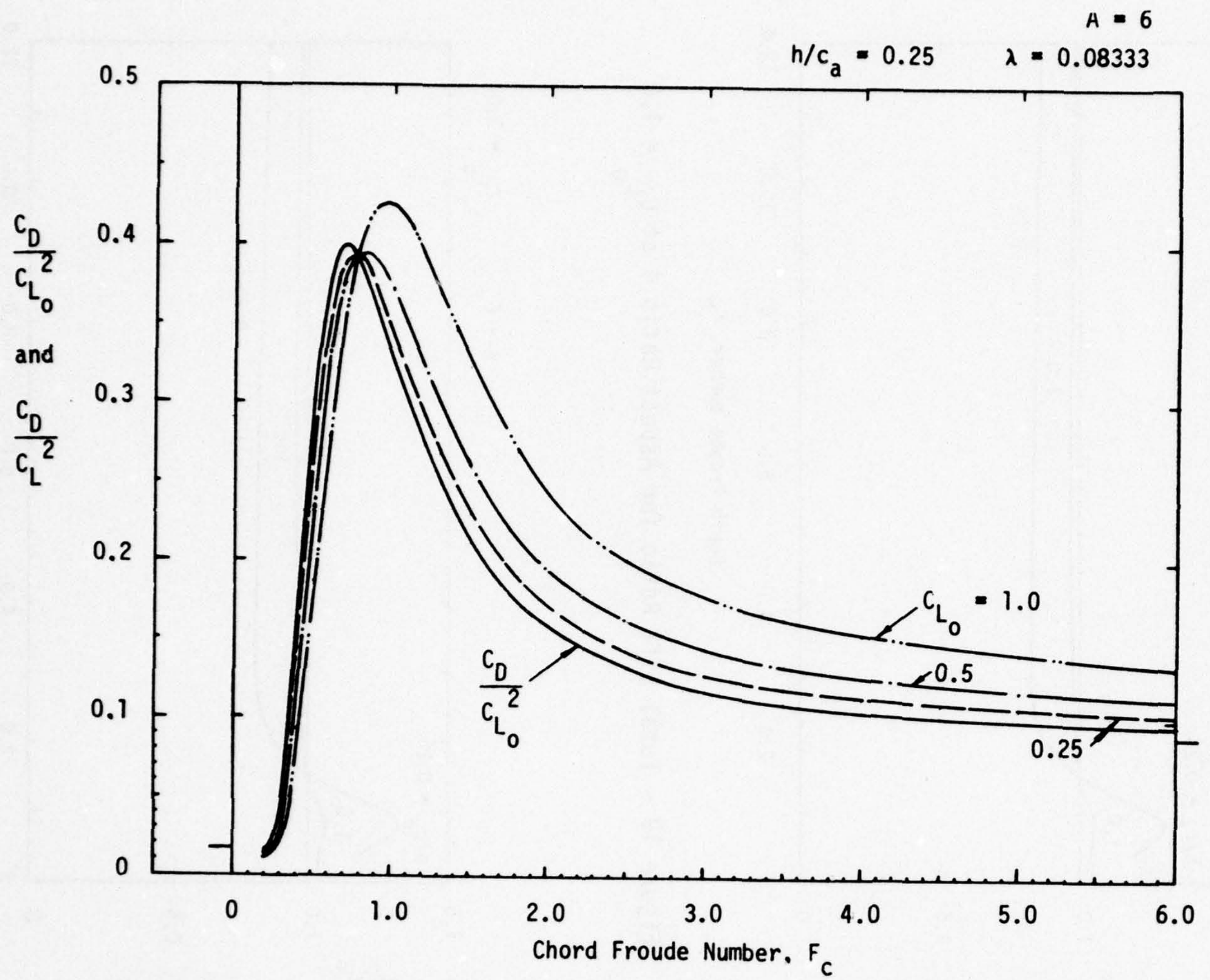

Figure 21 - Comparison of Total Lift-Dependent Drag Ratios for Aspect Ratio 6; Contours of Constant C_{L_o}

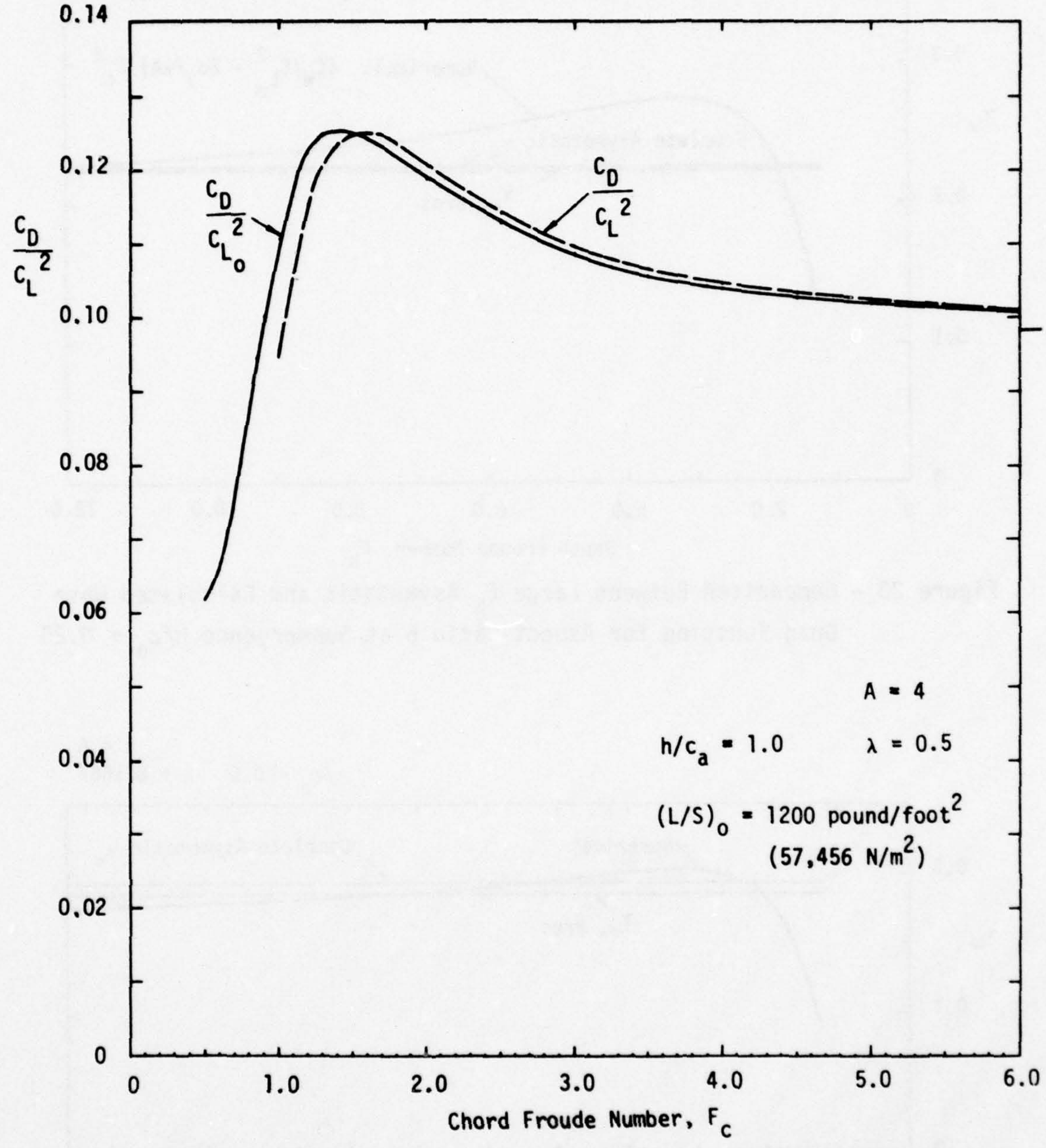

Figure 22 - Comparison of Total Lift-Dependent Drag Ratios for Aspect Ratio 4; Constant Reference Foil Loading

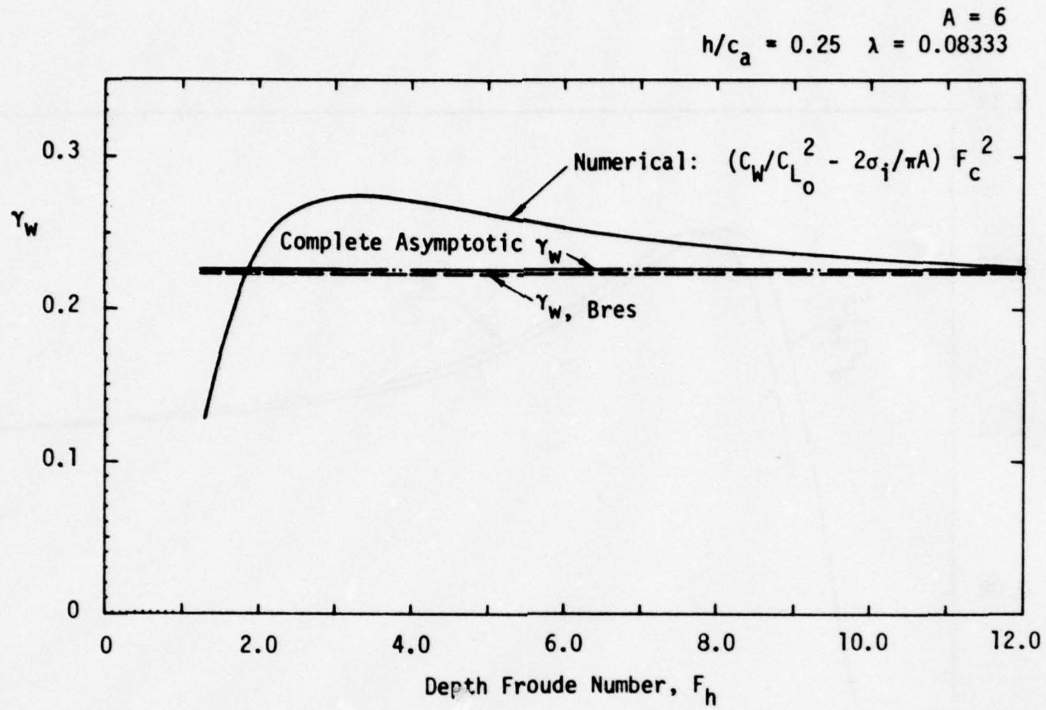

Figure 23 - Comparison Between Large F_h Asymptotic and Calculated Wave Drag Function for Aspect Ratio 6 at Submergence $h/c_a = 0.25$

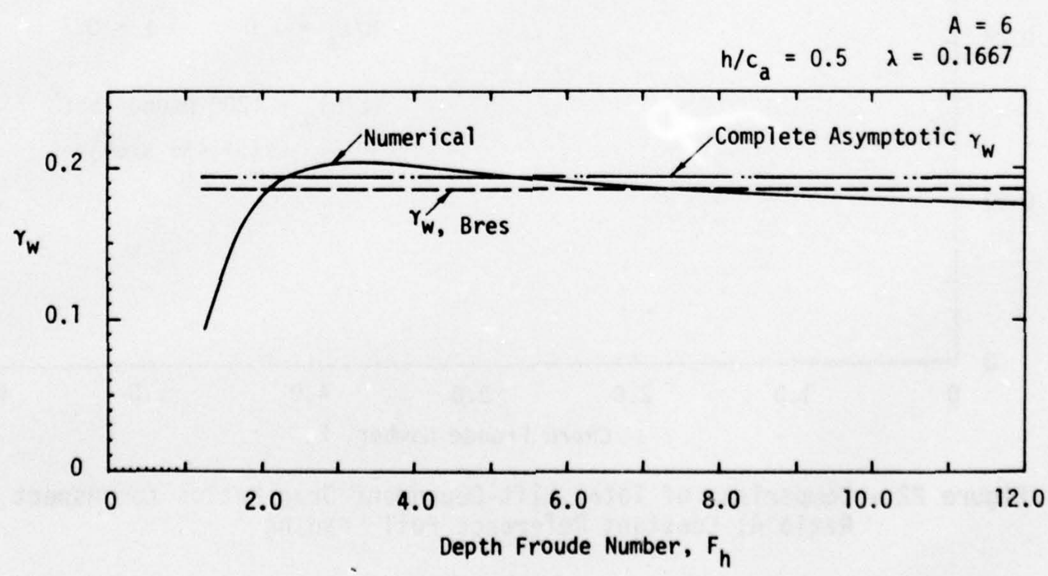

Figure 24 - Comparison Between Large F_h Asymptotic and Calculated Wave Drag Function for Aspect Ratio 6 at Submergence $h/c_a = 0.5$

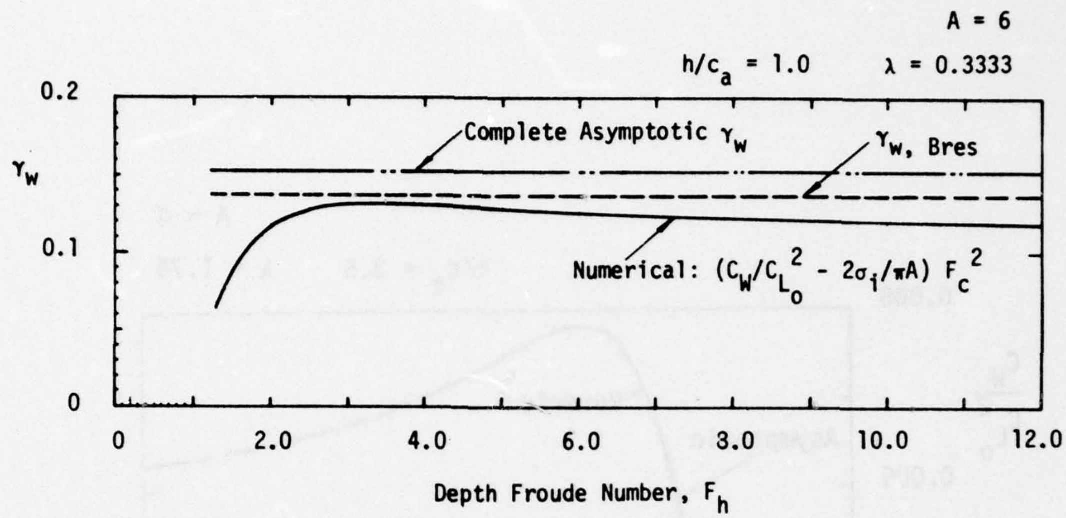

Figure 25 - Comparison Between Large F_h Asymptotic and Calculated Wave Drag Function for Aspect Ratio 6 at Submergence h/c_a = 1.0

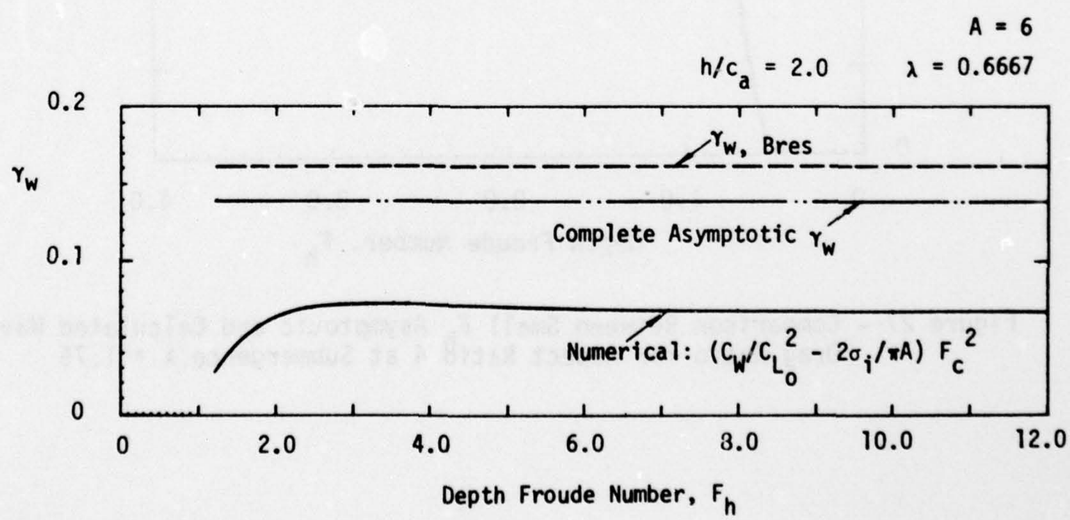

Figure 26 - Comparison Between Large F_h Asymptotic and Calculated Wave Drag Function for Aspect Ratio 6 at Submergence h/c_a = 2.0

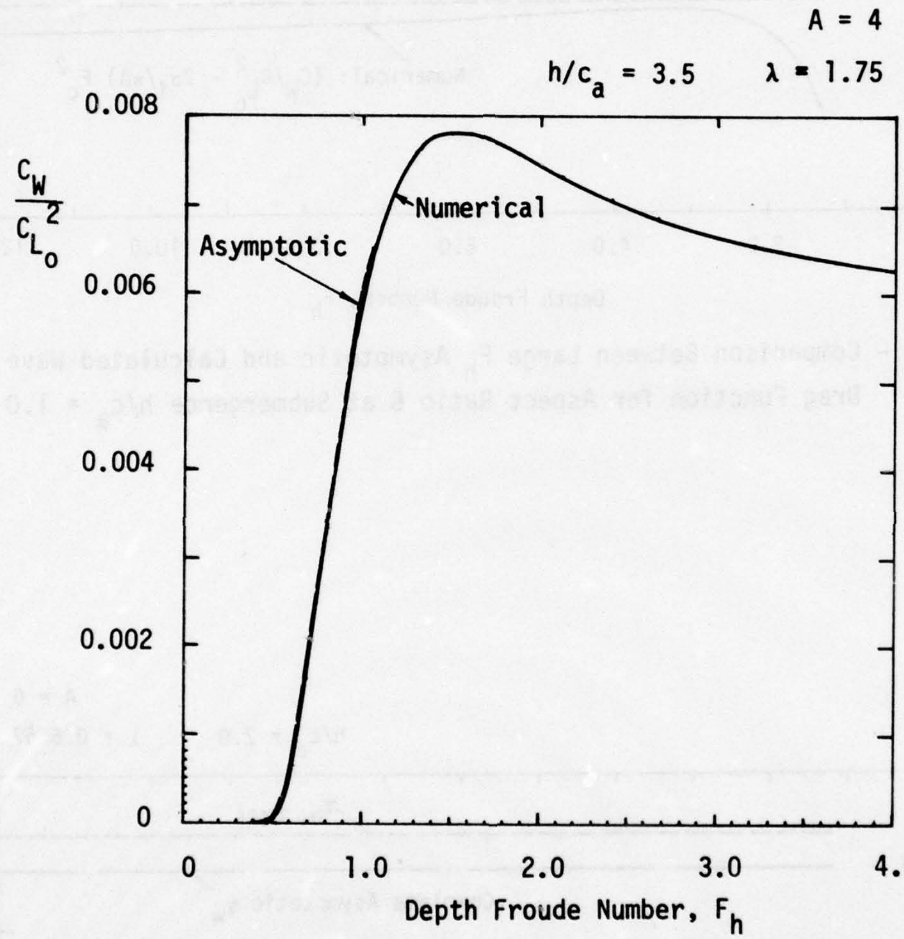

Figure 27 - Comparison Between Small F_h Asymptotic and Calculated Wave Drag Ratio for Aspect Ratio 4 at Submergence λ = 1.75

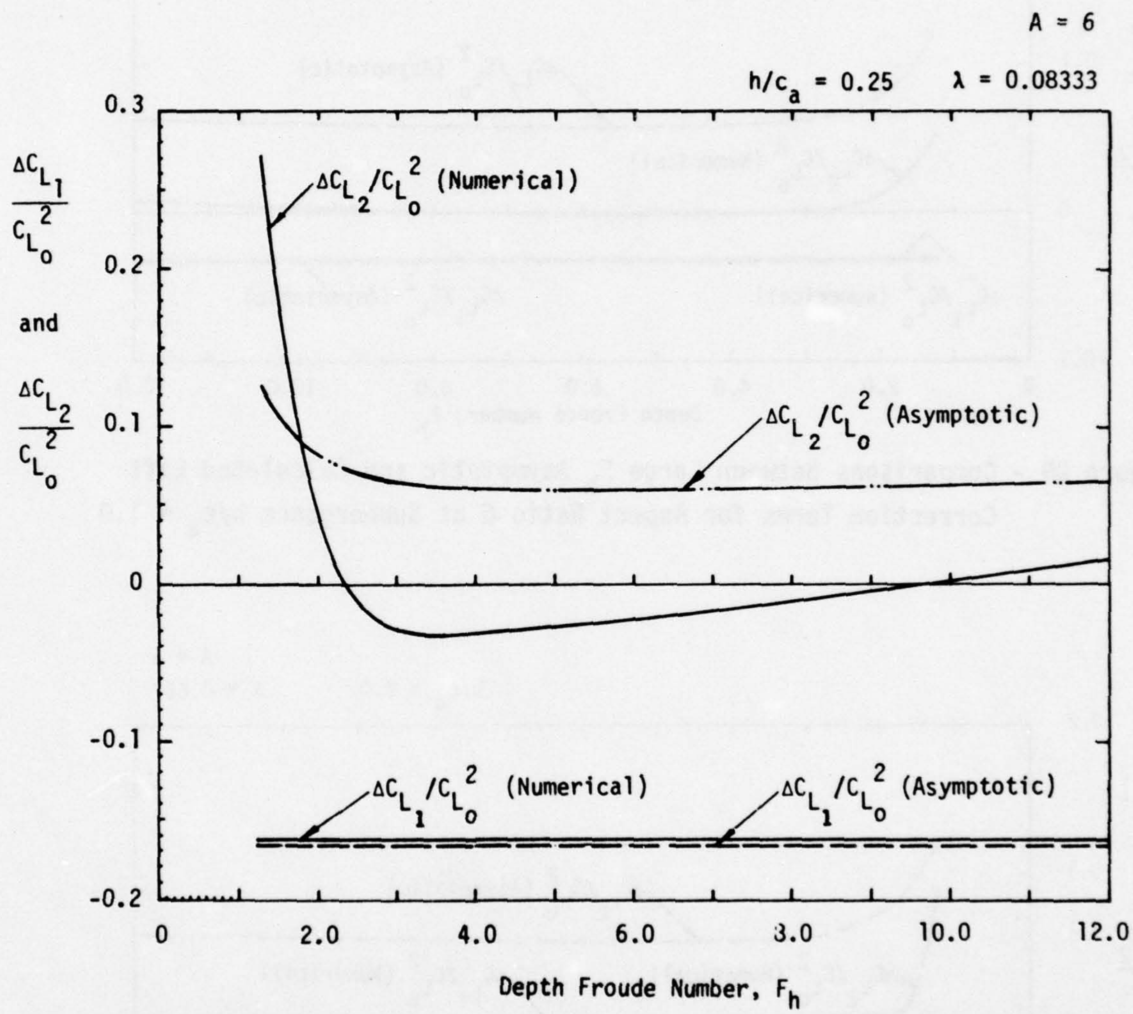

Figure 28 - Comparisons Between Large F_h Asymptotic and Calculated Lift Correction Terms for Aspect Ratio 6 at Submergence $h/c_a = 0.25$

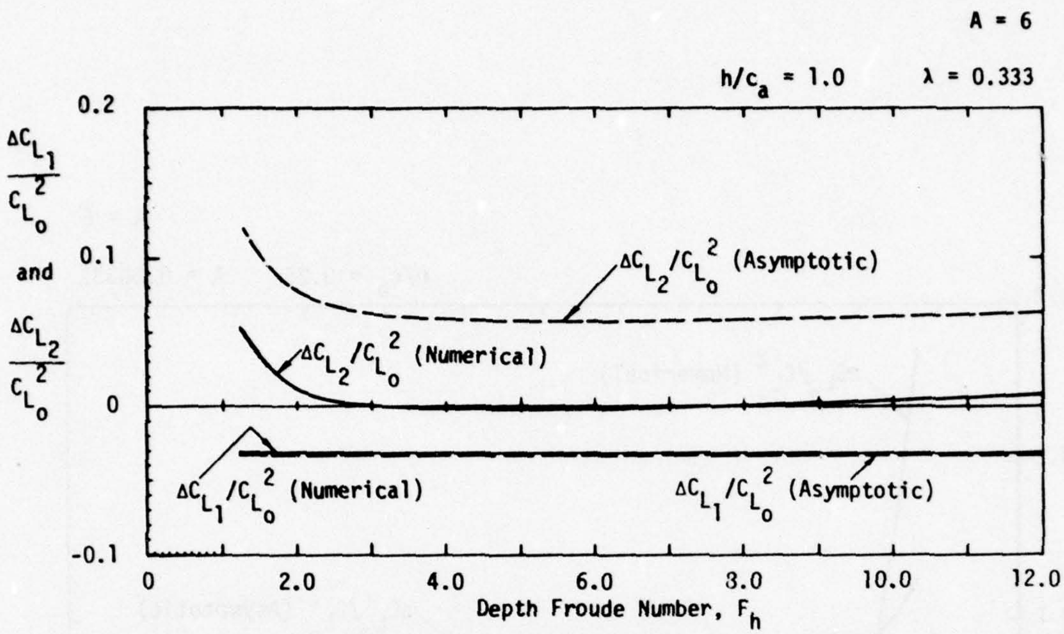

Figure 29 - Comparisons Between Large F_h Asymptotic and Calculated Lift Correction Terms for Aspect Ratio 6 at Submergence $h/c_a = 1.0$

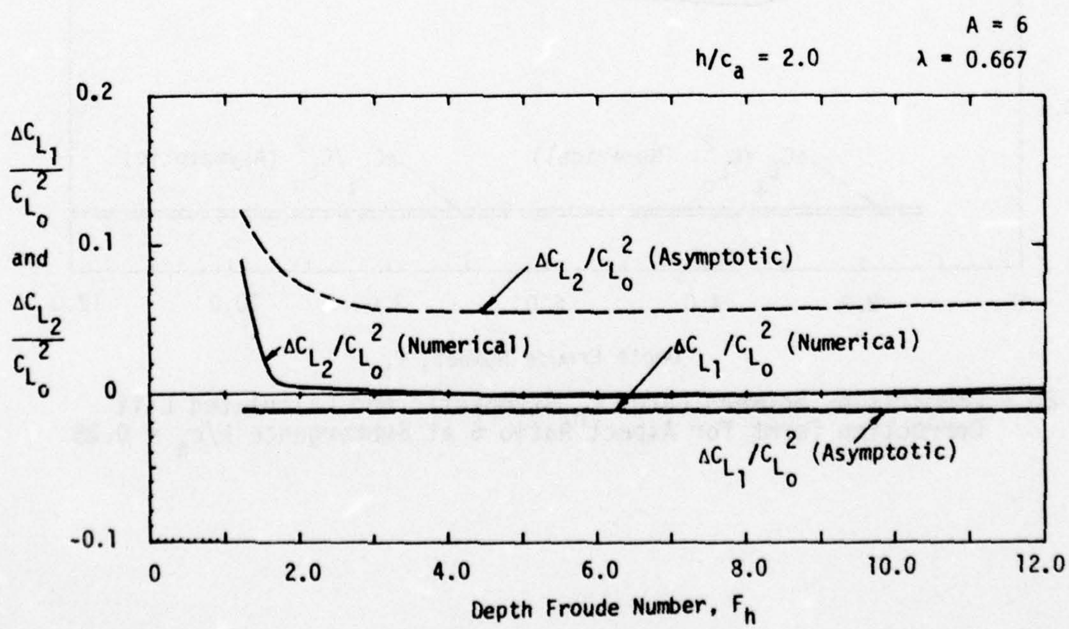

Figure 30 - Comparisons Between Large F_h Asymptotic and Calculated Lift Correction Terms for Aspect Ratio 6 at Submergence $h/c_a = 2.0$

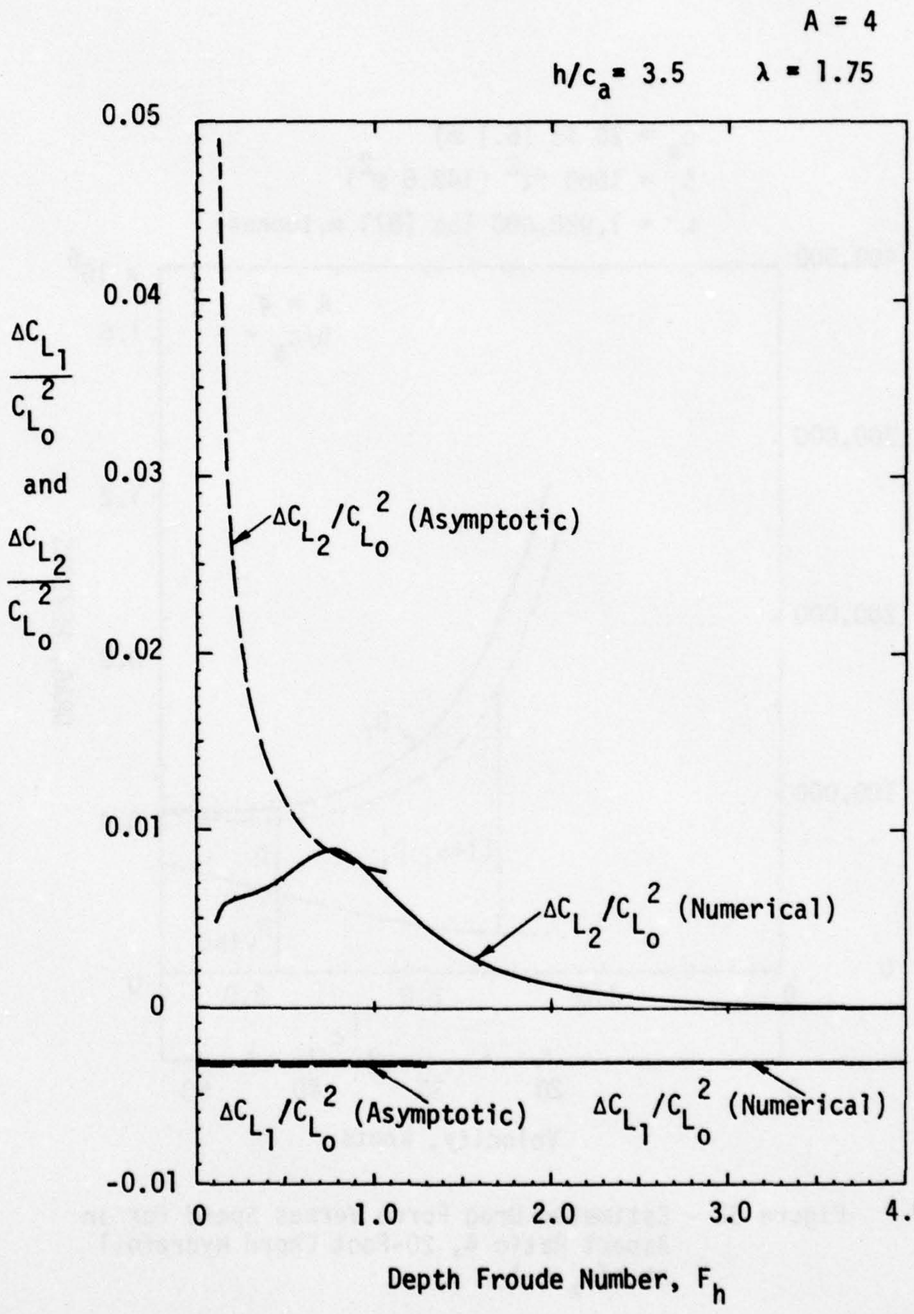

Figure 31 - Comparisons Between Small F_h Asymptotic and Calculated Lift Correction Terms for Aspect Ratio 4 at Submergence $\lambda = 1.75$

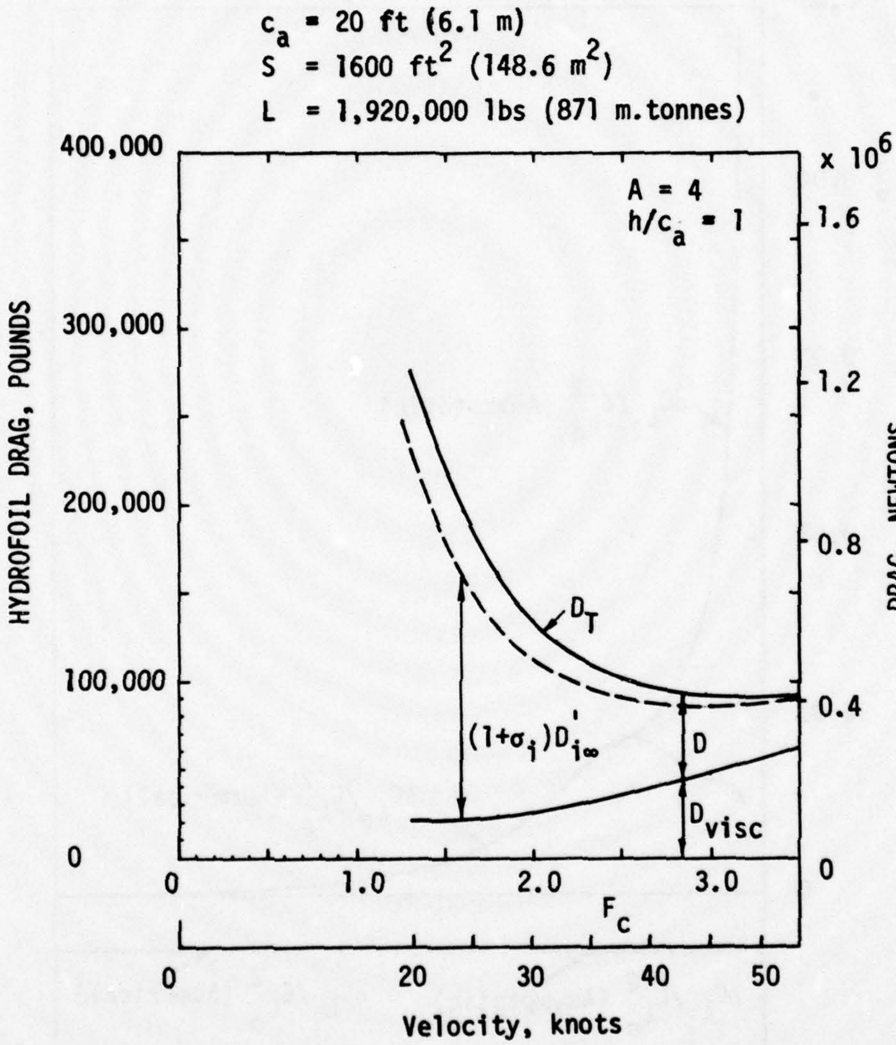

Figure 32 - Estimated Drag Force Versus Speed for an Aspect Ratio 4, 20-Foot Chord Hydrofoil at h/c_a = 1

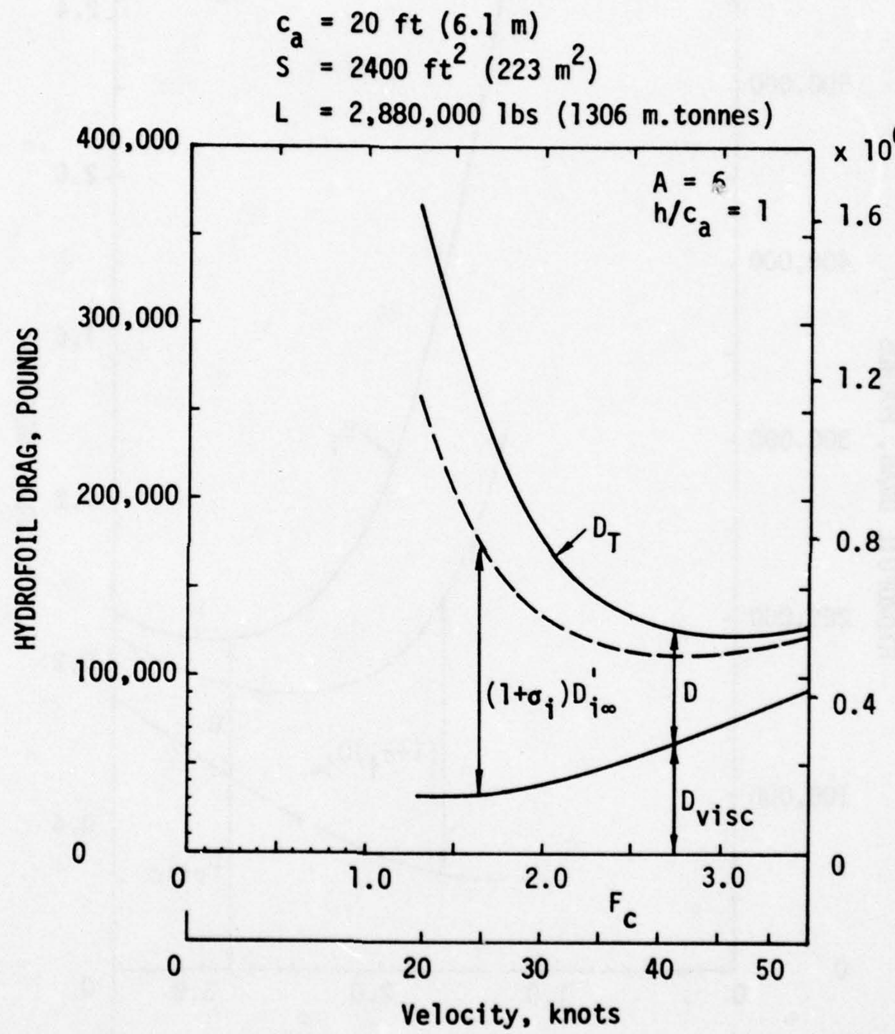

Figure 33 - Estimated Drag Force Versus Speed for an Aspect Ratio 6, 20-Foot Chord Hydrofoil at h/c_a = 1

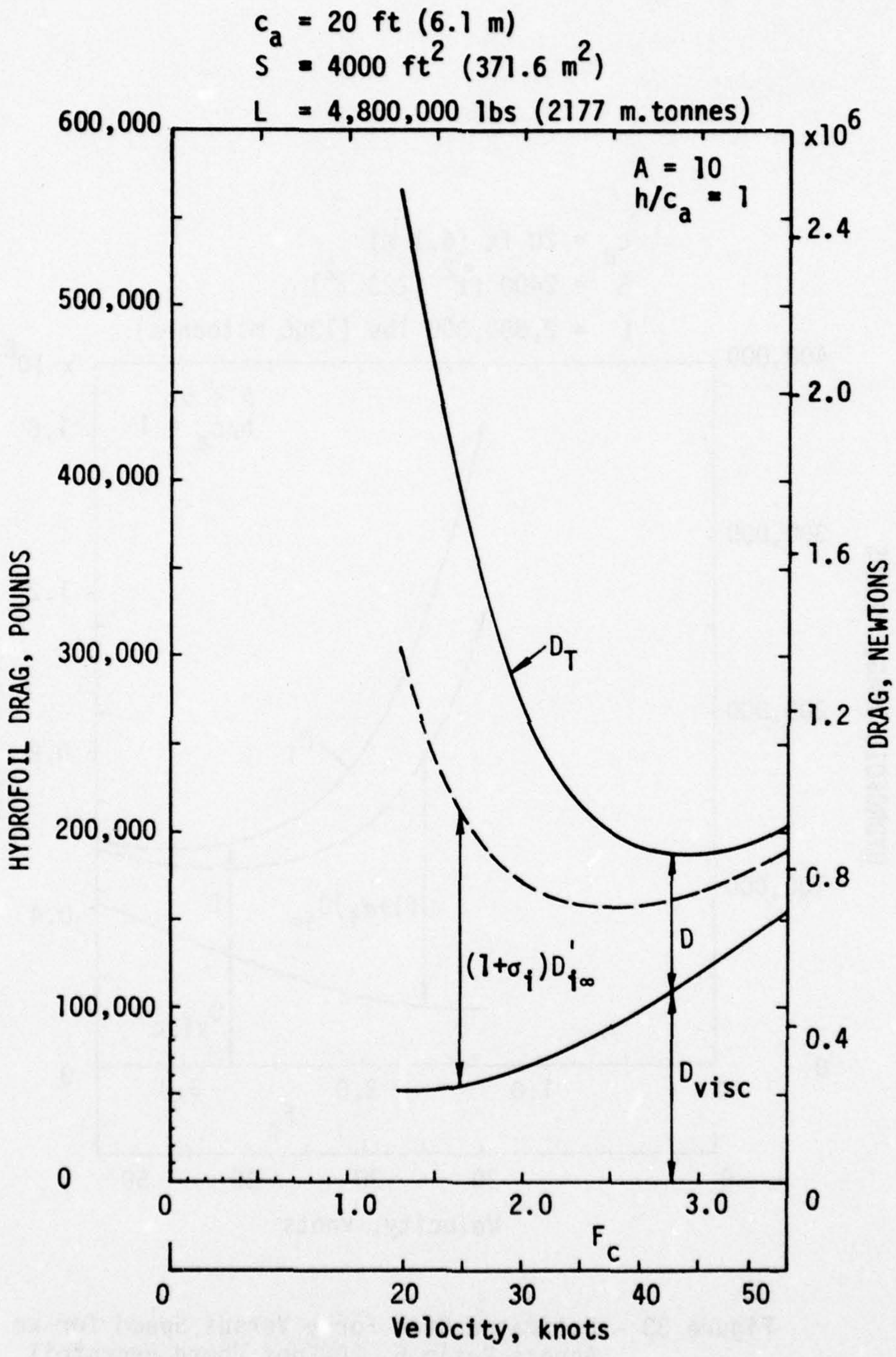

Figure 34 - Estimated Drag Force Versus Speed for an Aspect Ratio 10, 20 Foot Chord Hydrofoil at h/c_a = 1

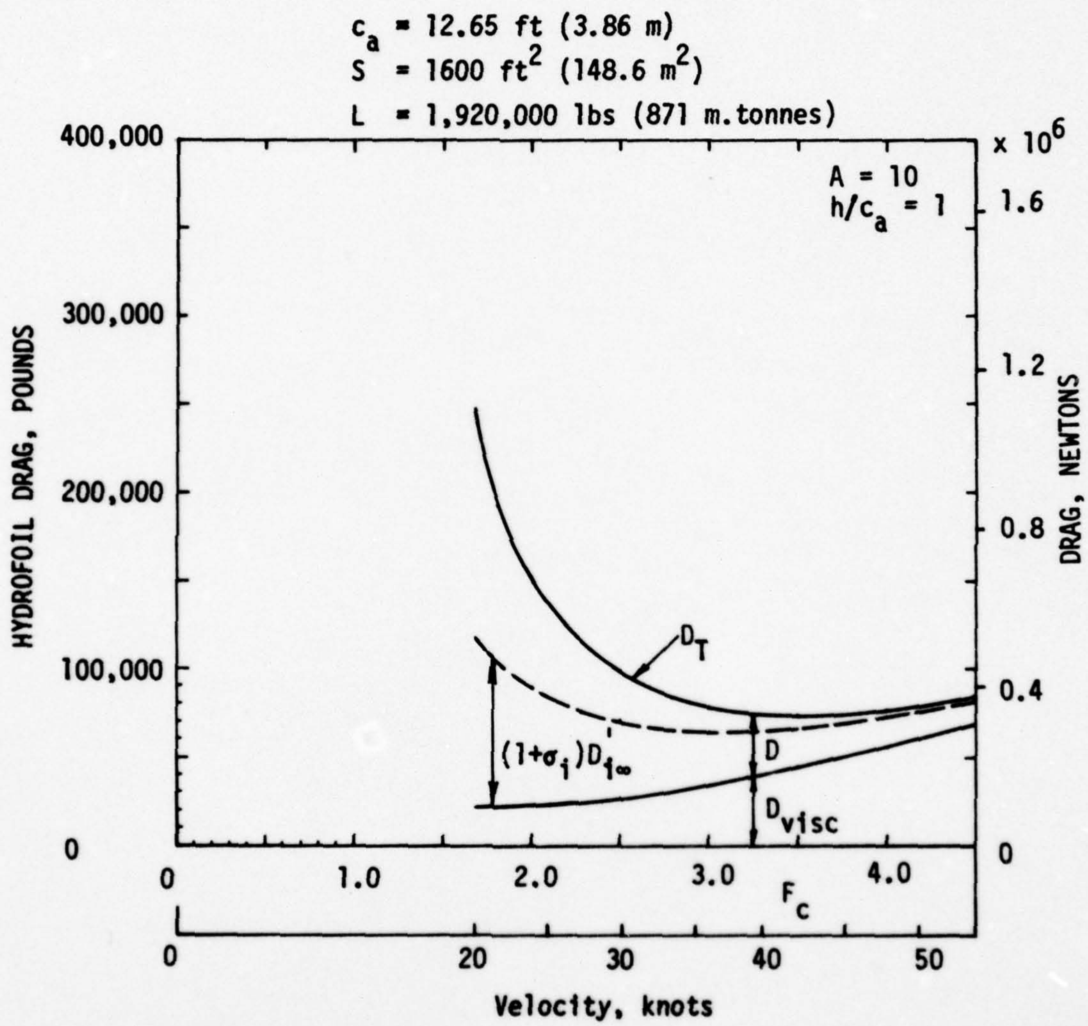

Figure 35 - Estimated Drag Force Versus Speed for an Aspect Ratio 10, 12.65-Foot Chord Hydrofoil at $h/c_a = 1$

APPENDIX A

LISTING OF COMPUTER PROGRAM

The computer program used to generate all the numerical data of the report is listed here for reference. Definitions of the input variables and the main output quantities are given in Tables 2 and 3.

TABLE 2

COMPUTER PROGRAM INPUT VARIABLES

Computer Notation	Symbol and/or Meaning
A	A = planform aspect ratio
HOCA	h/c_a = depth-to-chord ratio
TWMAX	Maximum allowable t-value in the C_W-integration (typically 70 to 100)
TLMAX	Maximum allowable t-value in the integration of $F_L(u)$ (typically 70-100)
EPS	Accuracy limit for integration of C_W and $F_L(u)$ (typically 0.000001)
NSPW	Number of spaces for numerical integration of loops in C_W and for ΔC_{L_1} (typically 100)
NSPL	Number of spaces for numerical integration of non-singular integrals of ΔC_{L_2} (typically 60)
NINDEX	Counting index for modified Simpsons Rule for Cauchy singular integral (typically 30)
NDATA	Number of input data cases of Froude number
FC	F_c = chord Froude number
CLO	C_{L_o} = reference lift coefficient

TABLE 3

MAIN COMPUTER PROGRAM OUTPUT VARIABLES

Computer Notation	Symbol and/or Meaning
CDIIR	$C_{D_{i\infty}}/C_{L_o}^2$
CDSIR	$C_{D_{si}}/C_{L_o}^2$
CDSWR	$C_{D_{sw}}/C_{L_o}^2$
CL1R	$\Delta C_{L_1}/C_{L_o}^2$
CL2R	$\Delta C_{L_2}/C_{L_o}^2$
CLRO	$C_L/C_{L_o} = (1 + \Delta_{LC} \cdot C_{L_o})$
CWR	$C_W/C_{L_o}^2$
CWR(T)	$C_{W_{(t)}}/C_{L_o}^2$
CWR(D)	$C_{W_{(d)}}/C_{L_o}^2$
DELW	$\Delta_{LC} = \Delta C_L/C_{L_o}^2$
DELCL	$\Delta C_L = C_{L_o}^2 \cdot \Delta_{LC}$
NLOOPS	Number of loops of integrand required to reach desired accuracy
SIGMAI	σ_i

TABLE 3 (Continued)

TE	End value of t-integration for C_W
WS	γ_W = Auxillary function for wave drag (see Equation (49))

```
C
C           CENTRAL PROGRAM TO COMPUTE HYDRODYNAMIC CHARACTERISTICS
C           OF DRAG AND LIFT FOR A SUBMERGED FLAT HYDROFOIL HAVING AN
C           ELLIPTICAL PLANFORM WITH SPECIFIED ELLIPTIC CIRCULATION
C           DISTRIBUTION.USING THE  1953  LIFTING LINE RESULTS OF
C           T.Y. WU.  COMPLETELY NUMERICAL EVALUATION OF INTEGRALS AT
C           ARBITRARY DEPTH AND FROUDE NUMBER
C
      PROGRAM SUBMFL(INPUT,OUTPUT,TAPE5=INPUT,TAPE6=OUTPUT)
      REAL LAMDA,JW,JWT,JWD,JL1,JL2,KE,LAMDA2
      COMMON/BLCK1/ZJ1(100)
      COMMON FH,FC,A,HOCA,LAMDA,BETA,EPS,PI,NSPW,NSPL
      PI = 3.1415926536
      PI2 = PI*PI
      PI3 = PI2*PI
      RPI = SQRT(PI)
      CONV = PI/180.0
C
      DO 22 N=1,100
   22 ZJ1(N) = 0.0
C
C        FIRST  20  ZEROS OF BESSEL FUNCTION  J1(T)  ARE KNOWN.
C        SEE ABRAMOWITZ AND STEGUN, PAGE 409
C
      ZJ1(1) = 3.83171
      ZJ1(2) = 7.01559
      ZJ1(3) = 10.17347
      ZJ1(4) = 13.32369
      ZJ1(5) = 16.47063
      ZJ1(6) = 19.61586
      ZJ1(7) = 22.76008
      ZJ1(8) = 25.90367
      ZJ1(9) = 29.04683
      ZJ1(10) = 32.18968
      ZJ1(11) = 35.33231
      ZJ1(12) = 38.47477
      ZJ1(13) = 41.61709
      ZJ1(14) = 44.75932
      ZJ1(15) = 47.90146
      ZJ1(16) = 51.04354
      ZJ1(17) = 54.18555
      ZJ1(18) = 57.32753
      ZJ1(19) = 60.46946
      ZJ1(20) = 63.61136
C
      READ (5,1001) A,HOCA
      READ (5,1001) TWMAX,TLMAX,EPS
      READ (5,1002) NSPW,NSPL,NINDEX
 1001 FORMAT (4F15.7)
 1002 FORMAT (3I10)
      READ (5,1000) NDATA
 1000 FORMAT (I10)
         DO 9999 ID=1,NDATA
      WRITE (6,9000)
 9000 FORMAT (1H1)
      READ (5,1001) FC,CLO
C
C
      FC2 = FC*FC
      LAMDA = (2.0/A)*HOCA
      LAMDA2 = LAMDA*LAMDA
      FH2 = (1.0/HOCA)*FC2
      FH = SQRT(FH2)
      FH3 = FH2*FH
      BETA = (2.0/A)*FC2
      FS = (1.0/SQRT(2.0))*SQRT(BETA)
C
C
      THETT = 35.26438968
      THETTR = THETT*CONV
      ST = SIN(THETTR)
      SECT = 1.0/COS(THETTR)
      SECT2 = SECT*SECT
      TT = (1.0/BETA)*SECT2*ST
      CONST = HOCA/FC2
C
      WRITE (6,2000) A,LAMDA,HOCA,BETA,FC,FH,FS,TT
 2000 FORMAT (/1X,8HGEOMETRY,/5X,22HASPECT RATIO,      A =F15.7,
     120X,7HLAMDA =F15.7,/5X,22HDEPTH-TO-CHORD, HOCA =F15.7,
     215X,12HFB2 = BETA =F15.7,/5X,22HCHORD FROUDE NO., FC =F15.7,
```

```
     35X,22HDEPTH FROUDE NO., FH =F15.7,/
     45X,22HSPAN FROUDE NO.,  FS =F15.7,5X,
     522HCRITICAL T-VALUE, TT =F15.7)
C
C                     DRAG
C
      WRITE (6,2001) NSPW,TWMAX,EPS
 2001 FORMAT (//1X,4HDRAG,/5X,6HNSPW =I10,/5X,7HTWMAX =F15.7,/5X,5HEPS =
     1E15.7,//8X,25HINDUCED DRAG COEFF RATIOS,35X,
     222HWAVE DRAG COEFF RATIOS)
      KE = 0.0
      EE = 0.0
      EMM1 = LAMDA2/(1.0 + LAMDA2)
      EMM = 1.0 - EMM1
         CALL ELLIP(VALK,VALE,EMM)
      KE = VALK
      EE = VALE
      ELL = 1.0 + LAMDA2
      RELL = SQRT(ELL)
      SIGMAI = 1.0 - (4.0/PI)*LAMDA*RELL*(KE - EE)
C
         CALL CALJW(JW,JWT,JWD,TT,TWMAX,NLOOPS,TE)
      C = (1.0/PI)*EXP(-CONST)
C
      WS = C*JW - (2.0*SIGMAI*FC2)/(PI*A)
C
      CDIIR = 1.0/(PI*A)
      CDSIR = -SIGMAI*CDIIR
C
      CWR = (C/FC2)*JW
      CWRT = (C/FC2)*JWT
      CWRD = CWR - CWRT
      CDSWR = (1.0/FC2)*WS
C
      CDIRUL = (1.0 + SIGMAI)/(PI*A)
      CDIRLL = (1.0 - SIGMAI)/(PI*A)
C
      CDR = CDIIR + CDSIR + CWR
      WRITE (6,2002) CDIIR,CWR,CDSIR,CWRT,SIGMAI,CWRD,CDIRLL,CDSWR,
     1CDIRUL,WS,CDR
 2002 FORMAT (/10X,7HCDIIR =E15.7,32X,
     125HWAVE DRAG(TOTAL),    CWR =E15.7,/10X,7HCDSIR =E15.7,/
     273X,32HTRANSVERSE WAVE PART,    CWR(T) =E15.7,/10X,
     38HSIGMAI =E15.7,40X,32HDIVERGING WAVE PART,     CWR(D) =E15.7,
     4//10X,18HCDI(LOWER LIMIT) =E15.7,21X,
     530HCDSWR =(CWR - 2*SIGMAI/PI*A) =E15.7,/10X,
     618HCDI(UPPER LIMIT) =E15.7,21X,
     730HSURFACE WAVE FACTOR,       WS =E15.7,//25X,
     838HCD(TOTAL)/CL02 =(CDIIR + CDSIR + CWR)=E15.7)
      WRITE (6,2003) NLOOPS,TE
 2003 FORMAT (/5X,8HNLOOPS =I10,/5X,4HTE =F15.7)
      WRITE (6,2005)
 2005 FORMAT (/5X,22HASYMPTOTIC RESULTS ---,6X,3HCWR,17X,5HCDSWR,15X,2HW
     1S,11X,11HWS(BRESLIN),12X,1HF)
         IF(LAMDA.GE.1.0.AND.FH2.LE.1.5) GO TO 170
         IF(LAMDA.LT.1.0.AND.FH2.GT.1.5) GO TO 171
      GO TO 172
  170 FAC1 = SQRT(2.0*PI)
      FAC2 = EXP(-2.0/FH2)
      FAC3 = LAMDA2*A*FH2*FH
      FAC4 = 6.0*LAMDA2*FH2*FH2
C
C   CWR ---  LAMDA.GE. 1.0,  FH2.LE.1.5
C
      CWR = (FAC2/(FAC1*FAC3))*(1.0 + 0.375*(1.0 - (1.0/FAC4))*FH2)
      WRITE (6,2004) CWR
 2004 FORMAT (28X,E15.7,11X,3H---,16X,2H--)
      GO TO 175
  171 FAK1 = 2.0/PI
      FAK2 = 1.5/PI2
      FAK3 = 4.0/(3.0*PI)
      ARGL = 4.0*RELL/LAMDA
      TLOG = ALOG(ARGL)
      F = FAK1*(2.0 - TLOG) - FAK2*((1.0/3.0) - TLOG)*(LAMDA2/ELL)
      WS = FAK3*(FAK1*RELL*ELL*EE - (1.5*LAMDA) -
     1(LAMDA2*RELL)*F)
      CDSWR = (1.0/FC2)*WS
      CWR = 2.0*SIGMAI/(PI*A) + CDSWR
      WSBRES = FAK3*((FAK1*ELL*RELL*EE) - (1.5*LAMDA))
C
```

THIS PAGE IS BEST QUALITY PRACTICABLE
FROM COPY FURNISHED TO DDC

```
      WRITE (6,2006) CWR,COSWR,WS,WSRRES,F
 2006 FORMAT (28X,E15.7,5X,E15.7,3X,E15.7,3X,E15.7,3X,E15.7)
      GO TO 175
  172 WRITE (6,2007)
 2007 FORMAT (/28X,27HNO ASYMPTOTIC RESULTS APPLY)
  175 NS = 2*NINDEX+1
C
C                    LIFT CORRECTION
C
      WRITE (6,2008) NSPL,NINDEX,NS,TLMAX,EPS
 2008 FORMAT (//1X,4HLIFT,/5X,6HNSPL =I10,/5X,8HNINDEX =I10,/5X,4HNS =I1
     +0,/5X,7HTLMAX =F15.7,/5X,5HEPS =F15.7,
     +//24X,28HLIFT COEFF CORRECTION RATIOS)
C
         CALL CALJL1(JL1)
      CL1R = -(8.0/(PI3*LAMDA*A))*JL1
C
         CALL CALJL2(JL2,TLMAX,NINDEX)
      CL2R = -(4.0/(PI2*A*FH))*JL2
C
      DELW = CL1R + CL2R
      CL02 = CL0*CL0
      DELCL = CL02*DELW
      CLR0 = 1.0 + DELCL
C
      WRITE (6,2009)CL1R,CL2R,DELW
 2009 FORMAT (27X,6HCL1R =E15.7,/27X,6HCL2R =E15.7,//27X,6HDELW =E15.7)
      WRITE (6,2010) CL0,DELCL,CLR0
 2010 FORMAT (/5X,9HFOR CL0 =F15.7,/10X,7HDELCL =E15.7,/10X,6HCLR0 =E15.
     +7)
      WRITE (6,2011)
 2011 FORMAT (/5X,22HASYMPTOTIC RESULTS ---,7X,6HCL1RAS,15X,6HCL2RAS)
C
         IF(LAMDA.GE.1.0) GO TO 50
      GO TO 51
   50 ELL2 = ELL*ELL
      ELL3 = ELL2*ELL
C
C   CL1RAS ---  LAMDA.GE.1.0
C
      CL1RAS =-(1.0/(8.0*PI*LAMDA*RELL*A))*(1.0 + (0.3125)/ELL +
     1(0.70703)/ELL2 + (0.0920105)/ELL3)
      GO TO 60
   51 EXL = RELL/LAMDA
      ALL = ALOG(EXL)
      AL2 = ALOG(2.0)
C
C   CL1RAS --- LAMDA.LT.1.0
C
      CL1RAS = -(8.0/(3.0*PI3*LAMDA*A))*(1.0 - (3.0*LAMDA2)*(AL2 -
     10.75 + 0.625*ALL))
   60    IF(LAMDA.GE.1.0.AND.FH2.LE.1.5) GO TO 70
         IF(LAMDA.LT.1.0.AND.FH2.GT.1.5) GO TO 71
      GO TO 72
   70 FACD = (2.0*PI)*SQRT(2.0*PI)
C
C   CL2RAS --- LAMDA.GE.1.0,  FH2.LE.1.5
C
      CL2RAS = (1.0/(FACD*LAMDA2*A*FH))*(1.0 + 0.5*FH2)
      GO TO 80
   71 GAM14 = 3.6256099082
      GAM34 = 1.2254167024
      GAM = 0.5772156649
C
C   CL2RAS,  LAMDA.LT.1.0,  FH2.GT.1.5
C
      RTWO = SQRT(2.0)
      ARG = 2.0/FH2
      CL2RAS = ((RTWO*GAM14)/(PI2*A))*(1.0 - (GAM34*LAMDA)/(RPI*GAM14*RE
     1LL))*(1.0 + (RTWO/RPI)*(1.0/FH)*(GAM + ALOG(ARG)))
      GO TO 80
   72 WRITE (6,2020) CL1RAS
 2020 FORMAT(30X,E15.7,5X,21HNO RESULTS APPLY HERE)
      GO TO 90
   80 WRITE (6,2012) CL1RAS,CL2RAS
 2012 FORMAT (30X,E15.7,5X,E15.7)
   90 CLR02 = CLR0*CLR0
      CDCL2 = CDR/CLR02
      WRITE (6,2013) CL0,CDCL2
 2013 FORMAT (//1X,21HINVISCID DRAG-TO-LIFT,//5X,9HFOR CL0 =F15.7,
```

```
     110X,15HCD(TOTAL)/CL2 =E15.7)
9999 CONTINUE
     END
```

```
      SUBROUTINE CALJW(JW,JWT,JWD,TT,TWMAX,NL,TF)
C
C        CALCULATES THE WAVE RESISTANCE INTEGRAL  JW
C        FOR A SUBMERGED HYDROFOIL
C
      REAL JW,JWT,JWD,J1,J12,LLOOP,LAMDA
      COMMON/BLCK1/ZJ1(100)
      COMMON FH,FC,A,HOCA,LAMDA,BETA,EPS,PI,NSPW,NSPL
      DIMENSION PS(100)
      CONV = PI/180.0
      SPACEN = FLOAT(NSPW)
      NSP1 = NSPW
      DO 1 N=1,100
    1 PS(N) = 0.0
C
      FC2 = FC*FC
      CONST = HOCA/FC2
      BETA2 = BETA*BETA
C
C
      ITT = 0
      J1 = 0.0
      N=1
      T=0.0
      JW = 0.0
      JWT = 0.0
      JWD = 0.0
      LLOOP = ZJ1(1)
      DT = LLOOP/SPACEN
      APS = EXP(-CONST)
         SIM1 = [illegible]
         SIM2 = 1.0
      IF (LLOOP.GE.TT) GO TO 200
   50 I = 0
  100 I = I+1
         IF (I.EQ.NSP1) GO TO 150
      T = T+DT
         IF (T.GT.TWMAX) GO TO 800
      T2 = T*T
      FORBT = 4.0*BETA2*T2
      ROOT = SQRT( 1.0 + FORBT)
         CALL CALJ1(VALJ1,T)
      J1 = VALJ1
      J12 = J1*J1
      EFACTR = EXP(-CONST*ROOT)
      FACT2 = (1.0 + ROOT)*(1.0 + ROOT)
      DAPS = (EFACTR*J12*FACT2)/(T2*ROOT)
         SIM = SIM1 + SIM2
      APS = APS + DAPS*SIM
         SIM2 = -SIM2
      GO TO 100
  150 APS = APS*(DT/3.0)
      PS(N) = APS
      JW = JW + PS(N)
      IF(ITT.EQ.0) GO TO 350
      GO TO 351
  350 JWT = JW
  351    RATIO = ABS(PS(N)/JW)
         IF (RATIO.LE.EPS) GO TO 700
  151    SIM1 = 3.0
         SIM2 = 1.0
      N = N+1
         IF (N.GT.20) GO TO 500
  152 T = ZJ1(N-1)
      LLOOP = ZJ1(N) - T
      TUL = (T + LLOOP)
      IF (TUL.GE.TT.AND.ITT.EQ.0) GO TO 200
      DT = LLOOP/SPACEN
      APS = 0.0
      I=0
```

```
160   I = I+1
         IF (I.EQ.NSP1) GO TO 170
      T = T+DT
         IF (T.GT.TWMAX) GO TO 800
      T2 = T*T
      FORBT = 4.0*BETA2*T2
      ROOT = SQRT(1.0 + FORBT)
      CALL CALJ1(VALJ1,T)
      J1 = VALJ1
      J12 = J1*J1
      EFACTR = EXP(-CONST*ROOT)
      FACT2 = (1.0 + ROOT)*(1.0 + ROOT)
      DAPS = (EFACTR*J12*FACT2)/(T2*ROOT)
         SIM = SIM1 + SIM2
      APS = APS + DAPS*SIM
         SIM2 = -SIM2
      GO TO 160
170   APS = APS*(DT/3.0)
      PS(N) = APS
      JW = JW + PS(N)
      IF(ITT.EQ.0) GO TO 352
      GO TO 353
352   JWT = JW
353      RATIO = ABS(PS(N)/JW)
         IF (RATIO.LE.EPS) GO TO 700
      GO TO 151
200   ITT = 1
         IF (N.EQ.1) GO TO 201
      DT = (TT - ZJ1(N-1))/SPACEN
      GO TO 202
201   DT = TT/SPACEN
202   I=0
203   I = I+1
      T = T+DT
         IF (T.GT.TWMAX) GO TO 800
      T2 = T*T
      FORBT = 4.0*BETA2*T2
      ROOT = SQRT(1.0 + FORBT)
      CALL CALJ1(VALJ1,T)
      J1 = VALJ1
      J12 = J1*J1
      EFACTR = EXP(-CONST*ROOT)
      FACT2 = (1.0 + ROOT)*(1.0 + ROOT)
      DAPS = (EFACTR*J12*FACT2)/(T2*ROOT)
         IF (I.EQ.NSP1) GO TO 204
      SIM = SIM1 + SIM2
      APS = APS + DAPS*SIM
         SIM2 = -SIM2
      GO TO 203
204   APS = APS + DAPS
      APS = APS*(DT/3.0)
      PS(N) = APS
         JW = JW + PS(N)
         JWT = JW
      RATIO = ABS(PS(N)/JW)
         IF (RATIO.LE.EPS) GO TO 700
      APS = DAPS
C
C        THIS SETS INITIAL VALUE FOR DOING THE AREA UNDER
C        THE REMAINDER OF THE LOOP
C
      DT = (ZJ1(N) - TT)/SPACEN
         SIM1 = 3.0
         SIM2 = 1.0
      GO TO 50
500   WRITE (6,2003)
2003  FORMAT (/2X,85HINTEGRATION MUST PROCEED BEYOND N=20 LOOPS, T = 63.
     161136 --- HEREAFTER ESTIMATE ZEROS)
      ENT = FLOAT(N)
      THET1 = (2.0*ENT - 1.0)*(PI/2.0)
      ALPHA0 = 2.35619449
      SUM = THET1 + ALPHA0
      SUM2 = SUM*SUM
      ZJ1(N) = (0.5*SUM)*(1.0 + SQRT(1.0 - (1.49995344)/SUM2))
      GO TO 152
800   WRITE (6,2006) TWMAX
2006  FORMAT (//10X,33HINTEGRATION TERMINATED AT TWMAX =F15.7)
700   JWD = JW-JWT
         TE = ZJ1(N)
         ROOTE = SQRT(1.0 + 4.0*BETA2*TE*TE)
         ARGE = (1.0/(2.0*BETA*TE))*(-1.0 + ROOTE)
```

```
      THETER = ASIN(ARGE)
      THETED = THETER/CONV
      NL = N
      RETURN
      END
```

```
      SUBROUTINE CALJL1(VJL1)
C
C        CALCULATES THE NESTED INTEGRAL JL1 FOR LIFT
C        CORRECTION
C
      REAL LAMDA,KX,KX2,KX4,KLAM,KE,LAMDA2
      COMMON FH,FC,A,HOCA,LAMDA,BETA,EPS,PI,NSPW,NSPL
      LAMDA2 = LAMDA*LAMDA
      SPACEN = FLOAT(NSPW)
      NSP1 = NSPW
      KLAM = 1.0/(SQRT(1.0 + LAMDA2))
      DKX = KLAM/SPACEN
         SIM1 = 3.0
         SIM2 = 1.0
      KX = 0.0
      VJL1 = PI/16.0
C
      I=0
  100 I=I+1
         IF (I.EQ.NSP1) GO TO 200
      KX = KX + DKX
      KX2 = KX*KX
      KX4 = KX2*KX2
      EMM = KX2
         CALL ELLIP(VALK,VALE,EMM)
      KE = VALK
      EE = VALE
      CE = (1.0/KX4)*((2.0 - KX2)*KE - 2.0*EE)
      RKKL = KX/KLAM
      RKKL2 = RKKL*RKKL
      FAC = SQRT((1.0 - RKKL2)/(1.0 - KX2))
C
      DVJL1 = FAC*CE
         SS = SIM1 + SIM2
      VJL1 = VJL1 + DVJL1*SS
         SIM2 = -SIM2
      GO TO 100
  200 VJL1 = VJL1*(DKX/3.0)
      RETURN
      END
```

```
      SUBROUTINE CALJL2(VJL2,TLMAX,NINDEX)
C
C         CALCULATES THE INTEGRAL  JL2  FOR LIFT CORRECTION
C
C                NSPL = NUMBER OF SPACES FOR ORDINARY
C                       (NONSINGULAR) INTEGRATIONS
C              NINDEX = COUNTING INDEX FOR CAUCHY SINGULAR
C                       INTEGRAL TREATED WITH SIMPSONS RULE
C
C                   H = SPACING FOR SINGULAR PART
C                     = 1.0/(2*NINDEX + 1)
C
C                  NS = NUMBER OF SPACES ON EACH SIDE OF ZERO
C                     = 2*NINDEX + 1
C
C         NUMERICAL COMPUTATIONS FOR INTEGRALS  I1,IN, AND IS
C
      REAL LAMDA,IS,IN,I1
      COMMON/BLCK1/ZJ1(100)
      COMMON FH,FC,A,HOCA,LAMDA,BETA,EPS,PI,NSPW,NSPL
      RPI = SQRT(PI)
```

```
      RTWO = SQRT(2.0)
      SPACEN = FLOAT(NSPL)
      NSP1 = NSPL
      FH2 = FH*FH
      NS = 2*NINDEX+1
      H = 1.0/FLOAT(NS)
         CALL CALFLO(FLO,TLMAX)
      UARG = 1.0/(2.0*FH2)
         CALL CALFL(FL,UARG,TLMAX)
      FL1 = FL
C
      UARG = 1.0/FH2
         CALL CALFL(FL,UARG,TLMAX)
      FL2 = FL
C
C             NONSINGULAR INTEGRALS  I1  AND  IN
C
         SIM1 = 3.0
         SIM2 = 1.0
      T = 0.0
      DT = 1.0/SPACEN
      FAEF = EXP(-1.0/FH2)
      I1 = 2.0*FAEF*(FL1 - FL0)
      IN = RTWO*FL2*FAEF
      I=0
  100 I=I+1
         IF (I.EQ.NSP1) GO TO 110
      T=T+DT
      EFTU = 1.0/(T*FH2)
         IF (EFTU.GT.500.0) GO TO 10
      GO TO 11
   10 E2 = 0.0
      GO TO 12
   11 E2 = EXP(-EFTU)
   12 E1 = EXP(-T/FH2)
      T12 = SQRT(T)
      T32 = T*T12
C
      ROOTT = SQRT((1.0 + T)/T)
      UARG1 = T/(2.0*FH2)
         CALL CALFL(FLT,UARG1,TLMAX)
      UARG2 = 1.0/(T*2.0*FH2)
         CALL CALFL(FLOT,UARG2,TLMAX)
      UARG3 = (1.0 + T)/(T*2.0*FH2)
         CALL CALFL(FLPOOT,UARG3,TLMAX)
C
      DI1 = (E1/T12)*(FLT - FL0) + (E2/T32)*(FLOT - FL0)
      DIN = FLPOOT*ROOTT*(E2/T)
C
         SIM = SIM1 + SIM2
      I1 = I1 + DI1*SIM
      IN = IN + DIN*SIM
         SIM2 = -SIM2
      GO TO 100
  110 DT03 = DT/3.0
      I1 = I1*DT03
      IN = IN*DT03
C
C             SINGULAR INTEGRAL  IS
C
         SIM1 = 3.0
         SIM2 = 1.0
      T = -1.0
      TM = 1.0
      EHPLUS = EXP(H/FH2)
      EHNEG = EXP(-H/FH2)
      HARGP = (1.0 + H)/(2.0*FH2)
         CALL CALFL(FLHP,HARGP,TLMAX)
      HARGN = (1.0- H)/(2.0*FH2)
         CALL CALFL(FLHN,HARGN,TLMAX)
      RHP = SQRT(1.0 + H)
      RHN = SQRT(1.0 - H)
C
      IS = RTWO*FAEF + (4.0/H)*(FLHP*RHP*EHNEG - FLHN*RHN*EHPLUS)
C
      I=1
  200 I=I+1
      T = T+H
      TM = TM - H
         IF (I.EQ.NS) GO TO 210
```

```
      E1R = EXP(-TM/FH2)
      E1L = EXP(-T/FH2)
      ROOTR = SQRT(1.0 + TM)
      ROOTL = SQRT(1.0 + T)
C
      HARGR = (1.0 + TM)/(2.0*FH2)
      HARGL = (1.0 + T)/(2.0*FH2)
         CALL CALFL(FL,HARGR,TLMAX)
      FLR = FL
         CALL CALFL(FL,HARGL,TLMAX)
      FLL = FL
C
      DISR = (FLR*ROOTR*E1R - FL1*FAEF)/TM
      DISL = (FLL*ROOTL*E1L - FL1*FAEF)/T
         SIM = SIM1 + SIM2
      IS = IS + (DISL + DISR)*SIM
         SIM2 = -SIM2
      GO TO 200
  210 IS = IS*(H/3.0)
      VJL2 = -RPI*FH*FL0 - I1 + FAEF*(IS + IN)
      RETURN
      END
```

```
      SUBROUTINE CALFL(FL,UARG,TLMAX)
C
C        CALCULATES THE FUNCTION   FL  DEFINED IN KERNEL OF
C        THE FROUDE-DEPENDENT LIFT CORRECTION INTEGRAL   JL2
C
      REAL LAMDA,LAMDA2,J1,J12
      DIMENSION PSL(100)
      COMMON/BLCK1/ZJ1(100)
      COMMON FH,FC,A,HOCA,LAMDA,BETA,EPS,PI,NSPW,NSPL
C
      CONV = PI/180.0
      SPACEN = FLOAT(NSPL)
      NSP1 = NSPL
      XVAR = 2.0*UARG
      UARG2 = UARG*UARG
      FL = 0.0
      J1 = 0.0
      IF (XVAR.GT.500.0) GO TO 3000
      DO 1 N=1,100
    1 PSL(N) = 0.0
      LAMDA2 = LAMDA*LAMDA
C
      N=0
  100    SIM1 = 3.0
         SIM2 = 1.0
      N=N+1
         IF (N.GT.20) GO TO 500
         IF (N.EQ.1) GO TO 101
  152 T = LAMDA*ZJ1(N-1)
      DT = (LAMDA*ZJ1(N) - T)/SPACEN
      APSL = 0.0
      GO TO 102
  101 T = 0.0
      DT = LAMDA*ZJ1(1)/SPACEN
      APSL = (0.5/LAMDA2)*(SQRT(XVAR))*(EXP(-XVAR))
  102 I=0
  110 I=I+1
         IF (I.EQ.NSP1) GO TO 170
      T = T+DT
         IF (T.GT.TLMAX) GO TO 800
      T2 = T*T
      ROOT = SQRT(T2 + UARG2)
      TOL = T/LAMDA
         CALL CALJ1(VALJ1,TOL)
      J1 = VALJ1
      J12 = J1*J1
      EFACTR = EXP(-2.0*ROOT)
      FACT32 = (UARG + ROOT)*(SQRT(UARG+ROOT))
C
      DAPSL = (EFACTR*J12*FACT32)/(T2*ROOT)
         SIM = SIM1 + SIM2
```

```
      APSL = APSL + DAPSL*SIM
        SIM2 = -SIM2
      GO TO 110
170   APSL = APSL*(DT/3.0)
      PSL(N) = APSL
      FL = FL + PSL(N)
        RATIO = ABS(PSL(N)/FL)
        IF (RATIO.LE.EPS) GO TO 700
      GO TO 100
500   ENT = FLOAT(N)
      THET1 = (2.0*ENT - 1.0)*(PI/2.0)
      SUM = THET1 + 2.35619449
      SUM2 = SUM*SUM
      ZJ1(N) = (0.5*SUM)*(1.0 + SQRT(1.0 - (1.4995344)/SUM2))
      GO TO 152
800   WRITE (6,2006) TLMAX
2006  FORMAT (//10X,33HINTEGRATION TERMINATED AT TLMAX =F15.7)
700     TE = LAMDA*ZJ1(N)
3000  CONTINUE
      RETURN
      END
```

```
      SUBROUTINE CALFLO(FLO,TLMAX)
C
C        CALCULATES THE FUNCTION   FLO  CONTAINED IN THE
C        KERNEL OF THE LIFT CORRECTION INTEGRAL  JL2
C
      REAL LAMDA,J1,J12
      DIMENSION PO(100)
      COMMON/BLCK1/ZJ1(100)
      COMMON FH,FC,A,HOCA,LAMDA,BETA,EPS,PI,NSPW,NSPL
C
      CONV = PI/180.0
C
      SPACEN = FLOAT(NSPL)
      NSP1 = NSPL
      DO 1 N=1,100
1     PO(N) = 0.0
      FLO = 0.0
      J1 = 0.0
      N=0
100     SIM1 = 3.0
        SIM2 = 1.0
      N=N+1
        IF (N.GT.20) GO TO 500
        IF (N.EQ.1) GO TO 101
152   T = LAMDA*ZJ1(N-1)
      DT = (LAMDA*ZJ1(N) - T)/SPACEN
      GO TO 102
101   T = 0.0
      DT = LAMDA*ZJ1(1)/SPACEN
102   APSO = 0.0
      I = 0
110   I=I+1
        IF (I.EQ.NSP1) GO TO 170
      T=T+DT
        IF (T.GT.TLMAX) GO TO 800
      T32 = (SQRT(T))*T
      TOL = T/LAMDA
        CALL CALJ1(VALJ1,TOL)
      J1 = VALJ1
      J12 = J1*J1
      EFACTR = EXP(-2.0*T)
C
      DAPSO = (EFACTR*J12)/T32
        SIM = SIM1 + SIM2
      APSO = APSO + DAPSO*SIM
        SIM2 = -SIM2
      GO TO 110
170   APSO = APSO*(DT/3.0)
      PO(N) = APSO
      FLO = FLO + PO(N)
        RATIO = ABS(PO(N)/FLO)
        IF (RATIO.LE.EPS) GO TO 700
      GO TO 100
```

```
  500 ENT = FLOAT(N)
      THET1 = (2.0*ENT - 1.0)*(PI/2.0)
      SUM = THET1 + 2.35619449
      SUM2 = SUM*SUM
      ZJ1(N) = (0.5*SUM)*(1.0 + SQRT(1.0 - (1.4995344)/SUM2))
      GO TO 152
  800 WRITE (6,2006) TLMAX
 2006 FORMAT (//10X,33HINTEGRATION TERMINATED AT TLMAX =E15.7)
  700    TE = LAMDA*ZJ1(N)
      RETURN
      END
```

```
      SUBROUTINE CALJ1(VJ1,TJ)
      IF (TJ.GE. 3.0) GO TO 300
      XT1 = TJ/3.0
      XT2 = XT1*XT1
      XT4 = XT2*XT2
      XT6 = XT4*XT2
      XT8 = XT6*XT2
      XT10 = XT8*XT2
      XT12 = XT10*XT2
      VJ1 = TJ*( 0.5 - 0.56249985*XT2+ 0.21093573*XT4
     1-0.03954289*XT6 + 0.00443319*XT8 - 0.00031761*XT10
     2+0.00001109*XT12)
      GO TO 301
  300 XT1 = 3.0/TJ
      XT2 = XT1*XT1
      XT3 = XT2*XT1
      XT4 = XT3*XT1
      XT5 = XT4*XT1
      XT6 = XT5*XT1
C
      THETA1 = TJ - 2.35619449 + 0.12499612*XT1 + 0.00005650*XT2
     1-0.00637879*XT3 + 0.00074348*XT4 + 0.00079824*XT5
     2-0.00029166*XT6
C
      F1 = 0.79788456 + 0.00000156*XT1 + 0.01659667*XT2
     1+0.00017105*XT3 - 0.00249511*XT4 + 0.00113653*XT5
     2-0.00020033*XT6
      CS1 = COS(THETA1)
      VJ1 = (F1*CS1)/(SQRT(TJ))
  301 RETURN
      END
```

```
      SUBROUTINE ELLIP(VK,VE,EM)
C
C        COMPUTES COMPLETE ELLIPTIC INTEGRALS OF THE FIRST AND
C        SECOND KIND ---  K  AND  E , RESPECTIVELY
C
C           EM = PARAMETER (= K**2)
C           EM1 =  1.0 - EM = COMPLEMENTARY PARAMETER
C
C        SEE ABRAMOWITZ AND STEGUN, PAGES 590,591,592 FOR
C        POLYNOMIAL APPROXIMATIONS
C
      EM1 = 1.0 - EM
      ALN = ALOG(1.0/EM1)
      EM12 = EM1*EM1
      EM13 = EM12*EM1
      EM14 = EM13*EM1
C
      VK = 1.38629436112 + (0.09666344259)*EM1 + (0.03590092383)*EM12
     1 + (0.03742563713)*EM13 + (0.01451196212)*EM14
     2+ (  0.50 + (0.12498593597)*EM1 + (0.06880248576)*EM12
     3+ (0.03328355346)*EM13 + (0.00441787012)*EM14)*ALN
C
      VE = 1.0 + (0.44325141463)*EM1 + (0.0626060122)*EM12
     1+ (0.04757383546)*EM13 + (0.01736506451)*EM14
     2+ ((0.2499836831)*EM1 + (0.09200180037)*EM12
     3+ (0.04069697526)*EM13 + (0.00526449639)*EM14)*ALN
      RETURN
      END
```

APPENDIX B

THE BIPLANE FACTOR

Routine and accurate calculation of the biplane factor σ_i for elliptic circulation distribution has been made easy by the existence of Wu's[3] formula, quoted in Equation (25), where the complete elliptic integrals are

$$K(k_\lambda) = \int_0^{\pi/2} \frac{d\phi}{\sqrt{1 - k_\lambda^2 \sin^2\phi}}$$

$$E(k_\lambda) = \int_0^{\pi/2} \sqrt{1 - k_\lambda^2 \sin^2\phi}\; d\phi \tag{B.1}$$

and $k_\lambda = 1/(1 + \lambda^2)^{1/2}$.

Polynomial approximations of great accuracy are available in Reference 12 (Chapter 17, pages 591 and 592) for the simple computation of K(k) and E(k). These are fourth order polynomials in the "complementary parameter"

$$m_1 = \frac{\lambda^2}{1 + \lambda^2} \tag{B.2}$$

where λ = depth-to-half span ratio.

A convenient collection of values for σ_i for a wide range of λ-values has been calculated using these formulas and is presented in Table 4.

TABLE 4

VALUES OF THE BIPLANE FACTOR σ_i

λ	$\sigma_i(\lambda)$	λ	$\sigma_i(\lambda)$
0.0	1.0	0.65	0.17095
0.01	0.9364	0.70	0.1555
0.02	0.8905	0.75	0.1418
0.03	0.8513	0.80	0.1298
0.04	0.8163	0.85	0.1191
0.05	0.7845	0.90	0.1096
0.06	0.7553	0.95	0.1011
0.08	0.7027	1.0	0.09351
0.10	0.6565	1.2	0.06999
0.15	0.5604	1.4	0.05406
0.20	0.4842	1.6	0.04285
0.25	0.4221	1.8	0.03472
0.30	0.3705	2.0	0.02865
0.35	0.3273	2.5	0.01889
0.40	0.2905	3.0	0.01334
0.45	0.2592	3.5	0.009904
0.50	0.2322	4.0	0.007635
0.55	0.2089	4.5	0.006061
0.60	0.1886	5.0	0.004927

APPENDIX C

NUMERICAL EVALUATION OF WAVE DRAG INTEGRAL

For the calculation of the integral in the wave drag formula of Equation (23), it is convenient to place the integrand in a form where the zero points of the oscillating factor (in this case the J_1-function) are most easily specified. To accomplish this, the transformation

$$t = \frac{1}{\beta} \sec^2 \theta \sin \theta \tag{C.1}$$

is applied to the integration variable to reduce the argument of the J_1-function to the linear variable t. This leads to the formula

$$\frac{C_W}{C_{L_o}^2} = \frac{e^{-1/F_h^2}}{\pi F_c^2} \int_0^\infty \frac{\exp(-F_h^{-2}\sqrt{1+4\beta^2 t^2})(1 + \sqrt{1+4\beta^2 t^2})^2}{t^2 \sqrt{1+4\beta^2 t^2}} \times J_1^2(t)dt \tag{C.2}$$

The entire t-integral is the wave drag integral, denoted by J_W. The technique of numerical integration proceeds in a sequence of steps, with each step being taken over an entire loop, whose value is then added to the cumulative sum. The current loop sum is then compared to the cumulative sum and when this ratio is found to be smaller than a specified accuracy, the approximate integration is complete.

Integration time is governed by the rate of decay of the integrand, and in general is slowest for shallow submergence (λ small) and for small Froude numbers.

APPENDIX D

NUMERICAL EVALUATION OF LIFT CORRECTION INTEGRALS

TERM ΔC_{L_1}

The numerical evaluation of the integral for ΔC_{L_1} given in Equation (32) involves a straight forward application of Simpsons Rule over the finite interval $(0, k_\lambda)$. As noted in Equation (34), the $\mathbb{C}(k_1)$ function appearing in the integrand is known in terms of the complete elliptic integrals $K(k_1)$ and $E(k_1)$ whose values can be computed using the polynomial approximations given in Reference 12, pages 591 and 592.

TERM ΔC_{L_2}

For the calculation of the double integral in the ΔC_{L_2} term in Equation (33), the θ-integral is treated first. The transformation

$$t_1 = \frac{\lambda u}{\beta} \sec^2\theta \sin\theta \tag{D.1}$$

leads to the final form

$$\frac{\Delta C_{L_2}}{C_{L_o}^2} = -\frac{4}{\pi^2 A F_h} J_{L_2} \tag{D.2}$$

where

$$J_{L_2} = \int_0^\infty \frac{e^{-u/F_h^2} F_L(u)}{\sqrt{u}\,(u-1)}\, du \tag{D.3}$$

with

$$F_L(u) = \int_0^\infty \frac{\exp(-2\sqrt{t_1^2+u^2/4F_h^4})\left(\frac{u}{2F_h^2} + \sqrt{t_1^2+u^2/4F_h^4}\right)^{3/2}}{t_1^2\sqrt{t_1^2+u^2/4F_h^4}} \times J_1^2\left(\frac{t_1}{\lambda}\right)dt_1 \tag{D.4}$$

The inner integral function $F_L(u)$ is dealt with numerically at any value u using the same procedure employed for the J_W integral in Appendix C.

The lift correction integral J_{L_2} has a Cauchy singular integrand and must be computed in terms of its principal value. By rewriting the integrand fraction $1/(u - 1)$ and by adding and subtracting the function $F_L(o)$ in the numerator, the singular part of J_{L_2} can be separated out, with J_{L_2} rewritten as

$$J_{L_2} = -\int_0^\infty e^{-u/F_h^2} F_L(o)\frac{du}{\sqrt{u}} - \int_0^\infty \frac{e^{-u/F_h^2}\left[F_L(u)-F_L(o)\right]}{\sqrt{u}}du + \int_0^\infty \frac{e^{-u/F_h^2} F_L(u)\sqrt{u}\,du}{(u-1)} \tag{D.5}$$

where
$$F_L(o) = \int_0^\infty \frac{e^{-2t}J_1^2(t/\lambda)}{t^{3/2}}\,dt \tag{D.6}$$

The first term of (D.5) involves a known definite integral

$$\int_0^\infty e^{-u/F_h^2}\frac{du}{\sqrt{u}} = \sqrt{\pi}\,F_h \tag{D.7}$$

The second term of (D.5) is not singular and can be handled easily by splitting the interval into $0 \le u \le 1$ plus $1 \le u \le \infty$; and then further transforming the second part by the substitution $u_1 = 1/u$ and integrating on u_1 from 1 to 0.

The third term of (D.5) contains the Cauchy singularity which is further isolated, first by substitution of $\xi = u - 1$, and then splitting the resulting interval $-1 \leq \xi \leq \infty$ into $-1 \leq \xi \leq 1$ plus $1 \leq \xi \leq \infty$. Ultimately the lift correction integral J_{L_2} can be written

$$J_{L_2} = -\sqrt{\pi}\, F_L(o) - I_1 + e^{-1/F_h^2} (I_N + I_S) \tag{D.8}$$

where

$$I_1 = \int_0^{\infty} e^{-u/F_h^2} \left[F_L(u) - F_L(o)\right] \frac{du}{\sqrt{u}} \tag{D.9}$$

$$I_N = \int_0^1 \frac{f(\frac{1}{\zeta})}{\zeta} d\zeta \tag{D.10}$$

$$I_S = \int_{-1}^1 \frac{f(\xi)}{\xi} d\xi \tag{D.11}$$

with

$$f(\xi) = F_L(\xi + 1)\sqrt{\xi + 1}\, e^{-\xi/F_h^2} \tag{D.12}$$

Numerical evaluation of integrals I_1 and I_N is accomplished by normal application of Simpsons Rule. The singular part, I_S, can be evaluated by a modified Simpsons Rule for a Cauchy singularity, which uses slightly modified Simpsons multipliers with a zero weight value on the integrand function at the singular point $\xi = 0$.

REFERENCES

1. Wilson, M.B. and J.R. Kelley, "Low Froude Number Hydrodynamic Performance of a Flat Plate Hydrofoil," DTNSRDC Departmental Report SPD-743-01, Dec 1976.

2. Nishiyama, T., "Linearized Steady Theory of Fully Wetted Hydrofoils," Advances in Hydroscience, Vol. 3, Edited by Ven Te Chow, Academic Press, 1966, pp. 237-342.

3. Wu, Y.T., "A Theory for Hydrofoils of Finite Span," (a) California Institute of Technology Hydrodynamics Lab Report No. 26-8, May 1953; (b) published in condensed form in Journal of Mathematics and Physics, Vol. 33, 1954/44, pp. 207-248.

4. Breslin, J.P., "Applications of Ship-Wave Theory to the Hydrofoil of Finite Span," Journal of Ship Research, Vol. 1, No. 1, 1957, p. 27.

5. von Kármán, T. and J.M. Burgers, "General Aerodynamic Theory - Perfect Fluids," Division E, Vol. II of Aerodynamic Theory, Edited by W.F. Durand, Julius Springer, 1935.

6. Bateman Manuscript Project, Higher Transcendental Functions, Vol. 2, Edited by A. Erdélyi, McGraw-Hill Book Co., 1953.

7. Lunde, J.K., "On the Linearized Theory of Wave Resistance for Displacement Ships in Steady and Accelerated Motion," Trans. SNAME, Vol. 59, 1951.

8. Kotchin, N.E., "On the Wave-Making Resistance and Lift of Bodies Submerged in Water," Translation from Russian, SNAME Technical and Research Bulletin No. 1-8, Aug 1951.

9. Wadlin, K.L., C.L. Shuford, and J.R. McGehee, "A Theoretical and Experimental Investigation of the Lift and Drag Characteristics of Hydrofoils at Subcritical and Supercritical Speeds," NACA Report 1232, 1955.

10. Hoerner, S.F., Fluid-Dynamic Drag, Published by the Author, 1965.

11. Burroughs, J.D., et al, "Hydrofoil Analysis and Design Program (HANDE), Theory Manual," Vol. II, The Boeing Co. Report No. D321-51312-2, Jul 1976.

12. National Bureau of Standards, Handbook of Mathematical Functions, Edited by M. Abramowitz and I.A. Stegun, U.S. Government Printing Office, Washington, D.C., 1964.

AD-A058 533 DAVID W TAYLOR NAVAL SHIP RESEARCH AND DEVELOPMENT CE--ETC F/G 13/10
LIFTING LINE CALCULATIONS FOR HYDROFOIL PERFORMANCE AT ARBITRAR--ETC(U)
JUN 78 M B WILSON

UNCLASSIFIED DTNSRDC/SPD-0839-01 NL

2 OF 2
ADA
058533

END
DATE
FILMED
11-78
DDC

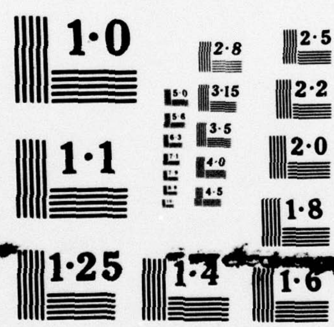

NATIONAL BUREAU OF STANDARDS
MICROCOPY RESOLUTION TEST CHART

DTNSRDC ISSUES THREE TYPES OF REPORTS

1. DTNSRDC REPORTS, A FORMAL SERIES, CONTAIN INFORMATION OF PERMANENT TECHNICAL VALUE. THEY CARRY A CONSECUTIVE NUMERICAL IDENTIFICATION REGARDLESS OF THEIR CLASSIFICATION OR THE ORIGINATING DEPARTMENT.

2. DEPARTMENTAL REPORTS, A SEMIFORMAL SERIES, CONTAIN INFORMATION OF A PRELIMINARY, TEMPORARY, OR PROPRIETARY NATURE OR OF LIMITED INTEREST OR SIGNIFICANCE. THEY CARRY A DEPARTMENTAL ALPHANUMERICAL IDENTIFICATION.

3. TECHNICAL MEMORANDA, AN INFORMAL SERIES, CONTAIN TECHNICAL DOCUMENTATION OF LIMITED USE AND INTEREST. THEY ARE PRIMARILY WORKING PAPERS INTENDED FOR INTERNAL USE. THEY CARRY AN IDENTIFYING NUMBER WHICH INDICATES THEIR TYPE AND THE NUMERICAL CODE OF THE ORIGINATING DEPARTMENT. ANY DISTRIBUTION OUTSIDE DTNSRDC MUST BE APPROVED BY THE HEAD OF THE ORIGINATING DEPARTMENT ON A CASE-BY-CASE BASIS.